Intracardiac mapping of atrial arrhythmias in humans: development and validation of new techniques

Linton, Nick William Fox

Awarding institution:
King's College London

Intracardiac mapping of atrial arrhythmias in humans: development and validation of new techniques

Nick Linton

Submission for PhD

King's College London

Acknowledgements

Embarking on a thesis that blends clinical cardiology and engineering has been an exciting and demanding undertaking. I am extremely grateful to my primary supervisor, Mark O'Neill, not only for challenging and enriching the ideas in this thesis but also for opening the door to clinical cardiac electrophysiology over the last 5 years. I am indebted to Reza Razavi who also supervised this work, providing direction and support. I am also grateful to Pierre Jaïs, and the team in Bordeaux, with whom I spent time during 2009/10 and continue to collaborate.

Steven Niederer undertook the arduous task of checking through the mathematical parts of the thesis, for which I am very thankful!

There are many colleagues to whom I owe thanks. However, I am particularly grateful to the other members of the research group - James, Steve and Matt - for their camaraderie and encouragement throughout the process.

Declaration

I confirm that the material presented in this thesis is my own work and references are cited accordingly. In Chapter 3, the initial publication on Ripple Mapping is presented. I was responsible for designing and writing the computer software for the Ripple Mapping and drafting the manuscript. I am grateful to Michael Koa-Wing who is a joint first author for that publication. He performed the data collection and initial analysis of the clinical cases. I performed all further software development, data collection, and analysis presented in Chapter 4.In Chapters 5 and 6, the suggestion to work on an electroanatomic approach to entrainment mapping was made by Pierre Jaïs. I then conceived and explored the concept for a new entrainment criterion that is presented in Chapter 5. I also designed and implemented the software presented in Chapter 6, as well as performing all data collection and analysis.

Abstract

In patients undergoing catheter ablation procedures for atrial tachycardia, successful ablation requires the mechanism and location of the tachycardia to be correctly determined. This thesis explores the integration of engineering and computational methods with electrophysiological principles for mapping atrial tachycardias.

The first objective of the thesis is to re-evaluate activation mapping. Ripple Mapping was created for this purpose. This is a method that displays each recorded electrogram as a bar on the shell that represents the cardiac surface: the length of the bar varies with time according to the electrogram voltage-time relationship. A proof-of-concept study evaluates Ripple Mapping in a small number of patients with a variety of different arrhythmias. After further development of the method, it is evaluated in patients with atrial tachycardia. Benefits include avoiding the need to annotate each electrogram with a Local Activation Time and also avoiding the need to select a Window of Interest.

The second objective is to investigate how macro-reentry tachycardias are detected. The classic entrainment criteria can be difficult to apply in the clinical setting of atrial tachycardia (particularly after prior ablation). A new entrainment criterion is described that utilises the response to entrainment from multiple locations. This can also detect double loop reentry from two entrainment manoeuvres. The theoretical basis for the criterion is developed within a mathematical framework. Clinical testing is performed in patients with typical flutter, left atrial macroreentry, and also analysis of previously published reports of double-loop reentry. The criterion is also incorporated into the overdrive pacing analysis software described below.

The final objective was to integrate information from overdrive pacing manoeuvres in combination with the electroanatomic information from 3D mapping systems. A theoretical basis for this has been developed and incorporated into a computer program. Initial clinical evaluation is presented from patients with simulated focal tachycardias as well as clinical localised reentrant and macroreentrant tachycardias.

Abbreviations

These have been kept to a minimum but are not given in expanded form at first use.

[1-1] – equation 1-1

AF – atrial fibrillation

AOP – atrial overdrive pacing

AT – atrial tachycardia

CL – cycle length

CS – coronary sinus

EP – electrophysiology

FBT – first beat of tachycardia

IVC – inferior vena cava

LA – left atrium

LAA – left atrial appendage

LAT – local activation time

PPI – post-pacing interval

RA – right atrium

RAA – right atrial appendage

SVC – superior vena cava

TCL – tachycardia cycle length

VT – ventricular tachycardia

Table of Contents

Supplemental CD:

Movie 4-1, Movie 4-2, Movie 4-3, Movie 4-4

1 Literature Review

1.1 Introduction

In 2003-2006, there were at least 21,000 ablation procedures performed worldwide for the treatment of AF.[1] As will be discussed, AT is common in the context of AF ablation and so there has been a concomitant rise in the number of ablation procedures involving AT and also a widespread increase in the use of 3D-mapping technology. However, the fundamental methods for mapping AT have changed little over the last 10-20 years, despite the pivotal role that mapping plays in choosing the correct ablation strategy. The purpose of the research underlying this thesis is to re-evaluate mapping techniques: by combining electrophysiological principles with engineering and computational methods, the aim is to create new mapping techniques to facilitate the treatment of AT.

In this chapter, the literature relevant to mapping AT is reviewed. Particular emphasis is given to the mechanisms of tachycardia: an understanding of mechanisms is crucial because it underpins the interpretation of electrograms that are recorded. Invasive activation mapping involves the integration and analysis of electrogram information from different locations within the heart. This is reviewed, including the electroanatomical mapping systems that are used. Another tool for identifying AT is entrainment mapping, and the history and evolution of entrainment mapping is described. Currently, its main use in AT procedures is to confirm the tachycardia mechanism that activation mapping has indicated.

1.2 Mechanisms of atrial arrhythmias

AT is a broad term that is used to describe sustained arrhythmias, where the mechanism depends only upon atrial tissue. This incorporates a number of different mechanisms that occur with different prevalence in different groups of patients. These mechanisms have previously been classified and described in a consensus statement from a working group formed by the European Society of Cardiology and the North American Society of Pacing and Electrophysiology.[2] Prior to this statement, AT classification had been based upon the ECG. However, the correlation between ECG appearance and tachycardia mechanism is not reliable, particularly in patients with diseased, previously ablated, or structurally abnormal atria.

The new classification placed greater emphasis upon intracardiac activation patterns and subdivides AT into: inappropriate sinus tachycardia, focal tachycardia or macroreentrant tachycardia. In the classification document, it is made clear that further mechanisms for AT might be discovered. Subsequently, localised reentry has been described, which involves reentry within a small area of tissue that has slow conduction (usually due to prior ablation).[3, 4] See Table 1-1 for a summary of terms which are described in further detail below.

Atrial Tachycardia Classification	Mechanisms
Inappropriate Sinus Tachycardia	see text
Focal Tachycardia	enhanced automaticity triggered activity microreentry
Reentry -	
Macroreentrant Tachycardia	typical flutter roof-dependent LA reentry perimitral reentry scar-related reentry
Localised Reentry Tachycardia	reentry in diseased tissue (<2cm diameter)

Table 1-1. The classification of AT.

1.2.1 Inappropriate sinus tachycardia

Inappropriate sinus tachycardia consists of an increase in the sinus node rate that is disproportionate to the level of physiological stimulation, i.e. it is an exaggerated response by the sinus node. The mechanism for this abnormality is poorly understood. Ablation can be performed, targeting the earliest site of atrial activation during isoprenaline infusion,[5] but results are mixed.[6, 7] Due to the small number of cases presenting for atrial mapping and ablation, inappropriate sinus tachycardia will not be considered further in this thesis.

1.2.2 Focal tachycardia

Prevalence

In a Finnish study, 3554 consecutive ECGs were examined from asymptomatic males aged 17-21 who were applying for a pilot's licence: the prevalence of AT was 0.34%.[8] The same authors performed a retrospective analysis of 3700 symptomatic patients attending an arrhythmia clinic, finding a prevalence of 0.43%.[8] However, these data were obtained from single ECG recordings and the prevalence would probably have been higher if longer recordings had been made, or more than one ECG from each patient had been examined. However, the data do indicate that sustained AT leading to ablation therapy is relatively uncommon. There is little contemporary data but studies have suggested that about 10% patients with tachycardia demonstrated at EP study have focal AT.[2, 9, 10]

Mechanism

Focal tachycardias arise from a small region of atrial tissue, with centrifugal spread of activation away from this region.[11] Three mechanisms have been proposed: enhanced automaticity, triggered activity, and microreentry.[12]

Automaticity is a normal property of cells within the sinus node, atrioventricular node and His-Purkinje system. The sinus node is usually at the top of the hierarchy in pacemaker function and so normal cardiac activation originates from this tissue. However, in abnormal circumstances other cells can develop automaticity. Automatic arrhythmias often initiate with acceleration ('warm-up') and terminate after deceleration ('warm-down'). Additionally, they are susceptible to suppression by overdrive pacing, which is usually followed by gradual re-acceleration of the tachycardia.[10]

Triggered activity is impulse initiation occurring consequent to a preceding impulse.[12] This can occur just before (phase 2), during (phase 3), or after repolarisation (phase 4). These arrhythmias are more likely to occur when the spontaneous heart rate is slow because, under these conditions, the action potential duration is longer. The effects of overdrive pacing upon triggered activity arrhythmias are variable. If pacing is fast enough for a long enough duration, then the rate of triggered activity

slows and may stop. However, if the pacing rate is only slightly faster than tachycardia, then it can cause overdrive acceleration of the tachycardia.

Microreentry is a form of reentry that occurs over an area too small to map with conventional 4mm tip electrodes.[12] There is rotation of the depolarisation wavefront around an area of slow conduction with fixed or functional block at its centre. Reentry will be discussed more fully below.

Human studies

In the 1980s surgical excision of the culprit region was employed as a treatment for focal AT[13] – this allowed histological and electrical study of the excised portion of atrium. In the largest series, there were 12 patients who did not have structural heart disease.[14] In these patients, there was fatty infiltration of uncertain significance (3/12) or normal histology (9/12). In the 4 other patients with structural heart disease, there was abnormal histology with patches of fibrosis between bundles of myofibrils: importantly, in these patients, AT could be reliably induced and terminated with paced atrial extrasystoli, suggesting a mechanism of reentry or triggered activity rather than enhanced automaticity.

Following these early studies, Chen et al. reported one of the seminal studies of focal AT mechanism.[9] They studied 36 patients referred for AT ablation to their centre over a 3 year period. Each patient underwent testing over 7 days, with ablation being performed on the last day. They attempted to categorise the mechanism of tachycardia based upon: 1) initiation with isoproterenol (automatic AT); 2) initiation or termination with programmed stimulation (microreentry or triggered reentry); 3) intracardiac after-depolarisations recorded (triggered activity); 4) entrainment phenomena observed (suggesting microreentry). On this basis 20/36 patients had microreentrant AT, 7/36 had automatic AT, and 9/36 had probable triggered activity.

The sites where focal AT originates are not uniformly distributed around the atria. In one of the largest series, 126 patients undergoing ablation for 130 focal AT were studied.[15] 63% AT originated in the RA, with sites being limited to the crista, tricuspid annulus, CS ostium, near the AV node, septum and the RA appendage. The remainder of AT originated in the LA near to the pulmonary veins, mitral annulus, CS,

septum, or LAA. The origin of LA focal AT has been confirmed by other investigators.[16-19]

1.2.3 Reentry

After a focal activation, a wave of depolarisation spreads away from the site of initiation with a centrifugal activation pattern, to depolarise the rest of the cardiac chamber. Propagation continues until the point is reached which has the greatest conduction time from the focal source. At this site of latest activation, the depolarisation wavefront collides with itself or with anatomical barriers so that propagation is terminated. The next activation then arises from the next focal impulse. Reentry is a different type of cardiac activation that can result in stable AT.

The mechanism for reentry was first described by Mayer, who devoted his life to the study of jellyfish.[20] He noted that it was possible to induce circular rhythms (that were visible due to the movement of the tissue) in rings cut from jellyfish. This work was applied to reptilian hearts by Mines (who also gave the first description of sinus arrhythmia and decremental conduction of the AV node in the same paper).[21] In contrast to focal tachycardias, tachycardias involving reentry have a single wavefront that propagates indefinitely across the heart's surface: the wavefront follows a path that re-enters tissue that it has already depolarised, and this allows self-perpetuation of the arrhythmia. Mines realised that reentry could only occur if certain conditions were met, and these conditions still hold today: 1) unidirectional block is required for initiation; and 2) the wavefront must pass around the circuit in a time long enough to allow the tissue to become repolarised. (See Figure 1-1.)

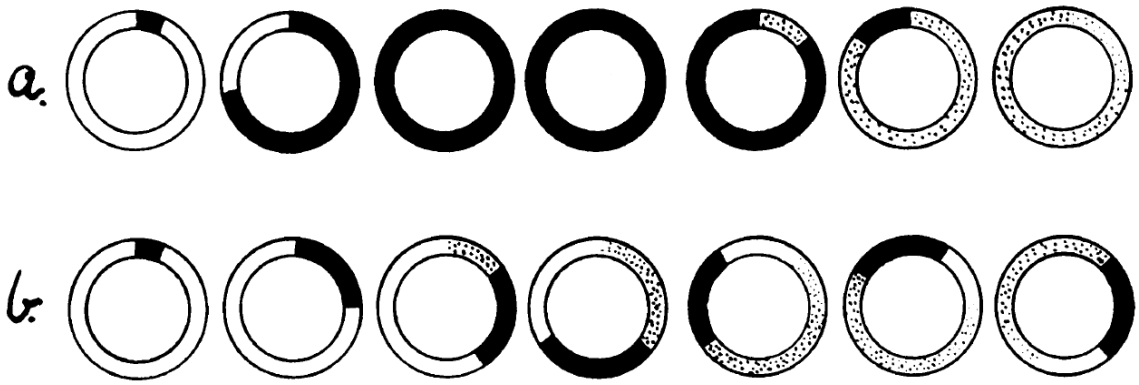

Figure 1-1. Reproduced from Mines.[21] The rings are schematic, using shading to represent activation: black, depolarised (i.e. refractory); stippled, partially recovered; white, excitable. There is unidirectional block next to an initial impulse (left side). In row [a], the impulse reaches depolarised tissue causing termination of wavefront propagation and then repolarisation of the ring. In [b], propagation is slower and so activation returns to the top of the ring when the tissue is excitable. Propagation can continue indefinitely around the ring because of this 'excitable gap'.

The first condition - unidirectional block - can occur if there is anatomical asymmetry of the conduction tissue, or if there is functional asymmetry in excitability (see Kleber and Rudy for a full discussion[22]). The second condition implies that there must be an excitable gap – i.e. that the circuit is long enough such that tissue at the trailing edge of the wavefront has time to become excitable before the leading edge of the next wavefront returns to that location. The circuit length that is required will depend upon the conduction velocity and the refractory period.

In human atria, reentry can give rise to arrhythmias in a number of ways. Reentry around relatively large fixed anatomical obstructions, such as vein orifices or valve annuli, gives rise to macroreentry. Reentry can also occur in the absence of fixed anatomical obstacles where there are areas of abnormal tissue. In microreentry, the reentry occurs within an area that is smaller than the resolution of standard intracardiac mapping catheters. The centre of the circuit has areas of fixed and functional block[22] and the activation away from this area has a pattern similar to other forms of focal tachycardia.[12] When the area of tissue involved in functional reentry is larger, then continuous activation can be recorded in a zone that is a few centimetres

in diameter and the term localised reentry is used.[3] Figure 1-2 shows a schematic of different tachycardia mechanisms that have been discussed.

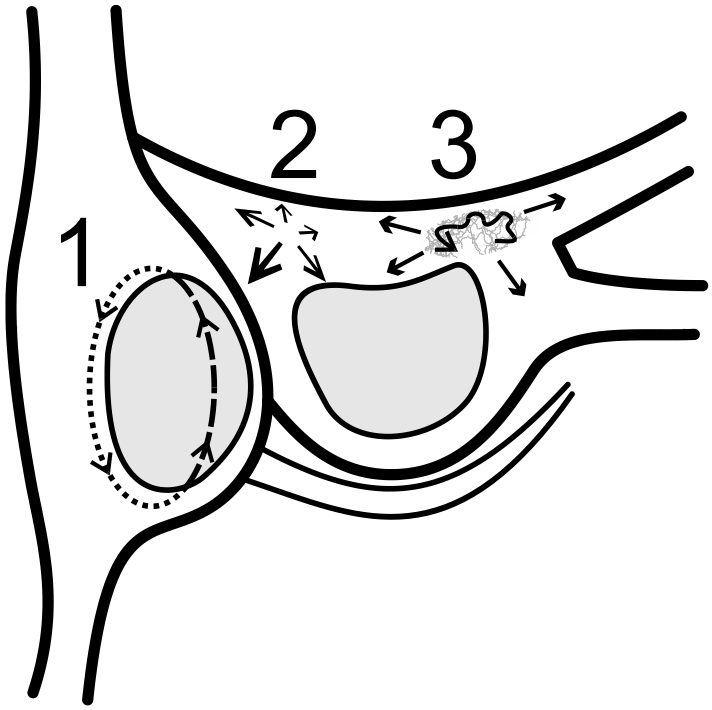

Figure 1-2. Schematic of different tachycardia mechanisms. 1) Cavotricuspid isthmus dependent macroreentry. The anterior part of the circuit is shown, coursing around the tricuspid annulus. 2) Focal. There is centrifugal activation emanating from a discrete source. 3) Localised reentry. There is an area of slow conduction with a reentry circuit within it.

An important property of atrial reentry tachycardias is that they can be entrained: when the atria are paced at a rate slightly faster than tachycardia then, at the termination of pacing, tachycardia continues without interruption. Entrainment is important because it allows the arrhythmia mechanism to be deduced and it also allows the re-entrant circuit to be located. This will be discussed more fully in Section 1.4.

1.2.4 Typical right atrial flutter

Prevalence

Typical atrial flutter refers to a regular tachycardia that has a characteristic appearance when recorded with a surface ECG. The incidence and risk factors were studied using analysis of a large database that captures almost all healthcare activity in Wisconsin.[23]

Incidence was approximately 88 per 100,000 but there were wide variations in different groups. In people younger than 50 years the incidence was 5/100,000 per annum but in those older than 80 years the incidence was 587/100,000 per annum. Atrial flutter was 2.5 times more common in men, and the relative risk was also greater in those with heart failure (relative risk 3.5) and chronic obstructive pulmonary disease (relative risk 1.9).

Mechanism

Typical flutter is the most common macroreentrant arrhythmia, and is confined to the RA with the LA being activated passively. Anteriorly the circuit forms a loop around the tricuspid annulus. Posteriorly, there is a combination of anatomical and functional obstacles that provide a long enough circuit so that there is an excitable gap.[24] Therefore there may coexist two potential circuits – one posterior to the SVC and one anterior – that are capable of sustaining tachycardia (this will be discussed further in Section 1.4.5).[25] However, all potential circuits pass through one area – the tissue between the IVC posteriorly and the tricuspid valve anteriorly. This area is known as the cavo-tricuspid isthmus (CTI). Termination and prevention of the tachycardia can be achieved by creating a line of ablation that prevents conduction through this isthmus.[26, 27]

The structure of the right atrium provides the fixed anatomical substrate for reentry. However, this is necessary but not sufficient for reentry to occur. There is a small amount of direct evidence that patients with atrial flutter also have abnormal electrical substrate: both slower conduction velocity and also increased dispersion of conduction.[28] This is consistent with the epidemiological data presented above – it is known that atrial conduction properties change with age[29] and with pulmonary hypertension (as is often found in chronic lung disease and cardiac failure).[30] The increased incidence of atrial flutter in males is more difficult to explain, but one reason might be the larger atrial size which would increase the excitable gap in any anatomically defined circuit.

1.2.5 Atrial tachycardia in the context of ablation for atrial fibrillation

Mechanisms and substrate for atrial fibrillation

AF is a disorganised arrhythmia where there is chaotic, irregular atrial activity: an episode of AF is defined as an episode >30 seconds with completely irregular RR intervals, no distinct P waves, and an atrial cycle length of <200ms (if visible) on the ECG. Patients with paroxysmal AF have episodes that terminate spontaneously within 7 days, and those with persistent AF have longer episodes.[31] It is the most common arrhythmia and is increasing in prevalence.[31, 32]

It is known that sleeves of conducting tissue extend into the pulmonary veins[33], and rapid firing from the pulmonary veins has become a well-established mechanism for the initiation and maintenance of AF.[34, 35] In the majority of patients with paroxysmal AF, this is the dominant mechanism of arrhythmia, although arrhythmogenic foci from other thoracic veins have been also reported. [36-38] This mechanism is likely to be influenced by other mediators, including autonomic control[39], hypoxia during sleep apnoea,[40] obesity and alcohol.[41]

The conduction properties of normal human atria are not uniform.[42] Patients with AF have altered electrical properties of the atria.[43] This may result from another condition that predisposes to AF, such as cardiomyopathy or valve disease. However, in pivotal experiments with chronically instrumented goats, Allessie's group demonstrated a causal effect between AF and electrical atrial remodelling.[44] They implanted pacemakers into the goats and used them to induce and maintain AF. They found that after maintaining AF for 7.1 ± 4.8 days the arrhythmia sustained itself for >24 hours in 10/11 goats, and this was accompanied by a 35% reduction in the atrial effective refractory period. By contrast, at the start of the experimental period, episodes of AF only self-sustained for 6 ± 3s. Additionally, in 5 goats after 2-4 weeks of AF, sinus rhythm was restored and the electrophysiological changes were reversed after one week.[44]

Further canine studies have confirmed the electrical remodelling that occurs in AF induced by chronic atrial pacing.[45, 46] Additionally, other models of AF have been developed, involving atrial changes induced by heart failure,[47] mitral regurgitation,[48] atrial ischaemia,[49] or cholinergic agonists.[50] The results of these studies may be

compared, and other investigators have also performed direct comparisons of these models.[45, 51]

In the canine model of AF with 6 weeks of rapid atrial pacing, the primary change is electrical remodelling manifested by a reduction in refractoriness as well as an increase in the dispersion of refractoriness. Structural changes in the atrium are small but an increased level of fibrosis has been observed,[45] although AF becomes sustained before this occurs.

In the canine models of AF with heart failure, induced by ventricular pacing at high rates, there was electrical as well as structural remodelling (although in contrast to pacing induced AF the atrial refractoriness *increased* slightly). There was pronounced interstitial fibrosis.[47, 52] After cessation of pacing and a 5 week recovery period, there was complete recovery of the electrical remodelling but AF vulnerability was still higher than baseline. Thus it is hypothesised that the fibrosis and structural changes led to continued AF susceptibility.[52] In the AF models with mitral regurgitation and atrial ischaemia, the atrial fibrosis was less marked but other microscopic structural changes were present and were likely to be the primary factor for increased AF susceptibility.[45]

In a comparative study of the canine models of AF, Everett et al. have demonstrated that the mechanism of perpetuation relates to the abnormality of the substrate.[45, 51] In models with primary *electrical* remodelling, the AF was characterised by multiple wavelets or multiple stable high frequency areas.[45] However, models with primary atrial *structural* changes were characterised by the presence of 'mother rotors'[45] consistent with the presence of micro-reentry due to altered conduction.

In humans, reversal of electrical remodelling has been demonstrated following treatment of AF by DC cardioversion.[43, 53] There is also evidence for a relationship between fibrosis and AF in patients with AF[54-56] and with mitral valve disease.[57] More recently, MRI has been used to detect atrial fibrosis non-invasively. In a group of 44 patients with lone AF, an increased burden of left atrial scar was associated with lower success rates after pulmonary vein isolation,[58] suggesting that further arrhythmic substrate was present in addition to the focal drivers from the pulmonary veins.

Ablation for atrial fibrillation

In patients with paroxysmal AF undergoing ablation, the majority of centres use radiofrequency ablation to achieve electrical isolation of the pulmonary veins.[1] For patients with persistent AF, further ablation is required.[59, 60] This includes electrogram-guided substrate modification, which can be based upon electrogram fractionation[61, 62] and also upon frequency analysis.[63] The aim of the electrogram-based ablation is to alter the atrial substrate in order to reduce its capability for supporting arrhythmia. However, the relationship of the underlying mechanisms to the electrogram (during AF) and the way in which modification by ablation reduces arrhythmia burden is poorly understood. Linear ablation lesions may also be performed and the aim of these is to prevent macroreentry and also to reduce the arrhythmia wavelength that can be supported.[64] Again, there is controversy about when these lesions should be deployed.[65]

During ablation for persistent AF, multiple ATs often occur during the procedure. These probably coexist and as the fastest tachycardia is ablated and terminates, a slower AT may then be revealed.[66] Better outcomes have been reported in those patients in whom sinus rhythm is achieved by ablation.[67-69]

Atrial tachycardia following atrial fibrillation ablation

As described above, the atria in patients with persistent AF are known to have abnormal electrical properties. Additionally, the atrial tissue is intentionally damaged during ablation procedures for AF. There are no studies formally examining atrial conduction in areas where 'substrate ablation' has been performed. However, it is likely that there are areas with heterogeneous electrical properties and also slow conduction velocity: both factors that are known to be pro-arrhythmic.

After an AF ablation, arrhythmia often does recur – either with AF recurrence but also with AT. When patients re-present with AT, as opposed to AF, then there is some evidence to suggest better outcomes. Ammar et al. studied 78 patients who underwent a repeat ablation procedure. At 9 month follow-up, 51% patients who had re-presented with persistent AT were free of arrhythmia without antiarrhythmic drugs, compared to 23% who had re-presented with persistent AF.[70] This prompted AT to be

considered as a 'stepping stone' to maintenance of sinus rhythm by some commentators.[31]

The reported incidence of AT, following AF ablation, varies widely (5-50%).[68, 71-73] Patients with AT have a high chance of recurrence if ablation is not performed.[74] The mechanism varies but there is evidence that previous ablation is an important factor. Takahashi et al. studied 9 patients with localised reentry after AF ablation and found that the circuit responsible for arrhythmia was in the vicinity of prior linear lesions or near the ablated ostia of pulmonary veins (it is known that conduction can recur across lesions created to isolate pulmonary veins[75]).[76] Cummings et al. studied 23 patients who developed AT in the LA following ablation that only involved PVI. In all patients, they repeated the PVI and did not perform any further ablation. In 11/12 patients, no LA low voltage areas were identified at the time of the repeat PVI and 11/12 of these patients remained arrhythmia free after 12 months follow-up. In contrast, in the other 11/23 patients with low voltage areas of the LA, only 4/11 remained arrhythmia free.[77]

There is also evidence that incomplete linear lesions can promote reentry. For example, an ablation line at the mitral isthmus that does not create conduction block may, instead, cause slow conduction. This zone of slow conduction will increase the conduction time to pass around a perimitral circuit, thus facilitating an excitable gap to promote reentry.[78] Whilst linear lesions may prevent AT,[79] if they are attempted and conduction block is *not* achieved then there is an increased risk of AT.[80, 81] In another recent study of patients after AF ablation, the circuit of 96% macroreentrant tachycardias crossed a line of prior ablation.[82]

Other studies have confirmed that the mechanism of AT varies according to the atrial ablation procedures that have been performed. Where only ostial PV isolation has been performed, the mechanism is usually localised reentry arising from reconnected PV ostia.[71, 72, 83-85] Wider encirclement of the PVs and linear ablation is associated with macroreentry.[73, 82] Where electrogram guided ablation is performed to modify the atrial substrate then this is associated with a higher proportion of focal and localised reentry AT recurrences.[3, 62]

The location of microreentry or localised reentry tachycardias varies widely.[86] However, the circuits causing macroreentry are more limited. Jaïs et al. successfully mapped 238/246 AT in a series of 128 patients undergoing ablation for AT, after a

previous AF ablation.[3] Importantly, there were multiple ATs in 77 patients. The mechanism was macroreentry in 109/238 (47%) and this was either CTI dependent, roof dependent or mitral isthmus dependent reentry (see Figure 1-3). Chae et al. also studied a large group of 78 patients undergoing ablation after AF ablation, and mapped multiple ATs in the patients.[82] Of 155 ATs, 73% were macroreentrant.*

Figure 1-3 illustrates the most common macroreentry circuits and the linear ablation lesions that are created to treat them.[87-91]

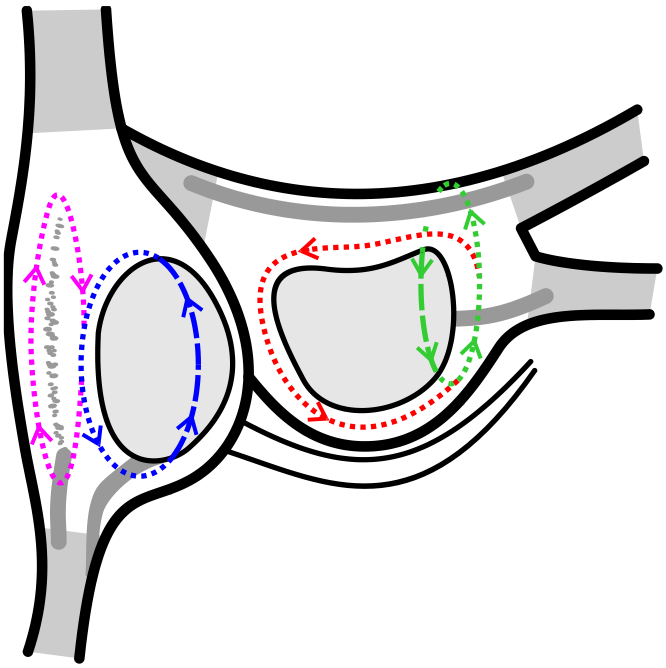

Figure 1-3. Some macroreentry circuits. Successful ablation for macroreentry requires the creation of an ablation line that 'cuts' the circuit by forming a line of electrical block between two inert structures – either a valve orifice or an electrically inert thoracic vein (depicted by grey). From left to right: **Magenta:** A circuit around a right atriotomy scar is usually disrupted by ablation from the scar to the electrically inert IVC (dark grey line). **Blue:** CTI dependent reentry is treated by creating an ablation line from the tricuspid annulus to the IVC. **Red:** Perimitral reentry is usually treated with ablation at the isthmus between the mitral annulus and the left inferior pulmonary vein, which must be isolated to create electrical block. **Green:** Roof dependent macroreentry (shown around the left pulmonary veins) can be prevented by an ablation line between the superior pulmonary veins.

* There is some inconsistency about which circuits are large enough to be called macroreentry rather than localized reentry. The convention is used here that macroreentry only occurs around a fixed (usually anatomical) obstruction to conduction.

1.2.6 Atrial tachycardia in the context of prior surgery

Cardiac surgery may involve the use of surgical incisions in the atria in order to access internal structures. For example, a lateral incision in the RA provides access to the interatrial septum for the surgical repair of atrial septal defects. A further incision in the atrial septum is also used as a standard approach to the mitral valve, following its introduction by Guiraudon,[92] (one of the pioneers in surgery for Wolff-Parkinson-White syndrome).

After surgery, the lines where these incisions are sutured back together remain inert (although conduction can sometimes recover to produce conducting channels through an old scar).[93] The non-conducting scar can provide a substrate for reentry and often these patients often have a dual-loop tachycardia: there are two macroreentrant circuits that coexist, with one circulating around the incisional scar and the other circulating around the tricuspid annulus. (See circuits 1 and 4 in Figure 1-3.) Frequently, these tachycardias can have an appearance similar to typical RA flutter on the surface ECG. However, ablation of the CTI is not sufficient to achieve arrhythmia termination because the CTI is not critical to the circuit that loops around the incisional scar. Therefore, an additional ablation line from the RA incision to IVC is often performed.[89, 94-97] Ablation results are better in those patients when this isthmus is short and has slow conduction velocities.[98]

There are many other forms of cardiac surgery that provide a substrate for arrhythmia. These are reviewed elsewhere.[12]

1.2.7 Overview of the substrate for atrial arrhythmia

It has been shown that focal tachycardias with triggered activity or enhanced automaticity can occur where there is minimal or no structural change. However, reentrant AT of all types occur in the presence of altered electrical properties, structural changes, or both. This explains the higher incidence of typical atrial flutter in older people and those with other forms of heart disease. Patients with prior cardiac surgery may develop AT around previous incision sites. In patients with prior AF ablation, the combination of altered underlying electrical properties, fibrosis, and changes caused by ablation itself all contribute to an increased susceptibility to

microreentry, localised reentry and macroreentry. These combine to increase the incidence of AT after AF ablation.

In all cases where ablation is considered for AT, then the electrophysiologist must be aware of the particular substrate in each individual patient because it is likely to have a significant impact upon the arrhythmia mechanism, and hence the mapping and ablation strategy. For focal tachycardias, ablation of the cardiac tissue at the location of the focal source results in arrhythmia termination. For localised reentry tachycardias, ablation must be performed over a slightly wider area in order to encompass and destroy the tissue responsible for arrhythmia. For macroreentrant arrhythmias, ablation must be used to prevent conduction around the circuit by creating an appropriate obstruction of inert tissue. Mapping is required to identify a critical isthmus by combining anatomical information with electrical information.

This thesis will seek to develop new methods for mapping AT. These will attempt to allow the electrophysiologist to relate the electrophysiological findings to possible mechanisms and to then plan an appropriate ablation strategy.

1.3 Activation mapping of atrial tachycardia

1.3.1 Introduction

In order to determine an ablation strategy for successful treatment of AT, the activation pattern and the mechanism of tachycardia must be ascertained. If reentry is the mechanism then this can only be proved by the use of another technique – entrainment – which is discussed in Section 1.4.

1.3.2 Surface electrical activity

Surface ECG

The surface ECG can be helpful in AT. In particular, the ECG appearance of typical (and also reverse typical) RA flutter is characteristic: the atrial rate is usually 240-360 beats per minute[99] and there is a 'saw tooth pattern'. In patients with no prior surgery or ablation, this appearance is specific for CTI dependent macroreentry. However, as described above, patients with an RA incisional scar can have double loop reentry despite similar ECG appearances. Additionally, patients with previous CTI ablation may also have an ECG with a similar appearance if activation originates to the septal side of

the CTI line and passes around the tricuspid annulus to the lateral RA: this is a similar activation pattern to flutter, but the mechanism of RA activation is passive and does not form a reentrant circuit.

For focal AT, P waves are usually separated by isoelectric intervals that are simultaneous in all ECG leads. A number of different ECG algorithms have been described for localizing the source of AT origin, and these assume normal atrial conduction.[100] In a comparatively large series, a proposed algorithm correctly identified the location of the focus in 93%.[15] However, the same data was used to develop and also to test the algorithm, which is likely to give an over-estimate of accuracy. Following AF ablation, attempts have been made to identify AT from the surface ECG, but these have been in the context of small amounts of LA ablation.[101] Establishing the mechanism and location of AT, from the ECG, in the presence of surgical incision scars, atrial ablation, or in the presence of abnormal atrial conduction is much more challenging and no accurate methods have been reported.[100, 102]

Electrocardiographic mapping

A surface ECG-based system has been used to map atrial tachycardias. This utilises recordings made from a large number (256) of surface electrodes all over the thorax.[103] The dispersion of the electric field from the epicardium to the skin surface is modelled (this is known as the 'forwards problems') with knowledge of the patients anatomy that has been obtained from a CT scan. An inverse solution (the 'backwards problem') is then found that estimates the epicardial electric potential.

The 'backwards problem' is mathematically ill-posed – the electric field tends to become 'smoothed' as it disperses through the body. Therefore, if the inverse problem is applied unconstrained to noisy electrical signals then this noise is amplified. Mathematical techniques such as Tikhonov regularisation must be used to constrain the solution and reduce the effects of recording errors.[104, 105]

The method was initially used to model ventricular activation.[106, 107] There was also a case report of a focal atrial tachycardia.[108] Recently, Shah et al. used a commercial system to evaluate AT in 52 patients undergoing an ablation procedure.[109] In 4 patients the AT changed during the procedure. In the other 48 patients, the

electrocardiographic mapping successfully identified the tachycardia mechanism in 44/48 (92%) patients.

The study by Shah et al. had a number of limitations.[109] In some patients with 2:1 atrioventricular conduction, the T wave obscured the P wave morphology. However, this could be overcome by mapping during changes in atrioventricular conduction induced by vagal manoeuvres or drugs. Many of the patients (18/48) had typical CTI dependent flutter, which usually does not present a diagnostic challenge from the 12-lead ECG. It is also not clear how many patients had low voltage regions of atrium: from a theoretical perspective areas of scar would be expected to give very low amplitude signals on the body surface. Nevertheless, the method provides promise for providing a much more accurate non-invasive assessment of atrial tachycardia than was previously possible.[110]

1.3.3 Invasive recordings of electrical activity

During ablation procedures, intracardiac catheters are used to record electrical signals. Typically, some catheters will be left stationary (for example, a catheter with multiple electrodes in the CS) and another catheter (the 'mapping' catheter) with fewer electrodes is moved around the atrium to explore the electrical signals at various locations. In this way, the timing of electrograms at different locations can be compared, using one of the stationary reference electrograms as a fiducial marker.

When recording an electrogram, the potential difference is measured between two electrodes. For *unipolar* electrograms, the potential difference is measured between the electrode of interest and a distant indifferent electrode. The indifferent electrode is often Wilson's central terminal but may also be an intravascular electrode that is positioned away from the heart. Wilson's central terminal is produced by connecting the limb leads (right arm, left arm, and left leg) together via a network of high impedance resistors.

For the majority of AT mapping, *bipolar* electrograms are used. These consist of the potential difference between a pair of electrodes on the same catheter and are usually recorded digitally with a sampling frequency of 1000Hz. The recording is affected most by tissue near to the electrode pair and so spatial resolution is improved by using narrowly spaced electrodes.[111] The most rapid changes in potential occur as

the depolarisation wavefront passes between the electrodes: in order to emphasise components of the signal that correspond to activation, the signals are band-pass filtered at 30-250Hz. (Frequencies above 250Hz are attenuated in order to reduce noise and avoid aliasing effects.)[112]

In normal homogeneous tissue, the first peak of the local bipolar electrogram is a good approximation to the activation time near to the electrode pair.[112] However, in other situations, local activation time can be more difficult to determine and the electrogram can also provide additional information about the underlying tissue activation. Figure 1-4 summarises some important electrogram characteristics that can provide clues to the electrophysiologist in the search for arrhythmia mechanism.

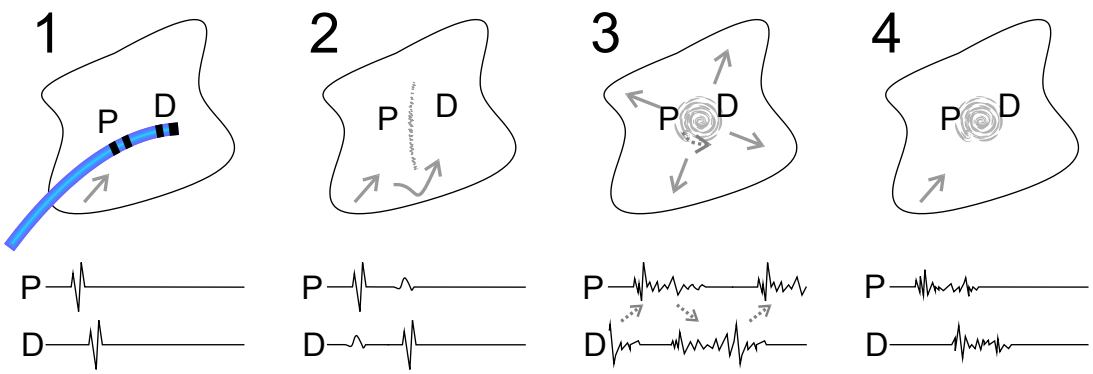

Figure 1-4. Some electrogram characteristics and their underlying mechanisms. 1) Normal conduction with corresponding bipolar electrograms recorded from 2 sites, for example the proximal (P) and distal (D) pairs of electrodes on a quadripolar catheter. 2) There is a line of slow conduction, such as might occur after a linear ablation lesion or after an atriotomy incision. This leads to double potentials, with an isoelectric period between them. At P, the first component is a normal electrogram and the second complex is a small far-field electrogram caused by activation on the other side of the line. At D, the first component is a far-field signal and the second component is normal. 3) In an area with localised reentry, the electrogram morphology will be of lower amplitude and appear fractionated. It is possible to record continuous activity – activity that spans the entire TCL. However, as shown in 4) this is not sufficient to prove that the area contains the tachycardia mechanism because passive activation can also create long fractionated signals.

The region of atrium influencing a pair of 2mm electrodes with 2mm separation is at least 6mm in diameter for a catheter lying parallel to the atrial tissue. (This is the distance from the end of one electrode to the end of the next.) Double potentials can

occur when electrical activity from both sides of a line of slow conduction, or conduction block, influence the potential difference between the recording electrodes. This can occur in normal atria, particularly at the crista terminalis[113, 114], or at the scar from previous incisions[96] or at the site of previous linear ablation lesions.[115] The time period between double potentials depends upon the conduction time to pass through the zone of slow conduction, or upon the time taken for activation to pass around the obstruction; whichever is shortest.

Double potentials occur where there is a relatively large, discrete barrier to conduction. However, patients with AT often have more subtle changes to electrical propagation. Where there are areas of fibrosis or heterogeneity in electrical conduction properties, the depolarisation wavefront can become less uniform.[116, 117] This gives rise to electrogram fractionation, which has been observed in simulation models of fibrosis[118], and during atrial pacing it is more marked in patients with paroxysmal AF than normal controls.[119] In addition to effects upon electrogram morphology, areas of scar also reduce amplitude because of a reduction in the amount of simultaneously conducting tissue in the vicinity of the recording electrodes. Electrode spacing also has an effect upon the electrograms that are recorded in areas of fractionation.[120]

Whilst mapping an AT, identification of electrograms that are fractionated or have double potentials is important. These characteristics indicate the presence of altered electrical conduction. As described above, this may be relevant to the tachycardia mechanism; for example, fractionation in a zone of localised reentry, or double potentials recorded at an incisional scar responsible for reentry. However, these electrogram characteristics can also occur at sites that are not part of the active tachycardia mechanism. As shown in Figure 1-4, fractionation can occur with passive activation of scarred tissue and double potentials can occur at lines of block in the absence of tachycardia. Therefore, in order to appreciate the significance of electrogram morphologies, they must be interpreted within the context of the activation sequence. This requires information about the positions where they were recorded.

Aside from the electrogram morphology, electrogram voltage is also altered in the presence of scarred tissue. This is due to altered velocity and dispersion of the

electrical wavefront as well as a reduced density of viable cardiac tissue in the vicinity of the recording electrode. Most evidence for this effect arises from studies of myocardial infarction in the ventricle and reports from atrial studies are limited.[121-125] Studies from our group indicate that the atrial bipolar peak-to-peak electrogram voltage in atrial tissue that has been scarred by ablation is less than 0.3mV, whereas normal atrial tissue is usually >2mV.[126] Previous investigators have used a bipolar peak-to-peak voltage of <0.05mV to indicate scar[124, 127] and <0.5mV to indicate 'low voltage',[124] although these thresholds appear to be arbitrary.

1.3.4 Assessing catheter position

X-ray guidance

X-ray guidance is the fundamental imaging modality for assessing the positions of intracardiac catheters. In order to navigate accurately and efficiently, the electrophysiologist is required to integrate the x-ray images with detailed anatomical knowledge and also electrogram recordings.[128] Ablation of accessory pathways and atrioventricular nodal reentry formed a large proportion of the cases performed around the world when catheter ablation was in its infancy. These tachycardias are ablated by placing a small number of ablation lesions at anatomically predictable sites. However, ablations for ventricular tachycardia and AF have increased in numbers. With this, there was a need for improved catheter localisation – both for mapping and also for documenting the positions of ablation sites. For treatment of these tachycardias, the ablation catheter may need to be positioned accurately anywhere in the cardiac chamber of interest. Ideally, a 3D mapping system should record the position of the catheters relative to other cardiac structures, accurately compensating for motion caused by respiration and cardiac contraction. Improved technology for this purpose became available in the late 1990s[129] and has led to a substantial reduction in patients' X-ray exposure.[130, 131]

Electromagnetic catheter location

This technology is primarily used in the Carto System (Biosense Webster, California, USA). Electromagnetic catheter location uses an attachment that is fixed to the operating table, with three separated electromagnets.[132, 133] Each electromagnet generates a magnetic field at a particular frequency. A purpose-built catheter is used

that has three small coils implanted in the tip with different orientations. The magnetic fields induce currents in these sensing coils, which are measured in order to calculate the distance to each electromagnet. The position of the catheter tip is then calculated by trilateration and the orientation of the catheter tip is also calculated. The position information from the catheter is gated with the ECG in order to reduce the effects of cardiac motion. Additionally, a reference patch is attached to the patients back and this can be used to detect and compensate for horizontal movement of the patient (but not rotation or rolling).

More recently, technology has been described to locate other catheters in the heart (aside from the catheter that contains induction coils) using an impedance-based method.[134] This utilises 3 skin patches attached to the front of the patient's chest, and 3 attached to their back. As the mapping catheter is moved around the heart, a small current is passed through it. It is then possible to calculate the impedance between the catheter and the six skin patches. Because the position of the mapping catheter is known (using electromagnetic catheter location), the relationship between position and impedance can be determined. This relationship is then used to calculate the position of other electrodes in the heart, after calculating their impedance between the skin patches.

Electric field based catheter location

With electric field based location, three pairs of electrodes are attached to the patient's skin and a small current is passed through them to create three high frequency electric fields.[135] A wide range of catheters can be used with the system, with up to 12 catheters or 64 electrodes at any one time. At each electrode, the potential from each of the 3 electric fields is recorded and then used to estimate the electrode position. It is assumed that the impedance of cardiac tissue and the blood pool is uniform. Due to the large and variable impedance of the lungs, this method can only be used to estimate catheter position relative to another catheter in the heart. Typically, the CS catheter is kept stationary and used for this purpose.

Defining the anatomy

The ability to track catheter position provides a means to establish the anatomical limits of catheter movement. All commercial systems provide for this. By dragging the

catheter around the cardiac surface, a shell is created to represent the chamber that is being studied. Computer software tracks all positions that have been reached and then applies an algorithm to overlay a shell upon these points. This can be manually edited in areas of anatomic complexity, and this is often necessary near the confluence of the left pulmonary veins and LAA.

The anatomical shell inferred from catheter movement around the atria tends to overestimate the true atrial volume.[136, 137] Additionally, the pulmonary vein ostial sizes are also overestimated but this can be improved by using respiratory compensation to correct for the movement of the heart that occurs with ventilation of the lungs.[138] It is also possible to merge anatomical information from CT or MRI scans[139, 140] and echocardiographic images[141], if this is available. Whilst this reduces the X-ray exposure it probably does not improve acute outcomes.[142, 143]

1.3.5 Integrating electrical activity with anatomical information

General principles

The goal of activation mapping is to combine electrogram information from multiple locations, in order to deduce the pattern of activation across the cardiac surface and to guide decisions about the likely tachycardia mechanism and appropriate ablation strategy. At its simplest, this involves comparing the electrograms at two locations that are in close proximity. The local activation time of each of the electrograms is assessed. It can then be inferred that direction of activation passes from the earliest site towards the later site.

When a mapping catheter is used, reference catheters are helpful because the mapping catheter can only sample electrograms from one site at a time. Often one of the electrode pairs on the CS catheter is used as a reference. In this situation, at the first mapping site, activation is compared to the CS. The mapping catheter is then moved a small distance and activation is compared to the CS again. This will give an indication of the direction of activation. When electrograms from multiple locations are sampled then a more accurate indication of wavefront propagation can be estimated.

Inferring the direction of activation in healthy tissue is relatively straightforward. However, when conduction is not uniform then more care must be taken. In particular,

where there is abnormal conduction the sequence of activation may not be so clear. For example, if there is a long delay between electrograms at two sites in the presence of a focal tachycardia then the order of activation depends upon correctly identifying electrograms from the same wavefront, rather than wavefronts from different beats.

Isochronal maps

To create an isochronal map, electrograms are recorded at different locations across the cardiac surface. Using the electrogram at each location, an LAT is assigned - this is the relative timing of activation compared to the reference. The representation of the cardiac surface is then coloured according to LAT so that points that have the same colour are activated at the same time (i.e. they are isochronal).[144] See Figure 1-5.

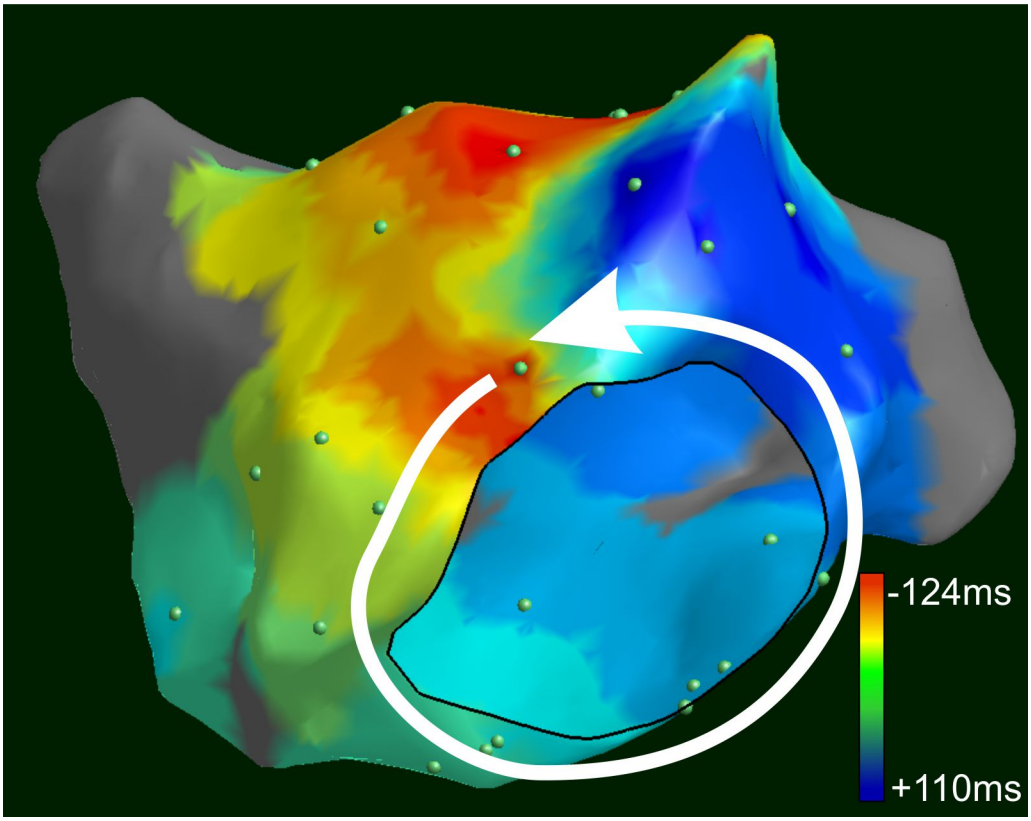

Figure 1-5. An isochronal map of the left atrium. Colours from red-green-blue correspond to timing that gets later. The white arrow indicates the direction of activation around the mitral valve. In this case, the diagnosis was perimitral reentry. The time taken to get from red to dark blue is similar to the tachycardia cycle length, i.e. the whole tachycardia cycle length has been mapped. Further methods for establishing macroreentry as the mechanism are discussed in the text.

Successful creation and interpretation of isochronal maps involves a number of steps:[144]

1) Each electrogram must be representative. This requires good catheter contact and stability. Recordings during ectopy must be discarded. This requires careful attention by the operators.[145]
2) Activation patterns should only be interpreted where there is a sufficient density of points.[145] The creation of an isochronal map involves colouring the anatomical shell beyond the locations where electrograms were recorded. This is done by interpolation. The extent of the interpolation can be set by the user in commercially available systems. However, the user must be cautious in using this interpolated data because it may not be a true reflection of underlying activation. One of the difficulties with creating a dense map is that hundreds of points must be acquired; whilst this improves map quality, it requires a significant amount of time to perform with a mapping catheter that only acquires one point at a time. This can be overcome by using catheters with multiple mapping electrodes.[86] However, a semi-automated method for annotating the LAT is required because so many electrograms are collected in a short space of time.
3) LAT must be assigned appropriately: this requires the appropriate electrogram complex to be identified, and also to the correct LAT assignment within that complex. This is discussed below.

Isochronal maps – the window of interest and LAT assignment

In a repetitive tachycardia, when an electrogram is recorded then there is a repeating sequence of electrogram complexes. One of these must be used to make measurements of LAT. This is done by selecting the LAT that falls within a window of interest, which has been chosen with a fixed time relative to the reference electrogram. The purpose of the window of interest is to ensure that electrogram complexes from the same beat of tachycardia are compared. Thus, for a focal tachycardia, the window should span a single activation of the chamber.[146, 147]

For a macroreentrant tachycardia, there is always activation within some part of the reentry circuit. Therefore, the window of interest covers one cycle of the

tachycardia. Some authors advocate using the P wave to set the window of interest, so that the start and end of the window correspond to the LAT where activation passes through a slowly conducting isthmus.[148, 149] However, this does not appear to have been widely adopted, in part due to problems identifying the P wave in AT.

Another difficulty with LAT assignment is that electrograms may have double potentials or fractionated signals, as discussed in Section 1.3.3. These signals often have particular significance because they give information about the underlying atrial substrate that may be relevant to the tachycardia mechanism. By reducing the displayed data to LAT alone, important information may be lost.

1.3.6 Interpreting activation

Relationship of activation to mechanism

After AF ablation, almost all macroreentrant tachycardias are either CTI dependent, roof dependent or perimitral reentry (see Figure 1-3).[150] Activation for these tachycardias involves reciprocal activation on opposite sides of the relevant atrium.[3] For example, in clockwise perimitral reentry, activation of the anterior portion of the LA is septal-to-lateral whereas activation of the inferior portion is lateral-to-septal. If activation of opposite sides of a reentrant circuit is in the same direction then this eliminates this mechanism from the differential diagnosis.

For a macroreentrant tachycardia, whilst passing around the circuit the LAT should change by one cycle length (see Figure 1-5). From any point on the circuit, it is possible to make a small movement which results in a slightly earlier LAT (as long as the electrogram complexes with the smallest change in activation time are chosen). By contrast, for a focal tachycardia, when a mapping catheter is placed over the source then movement in any direction will result in a later LAT.

On an isochronal map, macroreentry circuits present themselves in a similar way. For any potential circuit, the change in LAT around the circuit summates to one TCL. Therefore, there is a gradual change in colour from ‘early’ to ‘late’ whilst following the path of the circuit until the point where ‘late meets early’. It is important that the whole tachycardia cycle length is accounted for around the circuit of interest. For focal tachycardias, the isochronal maps show an area of early activation with LAT becoming later in a centrifugal pattern.

As discussed in Section 1.3.3, in localised entry tachycardias there is centrifugal activation of the atria away from the small area containing the active tachycardia mechanism. Within the localised reentry circuit, there are usually low-amplitude fractionated electrograms, to which it is often difficult to assign an LAT with confidence.

1.3.7 Key Issues - activation mapping

Activation mapping involves reconstruction of the activation pattern from the sequential collection of electrograms at different positions around the cardiac chamber. At the start of the chapter, tachycardia mechanisms were discussed and the importance of arrhythmia substrate was highlighted. In a patient with AT the prior information about heart structure and previous procedures is vital. As the electrograms are collected the activation pattern is constructed and interpreted within this context. However, the electrogram morphology also provides important clues about the underlying tissue's electrical properties.

Isochronal maps are the current gold standard for mapping AT. Creating an isochronal map that represents underlying activation requires 2 key steps: a tachycardia window must be chosen and the appropriate LAT for each electrogram must be selected. The resulting map only displays a small fraction of the information that may be relevant to the diagnosis. All electrogram characteristics (such as amplitude, fractionation, and double potentials) are lost in the process of reducing each waveform to a single corresponding activation time. As described above, these electrogram characteristics may be important in deducing the tachycardia mechanism. An additional source of error is that isochronal maps involve interpolation of LAT across the cardiac surface. This can be particularly problematic in the presence of LAT errors – because their influence is interpolated across the surface.[127]

The work presented later in this thesis will seek to address the problems relating to: the window of interest, assignment of local activation time, and interpolation of information across the cardiac geometry.

1.4 Entrainment

1.4.1 Background

Despite the fact that typical flutter is common, proof for the mechanism only emerged in the 1970s. Canine models of atrial flutter were consistent with macroreentry[151] and, in humans, the activation pattern had been described.[152] However, the activation pattern is not proof of reentry: a focal tachycardia next to the CTI with functional conduction block in the CTI could give the same pattern of activation.

Waldo and colleagues studied atrial flutter in patients with atrial flutter shortly after cardiac surgery.[153] Their primary interest was to investigate the use of pacing manoeuvres for terminating the arrhythmia. They used overdrive pacing – pacing at a constant rate slightly faster than the rate of tachycardia. The significance of their observations was not recognised at the time. The authors later recognised that the ECG changes that they had noted provided strong proof for reentry. Over the following decade these observations, and others, were combined to form 4 criteria for transient entrainment.

The key principle for entrainment is that part of the overdrive pacing wavefront travels antidromic to the tachycardia and collides with the tachycardia wavefront, whereas another part of the pacing wavefront travels orthodromically and reinitiates another cycle of tachycardia.[154] This continual antidromic collision and orthodromic reset is illustrated in Figure 1-6.

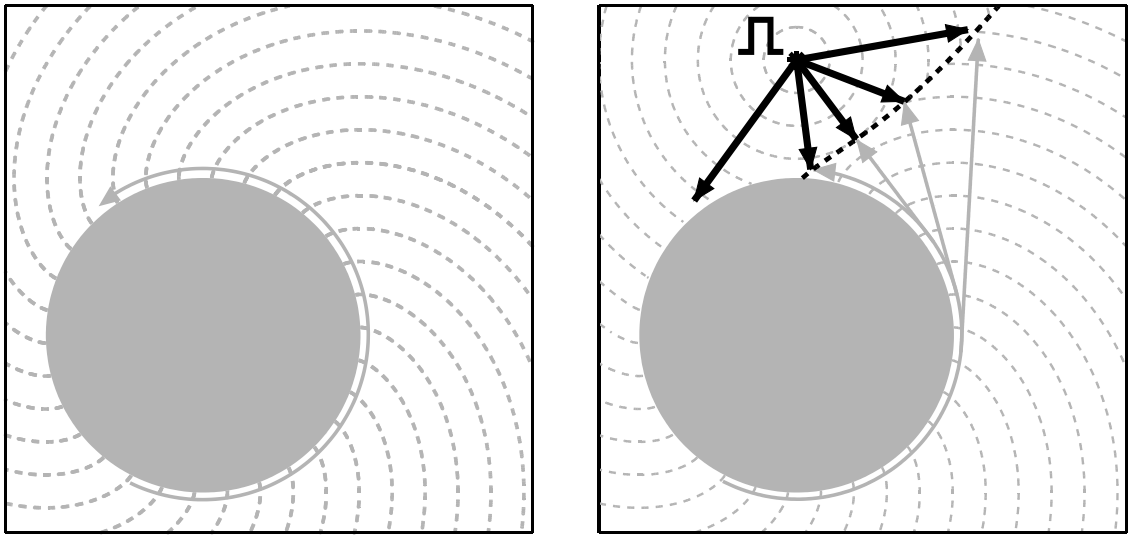

Figure 1-6. Left Panel. A schematic diagram shows reentry around a fixed anatomical obstruction (solid grey circle). Isochrones are shown as dashed-grey lines and are perpendicular to the direction of wavefront propagation. The solid grey arrow shows the shortest path around the obstruction – the 'tachycardia circuit'; the time taken to complete one loop is the 'tachycardia cycle length' (TCL). There is a gap in the arrow to indicate the excitable gap. **Right Panel.** During overdrive pacing, the paced activation (solid black arrows) travels i) antidromically to collide with the tachycardia wavefront (dashed black line), and ii) orthodromically to reset the tachycardia (leftward black arrow). This requires an excitable gap, such that pacing can excite the tissue before arrival of the tachycardia wavefront.

1.4.2 Criteria for entrainment

Despite attempts to introduce alternatives, the main criteria for entrainment have not changed for over 2 decades.[155] The criteria for entrainment prove the presence of reentry. They are presented in Table 1-2, with initial explanation given in the following figure (Figure 1-7).

		Criteria for Entrainment
ECG criteria	1	During overdrive pacing that fails to interrupt tachycardia, the demonstration of constant fusion beats in the electrocardiogram, except for the last captured beat, which is not fused.
	2	During overdrive pacing at two rates that fail to interrupt tachycardia, the demonstration of constant fusion beats of the ECG at each rate, but different degrees of constant fusion at each rate (progressive fusion).
Electrogram criteria	3	During overdrive pacing that interrupts the tachycardia, the demonstration of localised conduction block to a site(s) for 1 beat followed by activation of that site(s) by the next paced beat from a different direction and with a shorter conduction time.
	4	During overdrive pacing at two rates that fail to interrupt tachycardia, the demonstration of a change in conduction time to and electrogram morphology at an electrogram recording site.

Definition of **overdrive pacing**:
During tachycardia, pacing at a constant rate that is faster than the rate of spontaneous tachycardia.

Table 1-2. Criteria for transient entrainment. Adapted from Henthorn et al.[156]

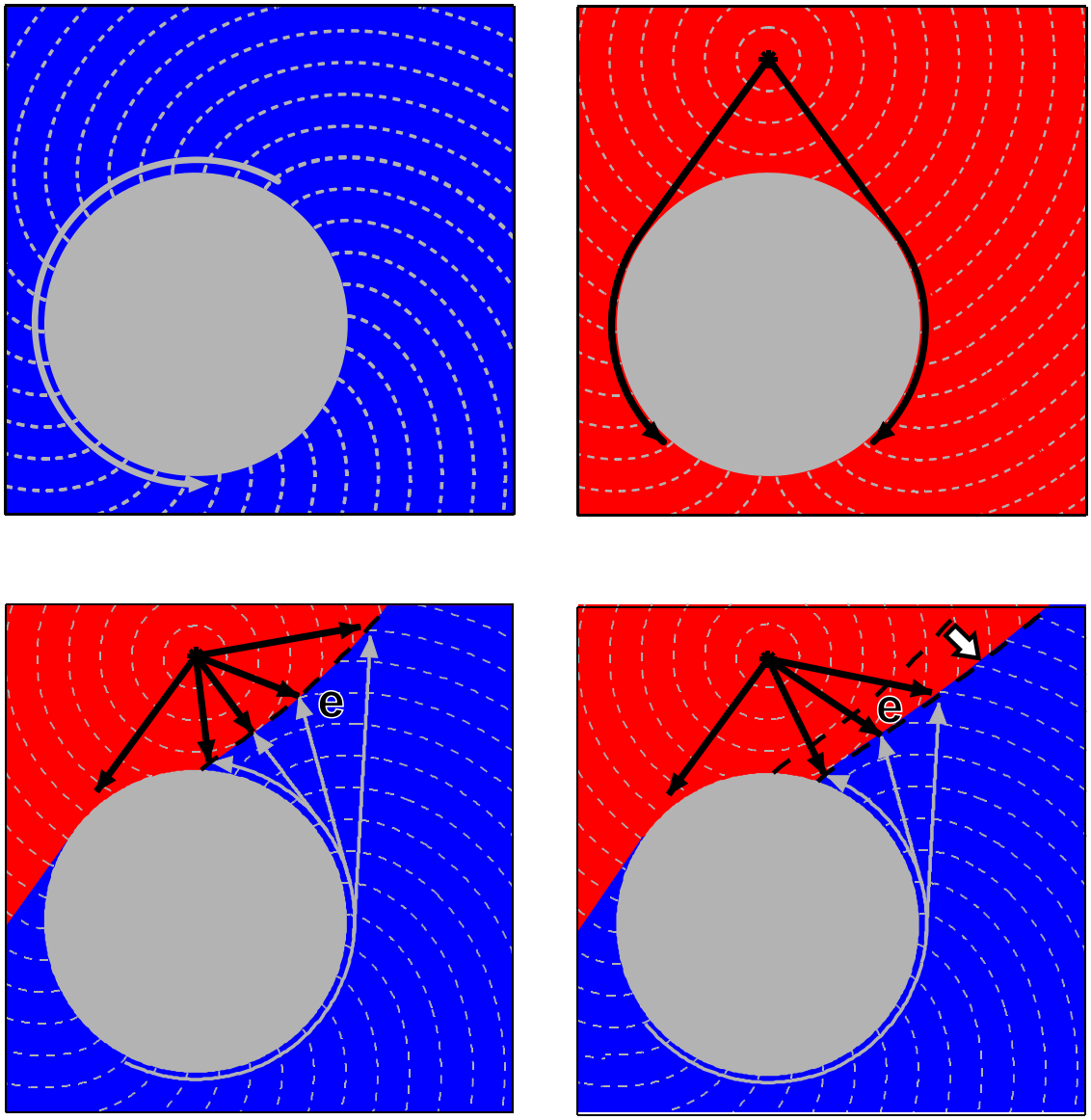

Figure 1-7. The same anatomical obstruction is shown, as in Figure 1-6. **Upper Left Panel.** Tachycardia is illustrated again, this sequence is indicated with blue. **Upper Right Panel.** During pacing, in the absence of tachycardia, the activation sequence is different. This is indicated with red. **Lower Left Panel.** During overdrive pacing, the chamber's activation pattern is partly similar to pacing (red) and partly similar to tachycardia (blue). The surface ECG morphology is therefore neither the pacing morphology nor the tachycardia morphology, but it is a fusion between the two (cf. 1st criterion of entrainment). At the site marked 'e', there is a long stimulus-to-electrogram time because activation must pass orthodromically around the circuit. However, if tachycardia terminates during pacing then the entire activation pattern will revert to the paced pattern (Upper Right Panel), and the stimulus-to-electrogram time will shorten (cf. 3rd criterion of entrainment). **Lower Right Panel.** This shows the effect of increasing the pacing rate. The antidromic penetration of the circuit has increased (thick arrow). This has resulted in a change in the degree of fusion between the pacing (red) and tachycardia (blue) activation patterns (cf. 2nd criterion of entrainment). At the site marked 'e', there is a shorter stimulus-to-electrogram time in comparison with the Lower Left Panel (cf. 4th criterion of entrainment).

The criteria for entrainment cannot be observed for focal tachycardias. During overdrive pacing of a focal tachycardia, the entire activation pattern is the same as for pacing in the absence of tachycardia. Theoretically, some degree of fusion could occur if an automatic tachycardia was accelerated by overdrive pacing. However, it is implausible that overdrive pacing could accelerate a focal tachycardia to the pacing rate and for it to remain constant (as required by the entrainment criteria).

Demonstration of any of the entrainment criteria is evidence for reentry. However, they are not always sensitive methods for detecting the tachycardia mechanism. For example, if the pacing site is near to a slowly conducting isthmus then the antidromic pacing wavefront may not have a significant effect upon the ECG. Therefore, although there is acceleration of the rate, the morphology is the same as in tachycardia. This is known as 'entrainment with concealed fusion' (i.e. fusion is presumed to occur but is not detectable).[157]

In the case of a microreentry tachycardia, the tachycardia circuit exists within a very small area of diseased tissue (Section 1.2.2). Theoretically, overdrive pacing will entrain the tachycardia but the fusion will be confined to the small area within which the tachycardia mechanism is confined. Therefore, the surface ECG will have the same appearance as during pacing in the absence of tachycardia. This is called 'concealed entrainment' by some authors[158, 159] (but the term is used interchangeably with 'entrainment with concealed fusion' by others).

1.4.3 Application of entrainment criteria to atrial arrhythmias

Entrainment has become a fundamental technique in electrophysiology.[160] For VT, the surface ECG and the relationship between the surface QRS complex and recorded electrograms is particularly important.[161] In scar-related VT, there is a zone of slow conduction and the onset of the QRS complex is associated with activation exiting this site. The appropriate site for ablation is dependent upon the detailed electrical substrate of the underlying scar and entrainment is critical in identifying this.

In macroreentrant AT, the use of the ECG is hampered by the low voltage of the P wave, particularly in atria with extensive scar. Even in patients with typical flutter and without any prior surgery or ablation, the sensitivity and specificity of concealed entrainment for detecting entrainment from the CTI are limited.[162] An additional

problem is interference with the P wave by the QRS-T components of the ECG. Therefore, the surface ECG is only routinely used when assessing entrainment manoeuvres during AT by some groups[163], but not others.[3, 69]

The 3rd and 4th entrainment criteria do not require use of the surface ECG. However, the 3rd criterion can only be observed when tachycardia terminates. In the context of ablation for AT, this is undesirable because further assessment of the tachycardia can only be performed if the same tachycardia can be re-induced. The 4th criterion of entrainment is most easily observed when multipolar catheters are placed around a tachycardia circuit.[164] However, this is not practical for many reentrant circuits. One goal of this thesis is to re-evaluate the principals underlying the criteria of entrainment to see if they can be re-synthesised into a more practical criterion for use during ablation procedures.

Currently, the most commonly used parameter after entrainment is the post-pacing interval.

1.4.4 Post-pacing interval

During entrainment, the orthodromic pacing wavefront resets the tachycardia and travels around the tachycardia circuit until it collides with the antidromic wavefront from the next paced beat (see Figure 1-6). If pacing has ceased, then there is no collision. Instead the paced wavefront continues around the circuit and also passes back to the pacing site. The time from the last paced atrial capture to the arrival of the next activation wavefront is the PPI. Therefore, at the pacing site the PPI is the time taken for paced wavefront to pass orthodromically around the tachycardia circuit and return to the pacing position.

In patients with VT, it was realised that the PPI gave important information about the position of the pacing site with respect to the tachycardia circuit.[161] Following this, analysis of PPI was applied to atrial macroreentry circuits.[158, 164, 165] If the pacing site is within the tachycardia circuit, then the shortest route that passes orthodromically around the circuit and back to the pacing site is the same as the tachycardia circuit: theoretically, the PPI is equal to one TCL. In Figure 1-6 the pacing site is not within the tachycardia circuit, and so the PPI would be greater than the TCL.

In reality, it is an assumption that PPI is equal to TCL for pacing sites within the tachycardia circuit. This assumption is only met if conduction is stable and unaffected by overdrive pacing. Often, atrial macroreentry circuits have an isthmus with relatively slow conduction. For typical flutter, this is located at the CTI.[166-168] Cosio et al.[164] studied conduction delay in 6 patients with typical flutter. Changes in conduction were dependent upon the rate of overdrive pacing, with faster rates causing greater conduction delay. When pacing with a CL equal to 20ms less than TCL, these delays did not exceed 30ms. Therefore, when choosing pacing rates, they must be fast enough to identify a difference in the pacing rate from the tachycardia rate. However, at faster rates the risk of conduction disturbance increases: this can change electrogram timings and can also change the tachycardia.

In this thesis, the methods are developed to detect macroreentry and also to obtain further information from the PPI (at the pacing site as well as remote catheters). The issues of decremental conduction are relevant and ideally should not have a significant effect upon their robustness.

Post-pacing interval for focal tachycardia

The development of entrainment methods, for AT, was based upon macroreentrant tachycardias. In these tachycardias it is possible to observe the entrainment criteria for reentry. For focal tachycardias it is not possible to observe constant, progressive, or concealed entrainment. However, as discussed in Section 1.2, some focal tachycardias do not appear to be interrupted by overdrive pacing and it was assumed that the mechanism in these cases was microreentry.[9]

More recently, the use of overdrive pacing for focal tachycardias was re-examined. Mohamed et al. studied 9 patients with AT and also performed measurements in 15 controls with sinus rhythm.[169] They used the scheme in Figure 1-8 to discuss their results. They found that the PPI did correspond to the distance from the tachycardia focus. The location of the focus was identified with activation mapping, and later confirmed by termination of tachycardia with ablation at that site. At the site of the focus in patients with AT, PPI-TCL ranged from 0-19ms. In patients with sinus rhythm, the PPI at the site of earliest atrial activation varied from 81-222ms.

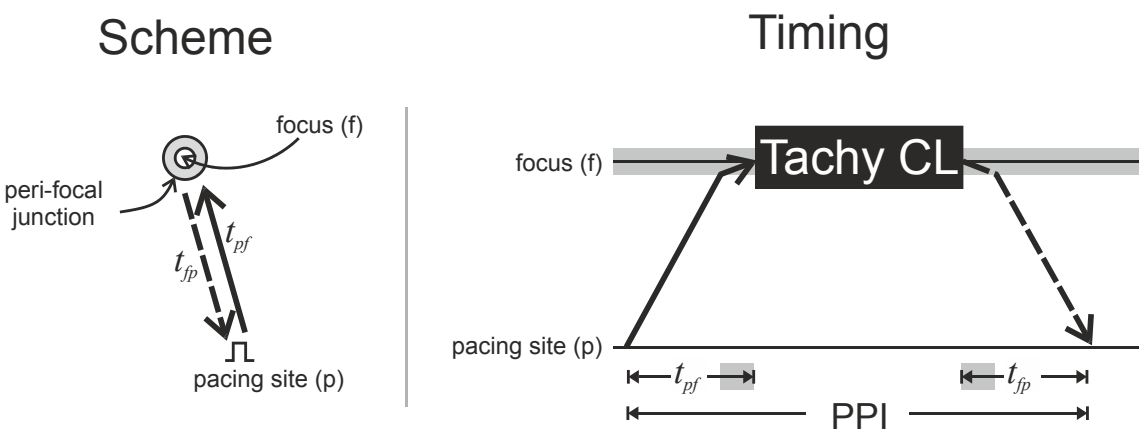

Figure 1-8. Left Panel. A schematic diagram shows the events after overdrive pacing with a focal tachycardia, adapted from Mohamed el al.[169] The last paced beat travels to the peri-focal junction, an area of slow conduction that is represented by grey shading. It then reaches the focus and resets the tachycardia. After one TCL, the focus fires and the wavefront must then exit the peri-focal junction before traversing the atrium back to the pacing site. For the sinus node, the time taken to traverse the 'peri-focal junction' is actually the sino-atrial conduction time.

Of the 8 ATs in this study[169], only 2 were classified as automatic on the basis of 'warm-up' and 'cool-down' phenomena in response to isoproterenol. This may partly due to the exclusion of patients where the atrial cycle length varied by more than 35ms. The study supports the use of PPI-TCL to give an indication of proximity to a focus. However, it is possible that PPI-TCL may underestimate the proximity if there is a long transit time at the peri-focal junction.

Post-pacing interval integrated into mapping

Miyazaki et al. developed a systematic approach to the use of entrainment for localizing AT.[170] Patients were only included if the cycle length variability was <20ms, if activation mapping was consistent with macroreentry, and if ablation successfully terminated the arrhythmia. They developed their algorithm using data from 90 patients and then applied it to a further 90 patients for prospective testing. Using a pre-determined strategy, the approximate location of the tachycardia could be identified with 2 or 3 manoeuvres in 93% of cases.

The algorithm by Miyazaki et al.[170] has not been evaluated for patients with localised reentry or focal AT. Additionally, one of the concerns about overdrive pacing

is that it can result in tachycardia modification or termination.[3, 93] For this reason, it is generally recommended to perform activation mapping before a limited number of entrainment manoeuvres.[3, 82, 86] This usually consists of identification of the potential macroreentry circuit by activation mapping and then using this information to guide the choice of entrainment manoeuvres. This can minimise the number of manoeuvres that are performed. After finding that activation is consistent with macroreentry, one group performs overdrive manoeuvres at two opposite segments of the proposed circuit; if the value of PPI-TCL is less than 30ms then this supports the diagnosis.[3]

Another use of PPI is to create complete electroanatomical maps, with colour coding according to the PPI-TCL at multiple locations around the atria. One group has used this approach in order to inform their ablation strategy.[171] This gave very accurate delineation of the active tachycardia circuit. However, the number of pacing manoeuvres was high (14-77 per patient) and the time taken for PPI mapping was long (12-200 minutes per tachycardia). This limits the practicality of the method and also restricts its use to very stable tachycardias.

Other investigators have used multiple entrainment manoeuvres combined with electroanatomical mapping.[25] By colour coding the electroanatomic map according to the PPI measured at each site (instead of the LAT), the regions of atrium with a PPI that closely approximates the TCL can be visualised. These have helped to clarify the activation pattern of typical right atrial flutter, revealing that there may be two active circuits in the RA – double loop reentry.

1.4.5 Double loop reentry

A PPI electroanatomical map from a patient with typical flutter is shown in Figure 1-9. It shows that there are two circuits that can be identified by short PPIs. One runs anteriorly, adjacent to the tricuspid annulus, and the other runs posterior to the SVC. These investigators found that the exact circuit(s) in patients with typical flutter is variable, although the cavotricuspid isthmus was a critical part of the circuit in all patients.

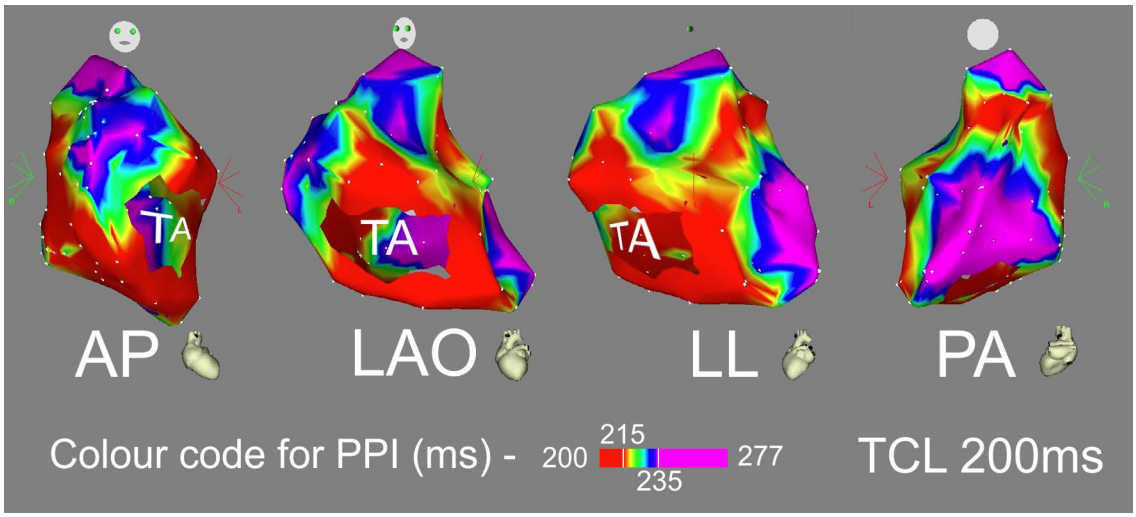

Figure 1-9. An RA PPI map in a patient with typical flutter (TCL 200ms), from Santucci et al.[25] The surface is coloured according to the PPI measured at each location. Red indicates areas with PPI<215ms and magenta indicates PPI>235ms (see colour bar at bottom). Four views are shown (AP – antero-posterior, LAO – left anterior oblique, LL – left lateral, PA – postero-anterior). There are 2 circuits with PPI<215ms. Both circuits share a common isthmus before separating (see LL) into: an anterior circuit around the tricuspid valve annulus and another coursing posterior to the SVC.

Fujiki et al. also studied entrainment manoeuvres in patients with typical flutter.[172] They performed fewer entrainment manoeuvres but they tracked activation with multipolar basket catheters. When pacing a circuit separately (i.e. not at the common isthmus) they identified 'paradoxical delayed capture' of the other circuit. For example, if they entrained from the top of the posterior circuit then the pacing wavefront had to pass through the common isthmus and also around the anterior circuit before activating the lateral anterior tricuspid annulus.

In addition to studying typical flutter, Fujiki's group also used similar methods to identify double loop reentry in patients with previous cardiac surgery. Although the principle appears to be sound, it does require the use of a basket catheter (a multipolar catheter that can gather electrodes from the entire atrium). It is more common to perform electroanatomical activation mapping with a limited number of entrainment manoeuvres.[94, 173]

1.4.6 Use of information from remote catheters

When overdrive pacing is performed from a location that is outside a reentrant circuit, then the PPI will be greater than the TCL. There has only been one investigation in which the distance to the macroreentrant circuit has been related to the PPI. In this study, mathematical equations were developed assuming a uniformly conducting two-dimensional sheet of conducting tissue, but not validated with electroanatomical mapping in animals or humans.[174] This issue will be further examined in this thesis in order to make stronger inferences about the tachycardia from the results of overdrive pacing manoeuvres.

When overdrive pacing is performed, the response at the pacing electrodes is usually analysed. The electrograms recorded from other sites are only used to help ensure that the tachycardia activation pattern has not changed. One study devised a scheme in which the timings at other electrode sites can be used more rigorously. The feasibility of using remote electrograms to estimate the PPI at the pacing electrode, when the electrogram is obscured by pacing artefacts, was demonstrated.[175] There are no studies that systematically explore the activation of remote catheters after entrainment, with respect to chamber geometry and tachycardia mechanism. This will be addressed further in Chapters 5 and 6.

1.4.7 Key issues – entrainment mapping

The development of entrainment was initially aimed at using pacing techniques to terminate atrial flutter. However, entrainment became a vital tool for the elucidation of macroreentry as the mechanism for flutter. Entrainment criteria were described that, if present, prove reentry. The use of entrainment was disseminated to other tachycardias: its development as a diagnostic tool for the invasive mapping of VT led to the PPI being used as a qualitative surrogate for ‘distance from the circuit’.

Entrainment continued to be used as a research tool, and this led to further characterisation of atrial flutter as well as accurate descriptions of double-loop circuits in patients with previous cardiac surgery. However, detailed PPI maps are impractical for most clinical situations – they take too long to create and the use of multiple manoeuvres risks altering the tachycardia. Therefore, the basis for most clinical diagnosis remains the use of a few PPIs to confirm a mechanism that has been

hypothesised on the basis of activation mapping. The established entrainment criteria are often difficult to apply to AT because the surface P wave is often too indistinct to provide clear evidence of fusion, and the electrogram-based criteria require electrograms to be recorded from specific locations. There are no existing entrainment criteria to detect double loop reentry.

If PPI information does not confirm the expected diagnosis then there is little previous work to indicate how this information can be integrated into a diagnostic strategy. There has not been an attempt to quantify the relationship between PPI and the distance from the tachycardia mechanisms. Additionally, the information from other catheters in the heart is not generally used. Despite some enthusiasm for using computational techniques to integrate the information from entrainment manoeuvres,[176] further research has not been forthcoming.

In this thesis, the analysis of electrogram information from overdrive manoeuvres will be reassessed. In particular, this will involve improved methods for detecting macroreentry and also improved methods for analysing the PPI.

1.5 Aims for this thesis

In this chapter, the mechanisms of atrial tachycardia were reviewed and then the current methods for performing activation mapping and entrainment mapping were examined. These enabled the identification of key issues that form the basis for the aims of the thesis.

1.5.1 Aims for activation mapping

A1 Design a new method for activation mapping that does not require a user-chosen window of interest.

A2 Avoid the need for local activation time assignment.

A3 Enable the display of electrogram characteristics, such as fractionation or double potentials.

A4 Create a prototype for analysis of clinical cases.

1.5.2 Aims for entrainment mapping

E1 Re-assess the criteria for entrainment to see if the principles can be reformulated into a method that is practical for use during AT procedures.

E2 Re-assess the criteria for entrainment, with a view to detecting double-loop reentry.

E3 Investigate the theoretical relationship between PPI and the trans-atrial distance from the tachycardia mechanism.

E4 Investigate the theoretical response to overdrive pacing for different tachycardia mechanisms, with respect to the PPI.

E5 Investigate the theoretical response to overdrive pacing for different tachycardia mechanisms, with respect to the response at electrodes distant from the pacing site.

E6 Integrate the theoretical findings from above into a clinical prototype for testing with patients.

2 Methods

2.1 Introduction

All aspects of this thesis involve the integration of mathematical and computing methods for assisting with the diagnosis of atrial tachycardia. In the first parts of this chapter, the methods used for collecting clinical data are discussed. Following this, some of the software methods are described. The purpose of the research was to use software as a tool, rather than to develop improved software techniques. Therefore, the methods for writing and testing software are kept to a minimum.

2.2 Patient studies

2.2.1 Patient setup, electrogram recording, Carto setup

All clinical procedures were performed in a clinical laboratory routinely used for electrophysiology procedures. Patients were monitored according to local protocols. Electrical signals were recorded using the LabSystem Pro Recording System (Bard Electrophysiology, Massachusetts, USA) and these typically included a 12-lead surface ECG as well as electrograms from intracardiac catheters. Surface ECG signals were filtered using a band-pass filter with cut-off frequencies set to 0.05Hz and 25 Hz. Bipolar intracardiac electrograms were also filtered with a band-pass filter but the passband was set at 30Hz to 500Hz. All signals were then digitised with a sample frequency of 1000Hz and stored.

A decapolar catheter was placed into the CS, using an SL3 sheath if necessary. For cases where connection of the pulmonary veins would require assessment, a circular mapping catheter was also used (Lasso Catheter, Biosense Webster, California, USA). The ablation catheter was selected according to the characteristics of the case.

For patients undergoing electroanatomic mapping, the Carto3 System was used (Biosense Webster, California, USA). The electromagnets were fixed to the operating table and skin patches attached to the patient, according to manufacturer instructions (see “Electromagnetic catheter location” on p27 for further information). A Navistar Thermocool ablation catheter (Biosense Webster, California, USA) was used for mapping.

In patients requiring LA access, a trans-oesophageal echocardiogram was performed in order to exclude thrombus in the left atrial appendage. This was

performed during the procedure, if general anaesthesia was used, or within 24 hours prior to the procedure otherwise. A transseptal puncture was performed if a patent foramen ovale was not present. This was accomplished using an SRO pre-shaped sheath and a BRK needle (St Jude Medical, Minnesota, USA) using fluoroscopic guidance and trans-oesophageal echocardiography if available. Immediately after access to the LA, heparin was given to achieve an activated clotting time of approximately 300s.

2.2.2 Creating isochronal maps for atrial tachycardia cases

If there was uncertainty about the location of the tachycardia mechanism, then RA activation was mapped and LA mapping was only performed if mapping indicated that an LA mechanism was likely. For all cases, one of the bipoles from the decapolar CS catheter was selected with a reproducible sharp atrial component to the electrogram. Selection of a window-of-interest was left to operator discretion. Generally, our approach is to gather information from an area of healthy myocardium first, as close as possible to the atrial timing reference, where the electrograms have unambiguous LAT. Mapping then proceeds with small movements around the atrial surface. The mapped area is gradually expanded, endeavouring to avoid crossing the edge of the window-of-interest or entering areas with abnormal electrograms where the LAT is unclear.

After this, the remaining areas of the surface are mapped and the electrograms are interpreted with knowledge of the likely tachycardia mechanism and activation of the previously mapped areas. For assignment of the LAT, the first peak of the near-field electrogram was assigned. In healthy tissue this is usually unambiguous. In the case of double potentials, the catheter was moved slightly so that one component was larger, and then this was annotated. This is similar to the approach of other investigators.[177]

2.2.3 Performing overdrive pacing

In order to perform overdrive pacing, the TCL was measured using the EP recording system. The desired catheter was then electronically connected to the stimulator and pacing was performed with a CL 10-30ms shorter than TCL. When electrograms recorded from electrodes distant to the pacing catheter were observed to have advanced their CL to the paced CL, then pacing was terminated.

In order to improve analysis of overdrive pacing manoeuvres, software was written to assist with the process. Figure 2-1 shows the GUI for electrogram annotation. This was implemented using Matlab (Mathworks, Massachusetts, USA). It allows the user to annotate the activation from each electrogram and see the corresponding cycle lengths plotted on the same interface, for a visual assessment. Once this has been done, then the activation time data is analysed.

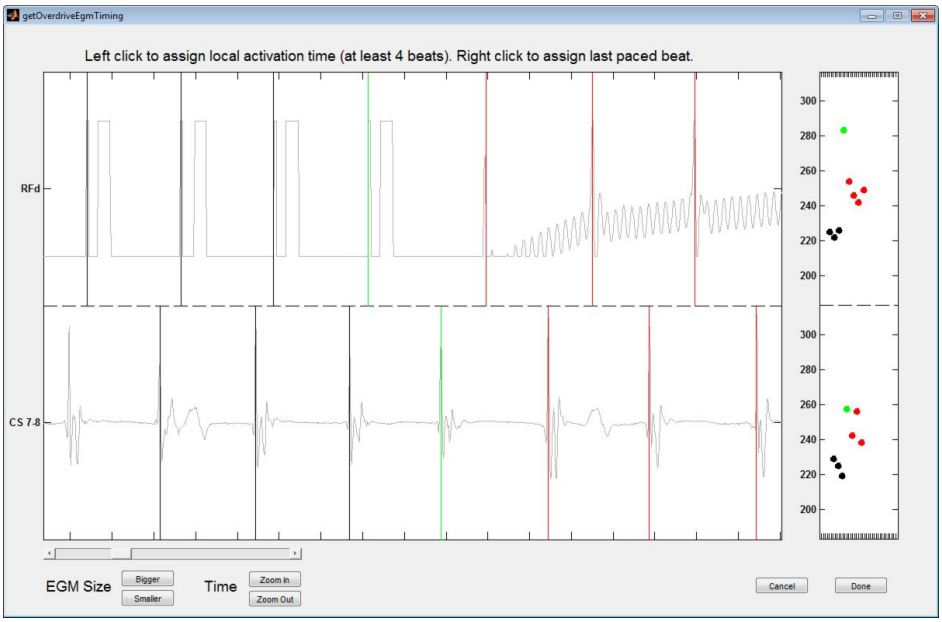

Figure 2-1. GUI for annotating electrograms. After an AOP, the electrogram data is imported from the Bard recording system. The user annotates the activation time from each electrogram and indicates the last pacing stimulus (green vertical line). The black vertical lines correspond to the previous paced beats, and the red vertical lines correspond to tachycardia. In the right panel, the cycle length (i.e. time between each activation) is shown. The cycle length that follows each activation is shown, e.g. the cycle length following the last paced stimulus is shown as a green circle.

For each electrogram, the pacing CL and the TCL are calculated. The software provides warnings if these are outside the expected range. Warnings are also provided if the difference between pacing CL and tachycardia CL are less than 10ms because this suggests that AOP may not have accelerated the atria to be faster than the tachycardia.

2.3 Accessing data

2.3.1 Electrophysiology recording system download

The LabSystem Pro Recording System allows the user to export recorded data in text format. Object-oriented code was written to import these files into Matlab and to manipulate them simply in that programming environment. The code utilises memory-mapping, a technique that involves re-storing data to file and then mapping that file so that the application can access it in the same way as it would access dynamic memory. This has the advantage that large amounts of data can be efficiently utilised and shared between applications.

2.3.2 Carto3 download

With the initial release of the Carto3 System, there was no facility for the user to access data from the cases. I acknowledge the help of Biosense Webster, who provided a workstation with an encrypted shared library, allowing for data to be extracted using Mathematica (Wolfram Research, Illinois, USA). Mathematica code was written to export data from cases in a format that could then be imported into Matlab, with which most code was written.

In later releases of Carto3, access to clinical data has been improved by including a facility for exporting the information directly from the clinical workstation. Matlab code was written to import this data.

2.4 Modelling reentry

In Chapters 5 and 6, mathematical and computer models of reentry are used to develop new approaches to the use of entrainment for mapping arrhythmias. These methods are described and discussed in those chapters.

2.5 Computational methods

In this section, computational methods for this thesis are briefly described. These were a critical tool for the research that is described but the goal was not to research these methods *per se*. Where quantitatively important code was written, it was validated as described below.

2.5.1 Shell reconstruction

Shells are represented in software as surfaces composed of multiple adjoining polygons. In this work, and most other software applications, triangles are used and the representation is referred to as a triangulation. This contains information about the vertices (a matrix of *x*, *y*, and *z* coordinates) as well as the triangulation matrix (a matrix in which each row lists the 3 vertices comprising a face). This provides the means with which to approximate curved surfaces in space. Typically, for an LA geometry produced using the Carto3 system, there are 5,000 – 10,000 vertices and 10,000 – 20,000 faces. The larger these matrices, the better the approximation of the geometry to the actual surface but the more computational power is required.

When a computer model of a surface is rendered as an image, the properties of each face can be controlled. These include colour, but also transparency, and the effect of reflected light. Whilst some of these aspects are computationally expensive, leading to slower refresh rates, they help to improve the 3D perception of the rendered surfaces.

For the Ripple Mapping application, each electrogram is represented as a moving cylinder on the surface of the heart. One of the difficulties was to achieve a sufficient speed of playback. In order to do this, the software adjusts the number of vertices and faces that are used to represent each cylinder depending upon the required frame rate. Further optimisation was also achieved by pre-storage of all calculated data within the graphics object (requiring faces to be turned ‘on’ or ‘off’ rather than fully re-rendered).

2.5.2 Graphical User Interfaces

For aspects of the research requiring repeated execution of code, GUIs were written. These were important to facilitate other users to test the software.

2.5.3 Calculating the distance across a shell

Finding the minimal geodesic between two points on a curved surface is non-trivial and considerably more complex than shortest-path problems in 2 dimensions. The requirement to calculate geodesics was encountered in the design of the software for electroanatomic analysis of entrainment manoeuvres. In this application, the distance

from the pacing electrodes to the rest of the atrial surface, including the other electrodes present, must be calculated.

Unfortunately, no suitable open-access software could be found. Therefore, a modified fast-marching algorithm was written, in which a virtual source was calculated for each face. Speed of the algorithm was optimised by storage of all intermediate variables in an object hierarchy, which reduced the need for repeated iterations when calculations were made between multiple catheters.

The 'virtual source' part of the algorithm determines the distance from the original source to a new vertex on a face where the distance to the other vertices in the face is known. This is explained further in Figure 2-2 below.

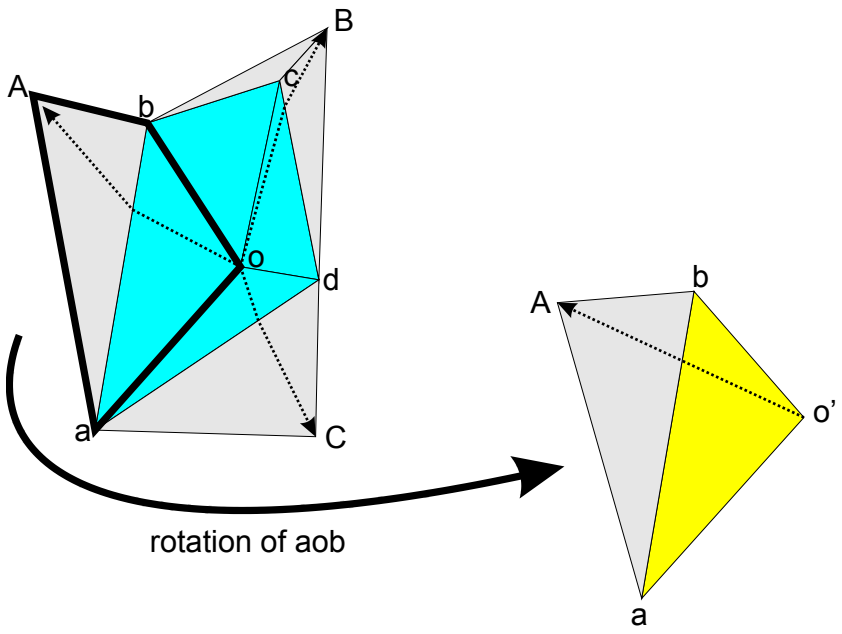

Figure 2-2. To the left is shown a small fragment of a triangulation. It is a 3 dimensional shell and so the shortest paths from *o* to *A*, *B*, and *C* are not straight lines. In order to calculate the shortest distances from *o* to *A*, *B* and *C*, virtual sources are used. For triangle *Aab*, the position of the source for its neighbour *aob* is known. Therefore, *aob* is rotated about *ab* so that it is coplanar with *aAb* (right part of figure). The position of the virtual source for triangle *aAb* is *o'* and the distance from *o* to *A* can easily be calculated because it is the same as the distance from *o'* to *A*.

There may be more than one route to reach vertices from the origin. Therefore, a 'fast-marching' type of algorithm is used to select which vertex should be calculated. This is an iterative process and is illustrated in Figure 2-3.

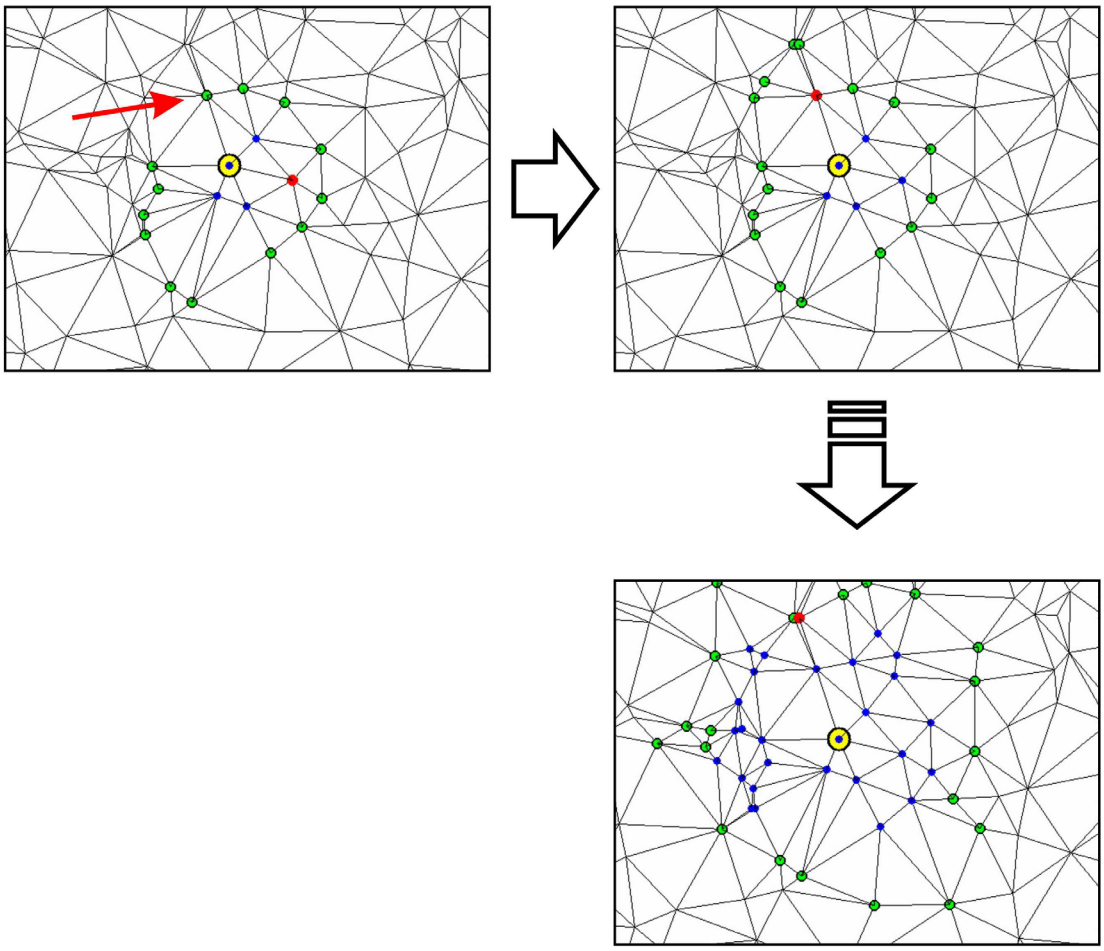

Figure 2-3. Fast marching algorithm. Part of a randomly generated spherical triangulated mesh is shown in each panel. Distances are being calculated from the yellow point to all of the other vertices. The green points represent locations to which a preliminary distance has been calculated. The blue points indicate locations where the distance has been 'fixed' (i.e. the algorithm will make no further modifications). The red location is the last point that was fixed. In the top right panel, the red arrow indicates the preliminary point that has the shortest distance from the yellow starting point. In the next iteration (top left), this point is fixed by the algorithm, and the surrounding vertices that are not fixed are then recalculated. This process is repeated to create an expanding number of fixed points (lower left panel).

In addition to verification of the subroutines that were written to calculate geodesic distances, validation was also performed by calculating the distance around a randomly generated spherical cloud of points. (The number of points was 4000, which is similar to the number in a Carto3 atrial geometry.) These were triangulated using a convex hull algorithm (available within Matlab) and the distance from a random vertex to all other vertices was calculated. This was compared with the mathematically

calculated distance: $d = r\theta$, where r is the radius of the sphere and θ is the angle separating the two points (in radians). As shown in Figure 2-4 the error is less than 1.5%, which is acceptable for its requirements.

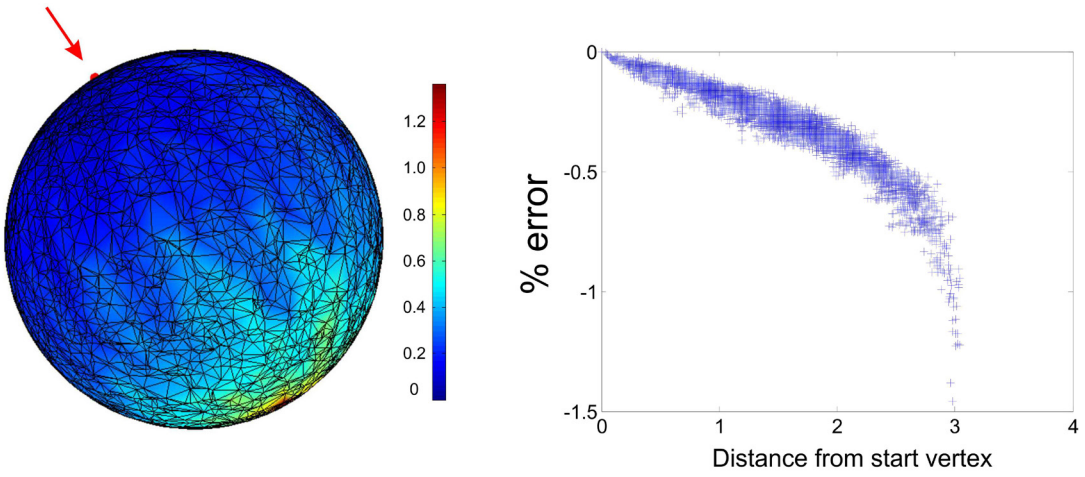

Figure 2-4. Validation of geodesic calculation. 4000 points were created on a unit sphere, which was triangulated with a convex hull algorithm (Left Panel). The red point shows the point from which geodesic distances were calculated to each other point. The error was calculated by comparing the result with the mathematical solution for a perfect sphere. The error increases as the distance around the shell increases. The main reason for this is that the geodesic on the triangulated surface traverses a series of straight chords that subtend the sphere.

2.6 Conclusion

This Chapter has outlined methods involved with patient studies, accessing clinical data, and some of the computational methods relating to cardiac surfaces. Further details are given in the following chapters.

3 Ripple Mapping to Assess Cardiac Activation

3.1 Ripple Mapping publication

The publication describing the initial development of Ripple Mapping is included on the following pages.[178]

Cardiac ripple mapping: A novel three-dimensional visualization method for use with electroanatomic mapping of cardiac arrhythmias

Nick W. F. Linton, MEng, MRCP, Michael Koa-Wing, MRCP, Darrel P. Francis, MD, MRCP, Pipin Kojodjojo, MRCP, PhD, Phang Boon Lim, MRCP, Tushar V. Salukhe, MD, MRCP, Zachary Whinnett, PhD, MRCP, D. Wyn Davies, MD, FRCP, FHRS, Nicholas S. Peters, MD, FRCP, FHRS, Mark D. O'Neill, MRCP, DPhil, Prapa Kanagaratnam, MRCP, PhD

From the Imperial College Healthcare NHS Trust, London, UK.

BACKGROUND Mapping of regular cardiac arrhythmias is frequently performed using sequential point-by-point annotation of local activation relative to a fixed timing reference. Assigning a single activation for each electrogram is unreliable for fragmented, continuous, or double potentials. Furthermore, these informative electrogram characteristics are lost when only a single timing point is assigned to generate activation maps.

OBJECTIVE The purpose of this study was to develop a novel method of electrogram visualization conveying both timing and morphology as well as location of each point within the chamber being studied.

METHODS Data were used from six patients who had undergone electrophysiological study with the Carto electroanatomic mapping system. Software was written to construct a three-dimensional surface from the imported electrogram locations. Electrograms were time gated and displayed as dynamic bars that extend out from this surface, changing in length and color according to the local electrogram voltage-time relationship to create a ripple map of cardiac activation.

RESULTS Ripple maps were successfully constructed for sinus rhythm (n = 1), atrial tachycardia (n = 3), and ventricular tachycardia (n = 2), simultaneously demonstrating voltage and timing information for all six patients. They showed low-amplitude continuous activity in four of five tachycardias at the site of successful ablation, consistent with a reentrant mechanism.

CONCLUSION Ripple mapping allows activation of the myocardium to be tracked visually without prior assignment of local activation times and without interpolation into unmapped regions. It assists the identification of tachycardia mechanism and optimal ablation site, without the need for an experienced computer-operating assistant.

KEYWORDS Catheter ablation; Computers; Electrophysiology; Mapping

ABBREVIATIONS **AF** = atrial fibrillation; **CTI** = cavotricuspid isthmus; **ECG** = electrocardiogram; **LA** = left atrium; **RA** = right atrium; **RV** = right ventricle; **VT** = ventricular tachycardia

(Heart Rhythm 2009;6:1754–1762)

Introduction

Successful catheter ablation of atrial or ventricular tachycardia requires an understanding of the mechanism and the ability to localize an anatomical site critical to the maintenance of arrhythmia. For example, typical atrial flutter can be effectively treated by ablation across the cavotricuspid isthmus (CTI).[1] However, many atrial tachycardias (including post–atrial fibrillation ablation tachycardias) and scar-related ventricular tachycardias (VTs) are more challenging.[2,3] While these arrhythmias can be mapped with conventional catheters using fluoroscopy only, three-dimensional (3D) electroanatomic mapping systems can often render the tachycardia mechanism more readily apparent and therefore amenable to effective ablation.[3–9]

Currently, accurate electroanatomic depiction of tachycardias requires precise annotation of local activation at all mapped points. One difficulty with current methods is that incorrect assignment of activation for a small number of electrograms can invalidate the entire activation map—manual adjustment is often required to achieve the optimal representation. A second difficulty is that data interpolation between mapped points is used to improve the quality of the display; however, areas of unmapped myocardium are then assigned simple estimates of timing and voltage information that may not be accurate.[5] Third, areas that may be most electrophysiologically and practically important are represented least well with current techniques: low-amplitude fractionated electrograms of long duration[10] or double po-

Dr. Linton and Dr. Koa-Wing made an equal contribution to the study. The authors' institution has filed a patent on some of the technology described. Dr. M. Koa-Wing and Dr. P. B. Lim are funded by the British Heart Foundation, London, United Kingdom. **Address reprint requests and correspondence:** Dr. P. Kanagaratnam, Waller Department of Cardiology, St. Mary's Hospital, Praed Street, London W2 1NY, United Kingdom. E-mail address: p.kanagaratnam@imperial.ac.uk. (Received July 27, 2009; accepted August 31, 2009.)

1547-5271/$ -see front matter doi:10.1016/j.hrthm.2009.08.038

tentials are often indicators of zones of deranged conduction critical to the maintenance of a reentrant arrhythmia, but with current methods only a single value of timing or voltage can be assigned to each coordinate.

We set out to develop and assess the feasibility of a novel method of electrogram visualization. We aimed to remove the need for an operator-determined window of interest, manual verification of local activation times, or data interpolation into regions of unmapped myocardium. In particular, we sought to preserve and display the entire electrogram voltage-time relationship rather than displaying a single electrogram characteristic at each location. We have carried out a proof-of-concept study in which cardiac ripple maps (available as movies on the *Heart Rhythm* website) were constructed using electroanatomical data acquired from the mapping of a variety of common cardiac rhythms.

Methods

Location and voltage data were obtained retrospectively for six patients who had undergone a clinically indicated electroanatomic mapping procedure using the Carto system (Biosense Webster, Diamond Bar, CA, USA). The data were then exported for offline processing with custom software written by the investigators using Matlab (Matlab 7, MathWorks, Inc., Natick, MA, USA). Each electrogram voltage-time relationship was displayed as a moving bar at the mapped location, perpendicular to a reconstructed 3D surface. Without any manual processing, this produced an activation map that was ready for clinical interpretation of the chamber activation sequence—a ripple map. These maps were then validated qualitatively against the original isochronal maps by confirming that the same activation sequence was identified. The ripple maps were also studied further for insights into electrogram interpretation or tachycardia mechanism that was not apparent from the isochronal maps.

Electrogram display

To create a ripple map, the electrograms from each location are timed relative to any chosen reference signal. For this pilot study we standardized on the peak of the QRS from the surface electrocardiogram (ECG). Each electrogram is displayed as a dynamic bar protruding from the constructed 3D surface (Figure 1). The color of the bars is graduated to give a further visual cue to their length because bars will be at various angles to the viewer. Any relationship between electrogram voltage and bar length could be chosen—we chose to make the length proportional to the absolute magnitude of the voltage, with the user able to limit maximal bar length by means of a control on the user interface (equivalent to clipping the electrograms). The 3D surface can also be shaded according to properties of the electrograms, for example, their maximum voltage.

For this study, the portion of the electrogram from 500 ms before to 500 ms after the QRS peak was stored for generation of the ripple map. This is a wide period and included more than one cycle length for some of the tachycardias. However, the user can see timing relative to the fiducial electrogram or the surface ECG, and this avoids defining electrogram components

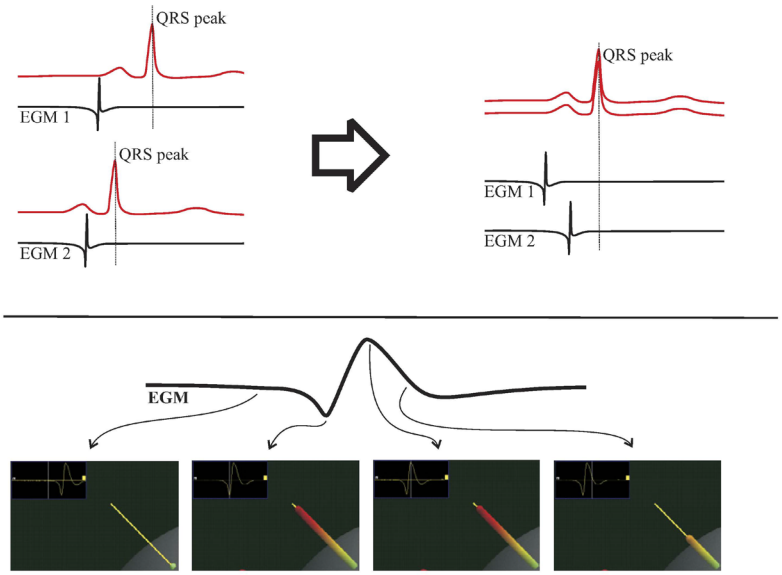

Figure 1 Creating the ripple map bars. Electrograms (egm1, egm2) are collected, and the corresponding QRS peak is identified (*dotted black line*). Next they are aligned according to this QRS peak, and 0.5 seconds of data are taken before and after this marker. The *lower panel* demonstrates that, for each electrogram, a bar is created, and the length varies according to the electrogram magnitude at each time frame (electrogram voltage shown in the top right of each frame). Negative deflections are displayed as positive changes in bar length in the current software.

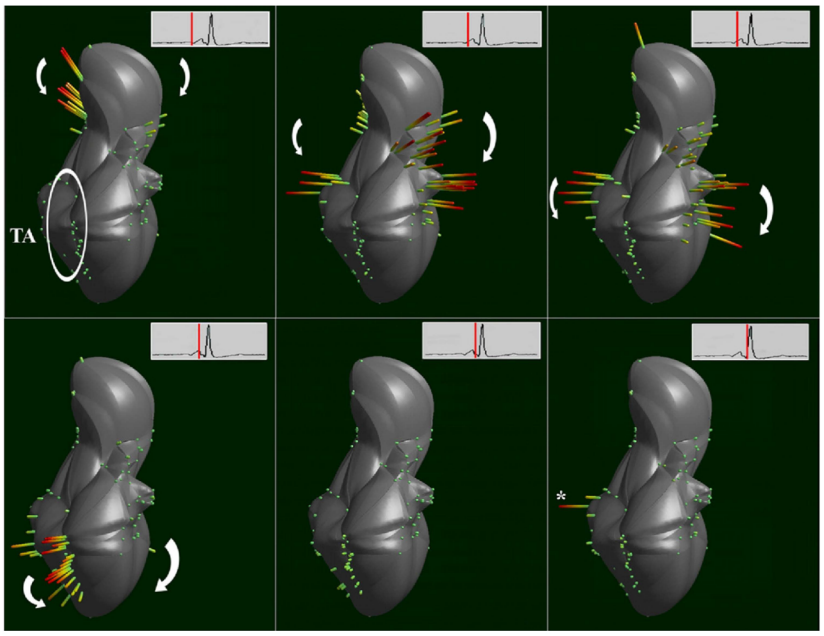

Figure 2 RA during sinus rhythm. Snapshots from the ripple map video (played left to right, top to bottom) of the RA during sinus rhythm. There are 99 points with complete electrogram and location information and seven points with location only. The tricuspid valve is marked by an ellipse (first image). *Arrows* show direction of activation. In the last image, a far-field ventricular signal is seen—isolated spike in electrogram magnitude during the QRS inscription (*asterisk*). The corresponding Carto maps are shown in Figure 3. Two corresponding videos are available from the *Heart Rhythm* website—sinusRA_1 gives a view of the whole chamber, and sinusRA_2 shows a closer view of the signals with a far-field ventricular component.

as "early" or "late" according to a predefined narrow window of interest.

Three-dimensional surface reconstruction

Three-dimensional surface reconstruction algorithms are used to construct a smooth shell intersecting the imported electrogram locations (Figures 2 and 4–8 have examples of reconstructed surfaces). For improved visualization of neighboring electrograms, the ability to smooth the surface was added to the software. Technical details of the surface reconstruction are available in an appendix on *Heart Rhythm*'s website (see SurfaceMethod.pdf).

User interface

Controls allow visualization of electrogram voltage throughout the entire chamber at any time point. This can be played as

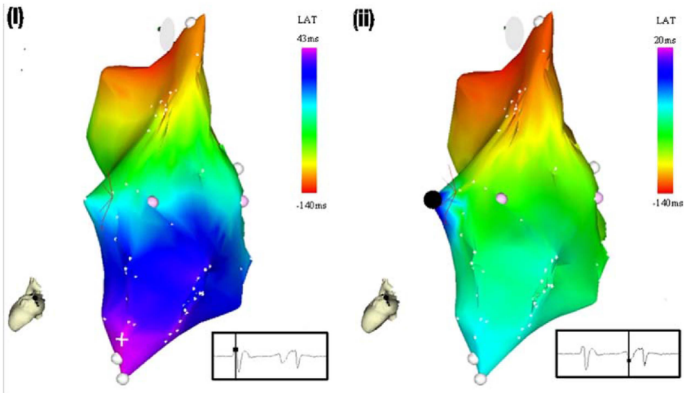

Figure 3 Isochronal maps corresponding to Figure 2. *Left panel*: atrial activation has been correctly annotated. *Right panel*: the same isochronal map, except that a single point has been incorrectly annotated to the ventricular component of the electrogram (at the *black sphere*). The difference between the maps is substantial, despite correct annotation at all but one of the electrogram locations.

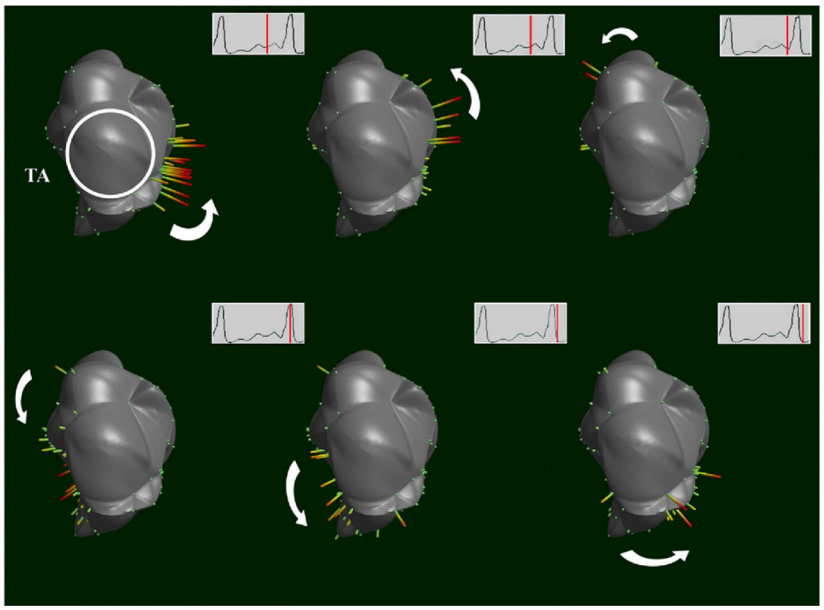

Figure 4 RA during typical atrial flutter. Left anterior oblique projection, 120 points. The tricuspid valve is marked by a *circle* in the first image. *Arrows* show direction of activation. The ripple map clearly demonstrates anticlockwise activation of the whole atrium, encompassing the whole cycle length of the tachycardia. The corresponding video, available from the *Heart Rhythm* website, is flutterRA.

a movie to demonstrate the sequence of chamber activation by creating a visual ripple of electrograms. Local activation can also be examined by selecting and displaying the relevant electrograms as well as by stepping through the ripple map millisecond by millisecond.

Results

Using the current software

The data from each case were downloaded from Carto. Matlab imports electrogram location and voltage data and

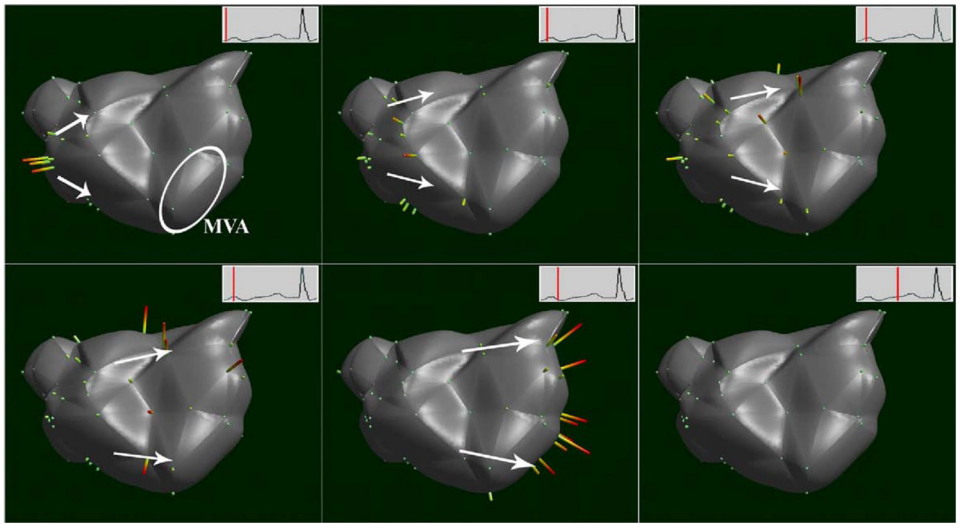

Figure 5 Focal LA tachycardia. Anteroposterior view, 70 points and 12 location-only points. An ellipse on the first image marks the mitral valve. At the last snapshot, there is electrical silence because LA activation from the focal site does not span the cycle length of the tachycardia. The corresponding videos, available from the *Heart Rhythm* website, are focalLA_1 (overview of LA activation), focalLA_2 (rotation to the area of interest), and focalLA_3 (area of interest played more slowly to demonstrate fractionated electrograms). Note the activation relating to ventricular depolarization that corresponds to the QRS of the surface ECG.

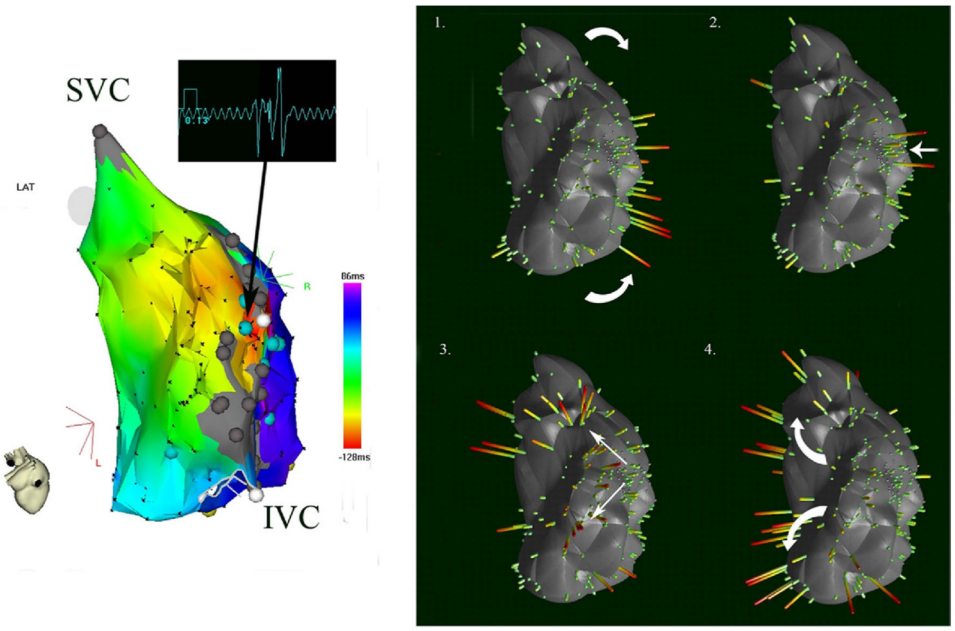

Figure 6 Macroreentrant RA tachycardia. RA scar-related tachycardia with ripple map (*right panel*, 211 points and 41 location-only points) and corresponding isochronal activation map (*left panel*). The ripple map shows the wave front approaching and subsequently traversing the isthmus of slow conduction, exiting in a figure-of-eight fashion around the two islands of scar. An electrogram within the critical isthmus is shown (*left panel*) to illustrate the low-voltage, fractionated signals seen in this area. SVC = superior vena cava; IVC = inferior vena cava.

reference ECG data. For some of the Carto points, there will be no electrogram voltage data where a location-only point has been selected. The ripple map software automatically reconstructs a surface from all of the point locations. The user then selects the maximum plotted voltage for the electrograms—this clips the electrogram voltages to the chosen

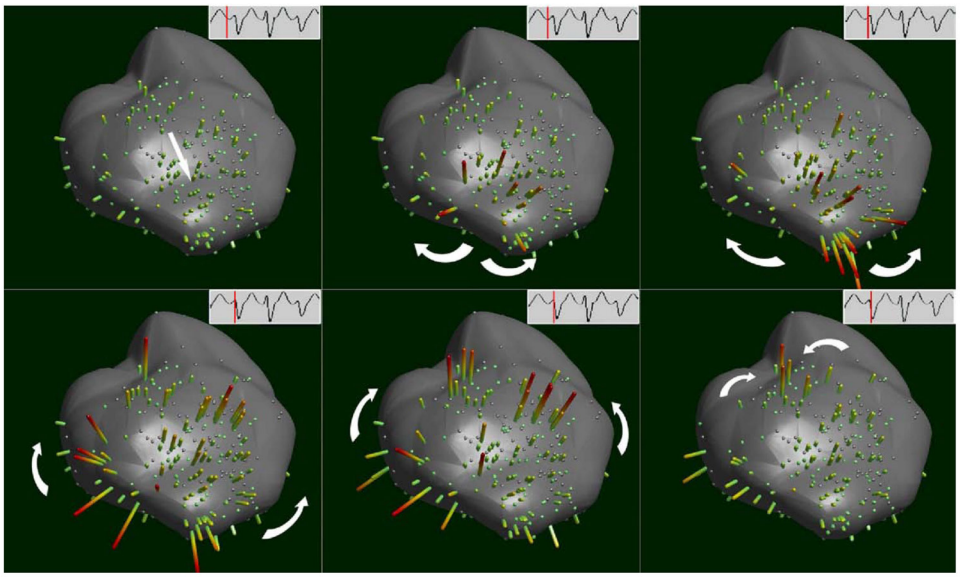

Figure 7 Left ventricular tachycardia. Ripple map of the left ventricle (caudal left anterior oblique view, 120 points and 158 location only points) during scar-related VT. Earliest activation was seen anteroapically. *Arrows* show postulated direction of activation in a figure-of-eight fashion.

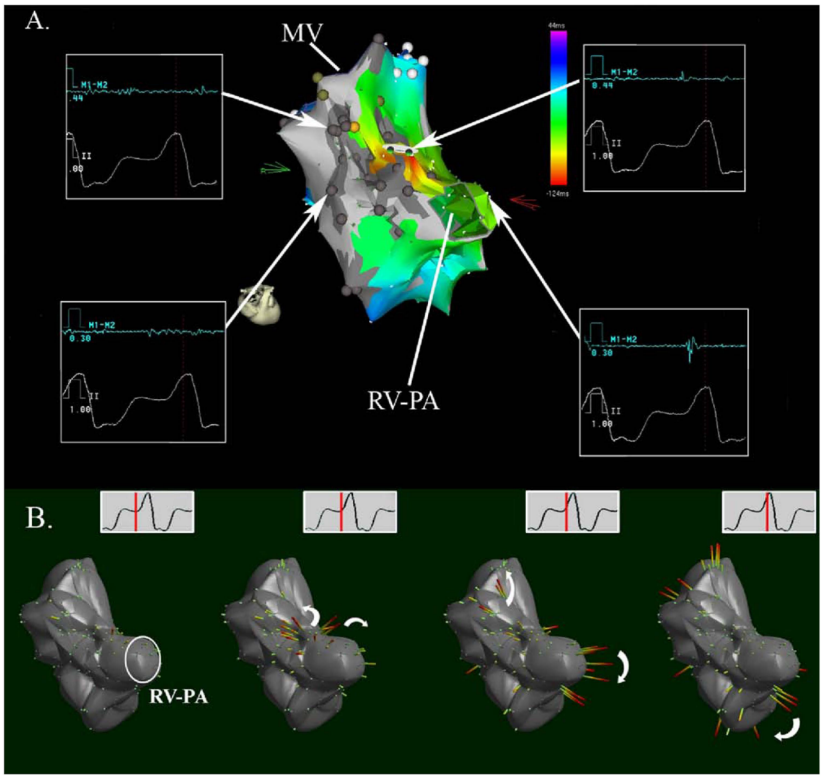

Figure 8 RV tachycardia. **A:** Activation map of an RV scar-related VT (oblique cranial, lateral view). RV-pulmonary artery conduit (RV-PA) insertion and mitral valve (MV) are marked. Note the large anterolateral scar. Several signals around the scar and scar border are shown to illustrate the fractionated signals seen during activation mapping. The corresponding ripple map (panel B, 103 points and 144 location only points) clearly showed the earliest electrogram with exit occurring at the base of the conduit (marked by *circle*) with activation posterior and laterally around the base of the conduit.

value. A movie can then be played (e.g., movie: focalLA_1 from the *Heart Rhythm* website). At each frame, the electrogram bars are plotted according to voltage at the displayed timing (relative to the reference). This timing is shown in a small panel (top right of the ripple map).

The user can then replay the ripple map with different orientations to get an overview of activation (e.g., movie: focalLA_2). Then it is possible to step through the different frames manually or at slower speeds to assess carefully the regions of interest. Individual electrograms can also be selected and displayed to give more precise information about morphology and timing (e.g., movie: focalLA_3). Initial analysis of ripple maps was completed within 5–10 minutes of starting the ripple map software.

Clinical cases

The activation sequences studied were (1) right atrial (RA) activation during sinus rhythm (Figure 2); (2) RA activation during CTI-dependent atrial flutter (Figure 4); (3) left atrial (LA) activation during a focal reentrant tachycardia (Figure 5); (4) scar-related reentrant RA tachycardia (Figure 6); (5) left ventricular activation during postinfarction scar-related VT (Figure 7); and (6) right ventricle (RV) activation in a patient with congenital heart disease and scar-related VT (Figure 8).

In addition to the figures, movies showing examples of ripple maps are available from the *Heart Rhythm* website (these are described in the legends to Figures 2, 4, and 5).

Sinus rhythm

The sinus rhythm ripple map correlated well with the original electroanatomical activation and propagation map. Activation occurred earliest at the high RA and propagated inferiorly toward the tricuspid annulus (Figure 2). After atrial depolarization had finished, a late signal is seen that is separate from the rest of activation and is consistent with ventricular activation (see Figure 3 for confirmation). In isochronal mapping, inaccurate annotation produces a marked difference in the appearance of the activation sequence (Figure 3). However, the ripple map displays a view of atrial activation ready for interpretation by the operator without relying on any further data processing, that is, 'what you see is what you get'.

Atrial tachycardias

A CTI-dependent flutter (confirmed by surface ECG analysis, entrainment, and flutter termination during ablation at the CTI) was used to construct a ripple map of atrial macroreentry (see Figure 4). Activation can be followed in a counterclockwise direction around the tricuspid annulus, in keeping with the interpretation from Carto-acquired data and conventional electrophysiological diagnostic maneuvers.

Another patient with previous pulmonary vein isolation for paroxysmal AF presented with a regular atrial tachycardia (cycle length 270 ms). Isochronal mapping demonstrated centrifugal activation of the LA from a site on the left superior aspect of the interatrial septum. A single ablation lesion at this site terminated the tachycardia. A ripple map of this tachycardia was constructed offline and demonstrated septal-to-lateral activation of the anterior LA (Figure 5) and a long period of atrial electrical silence coincident with the isoelectric line on the surface electrocardiogram—suggestive of either a localized reentry or a true focal point atrial tachycardia. The septal site of early activation on the reconstructed atrial shell corresponded with the site of successful ablation on the original isochronal map. Additionally, the ripple map conveys the fractionation of the electrograms in this region, confirming the capacity of the system to demonstrate anatomically relevant detail together with useful electrical information.

A patient with a previous atrial septal defect repair underwent high-density electroanatomic mapping, revealing an RA tachycardia with a cycle length of 265 ms. The entire tachycardia cycle length was accounted for within the chamber of interest, and the isochronal activation map was consistent with a scar-related macroreentrant circuit traversing an isthmus of slow conduction between two separate islands of scar (Figure 6). Activation within this isthmus was characterized by low-amplitude fractionated electrograms (an example of the signal can be seen in Figure 6), which are difficult to annotate with isochronal mapping as only one value for timing can be assigned. Ripple mapping not only corroborated atrial activation passing around the two scars and through the isthmus but also retained electrogram morphology within the slow conduction zone. Ablation across this isthmus terminated the tachycardia and rendered it noninducible by programmed stimulation.

VTs

Two cases of ischemic left ventricular tachycardia were analyzed. An isochronal activation map during VT (cycle length 420 ms) in a patient with an inferolateral left ventricular scar showed the exit site on the isochronal map. However, the ripple map was also able to show the exit site as well as activation around the scar consistent with reentry through a diastolic pathway (Figure 7; see also Discussion).

A sinus rhythm left ventricular ripple map of another patient with a well-defined inferobasal scar highlighted an area of fractionated potentials late in the QRS. This area corresponded with the Carto scar map where late fractionated potentials were marked separately. During VT (cycle length 380 ms), a limited activation map of the same tachycardia showed that the site of earliest ventricular activation (i.e., the exit site) was near to the site of late fractionated potential that is demonstrated in sinus rhythm.

An RV tachycardia (cycle length 550 ms) was studied in a patient with transposition of the great arteries, ventriculoseptal defect, and pulmonary stenosis corrected by a Rastelli repair. A sinus rhythm Carto scar map of the RV revealed a large anterolateral scar extending from the tricuspid annulus as far as the insertion of the RV to pulmonary artery conduit situated in the outflow tract (Figure 8). Activation mapping in VT showed multiple low-amplitude fractionated signals of long duration within and around the scar border. Annotation of discrete local activation in this setting was not possible, but the remainder of the map was consistent with a circuit traversing the scar zone: ablation across the scar from tricuspid annulus to conduit terminated the previously incessant tachycardia, rendering it noninducible. Construction of a ripple map encompassing the RV and RV outflow tract demonstrated the direction of activation through the scar and preserved the electrogram amplitude and duration information at the sites of ambiguous activation.

Discussion

This study has (1) described a novel technique for representation of endocardial activation (ripple mapping) and (2) evaluated feasibility with the technique across a spectrum of cardiac rhythms. Ripple mapping is the first 3D mapping technique to offer a dynamic representation of local voltage in the time domain across the whole chamber. The study confirms that activation sequences produced by a ripple map concur with those of conventional isochronal activation maps. Additionally, ripple maps preserved information relating to fractionated and low-voltage signals, giving further insight into the arrhythmia mechanism.

Isochronal and isopotential mapping

The last decade has seen substantial development of 3D electroanatomic mapping systems that integrate catheter location with electrical information. However, the mechanisms of atrial and ventricular tachycardias may not be apparent, despite meticulous activation mapping and visualization using existing techniques.

Isochronal mapping using the Carto system allows acquisition of points in 3D, to which timing values are assigned. For regular tachycardias, the resultant color-band maps are an effective method for displaying activation when timing of activation is unambiguous and when the point density and distribution minimizes data interpolation. Difficulty can arise when assigning a single timing value to a fractionated or a double potential or when the signal-to-noise ratio is low, as is frequently the case in areas of myocardial scar.[11] The ideal adjunctive technique would therefore obviate the need for a single timing value for each site and instead simply display all timing and voltage data dynamically, allowing the observer to “see” all chamber

electrical activity simultaneously from onset to termination of activation.

In isopotential mapping, unlike isochronal mapping, activation is assumed to occur when the electrogram voltage reaches a predefined magnitude and can be displayed as a moving image over the surface. This method is used with simultaneous noncontact voltage data collected from a multielectrode array (EnSite System, St Jude Medical, St Paul, MN, USA).[12] However, there are important limitations to this technique: the accuracy of the noncontact data as a representation of true contact data decreases with distance from the array; the array restricts ablation catheter manipulation within the chamber; and low-amplitude signals at sites of critical isthmuses may require manual manipulation of voltage filter settings,[13] which can be time-consuming and dependent on a high level of expertise and system familiarity.

Ripple mapping—The rationale

In reviewing the process of activation mapping and identification of tachycardia mechanisms, we identified three important criteria for consideration: (1) there should be minimal user-dependent offline processing; (2) there should be no interpolation of data between mapped points; and (3) fractionated and single-deflection electrograms should be easily interpreted.

In minimizing user-dependent offline processing, we sought to provide a visual representation that included as much information as possible to exploit the top-down pattern recognition[14] of the electrophysiologist. Current visualization methods involve a bottom-up approach to identifying the myocardial activation pattern: each electrogram is analyzed in isolation to identify local activation, and then the overall pattern is inferred from interpolation of this information around the chamber. This requires a certain degree of familiarity and postprocessing to produce a color-coded map that is interpretable and quickly identifies areas of interest critical to the arrhythmia mechanism. Ripple mapping minimizes the offline processing to no more than selection of appropriate electrograms in a time window either side of a particular ECG component. Activation is then assessed by using the human ability to detect and interpret movement—the ripple—enabling the morphology of electrograms to be assessed within the context of other electrograms locally and elsewhere within the chamber. This reduces the potential for rogue points to significantly impact upon overall interpretation of chamber activation, which can be seen with isochronal mapping (Figure 3).

When complex tachycardias are mapped conventionally (without using 3D technology), the direction of activation in a region is determined from sequential point mapping over a small area. Repeating this process around the chamber enables the activation sequence and therefore mechanism of the tachycardia to be determined. This can be confirmed with entrainment maneuvers and has been used effectively to treat atrial tachycardias after catheter ablation for AF.[15–17] Ripple mapping simplifies the storage and 3D comparison of electrograms that have been collected in this way. Each bar will change according to the local voltage change, with the earliest occurring first: this can be examined frame by frame, within a local region, or as a rapid movie to display the ripple across the entire chamber. There is no interpolation, but the direction of activation will be more obvious with increasing density of points.

In this study, we used data from completed Carto maps to create the ripple maps, and so the number of points used was the same for each. When an online version of the software is available, then the number of points required for prospective clinical cases can be assessed. We anticipate that the total number of points required will often be similar to the number of points collected for creating Carto maps. However, it is also possible that ripple mapping could be used in conjunction with other diagnostic maneuvers to identify arrhythmias using a smaller number of collected points—for example, using a recently described approach that combines activation mapping with entrainment mapping in a limited number of regions for atrial tachycardias.[17]

We were able to demonstrate qualitatively that ripple mapping is effective in determining activation patterns in both simple and complex cardiac rhythms without the need for data interpolation. Additionally, the technique may provide useful information on arrhythmia mechanism. In the macroreentrant CTI-dependent flutter (Figure 4), activation around the tricuspid annulus is seen for the whole atrial cycle length. In the case of focal atrial tachycardia (Figure 5), a period of electrical silence before subsequent focal firing was noted, which would not be the case for macroreentry. At the origin of this tachycardia, the ripple map demonstrated fractionated electrograms. Ripple mapping also allowed rapid visualization of an area of fractionated late potentials in sinus rhythm, which corresponded to the early exit site during VT. This confirmed our hypothesis that zones of slow conduction, such as occur within reentrant circuits,[18] can be readily visualized with ripple mapping and may identify target ablation sites in sinus rhythm for patients with VT related to postinfarction scar.

Limitations

In this proof-of-concept study, the clinical operator had no access to the ripple map analysis. Ripple mapping shares some of the inherent limitations of isochronal tachycardia mapping: it relies upon a stable tachycardia and a high density of data at sites of interest. The electrograms could be gated to fiducial markers other than the surface ECG, for example, an atrial reference electrogram, would be more appropriate for atrial tachycardias. For some atrial tachycardias, with 1:1 A:V conduction, far-field ventricular signals might complicate the interpretation of atrial electrograms near the mitral or tricuspid annulus. Larger, prospective studies are needed before this technique can be widely recommended; further refinement and implementation with clinical real-time tools will be necessary to make such trials practical.

Conclusion

Ripple mapping is a novel method of displaying electroanatomical data. Operator-dependent annotation and data interpolation are eliminated, and dynamic voltage-time relationships are displayed at each site of electrogram acquisition. This results in a propagation map that incorporates all collected information, potentially leading to improved understanding of arrhythmia mechanism and therefore treatment.

Appendix

An electronic Appendix, SurfaceMethod.pdf is available on *Heart Rhythm*'s Web site. This describes the construction of a surface from the electrogram locations.

References

1. Tai CT, Chen SA, Chiang CE, et al. Long-term outcome of radiofrequency catheter ablation for typical atrial flutter: risk prediction of recurrent arrhythmias. J Cardiovasc Electrophysiol 1998;9:115–121.
2. Dixit S, Callans DJ. Mapping for ventricular tachycardia. Card Electrophysiol Rev 2002;6:436–441.
3. Marchlinski F, Callans D, Gottlieb C, et al. Magnetic electroanatomical mapping for ablation of focal atrial tachycardias. Pacing Clin Electrophysiol 1998;21: 1621–1635.
4. Earley MJ, Showkathali R, Alzetani M, et al. Radiofrequency ablation of arrhythmias guided by non-fluoroscopic catheter location: a prospective randomized trial. Eur Heart J 2006;27:1223–1229.
5. Nakagawa H, Jackman WM. Use of a 3-dimensional electroanatomical mapping system for catheter ablation of macroreentrant right atrial tachycardia following atriotomy. J Electrocardiol 1999;32(Suppl):16–21.
6. Nakagawa H, Shah N, Matsudaira K, et al. Characterization of reentrant circuit in macroreentrant right atrial tachycardia after surgical repair of congenital heart disease: isolated channels between scars allow "focal" ablation. Circulation 2001;103:699–709.
7. Schilling RJ, Peters NS, Davies DW. Mapping and ablation of ventricular tachycardia with the aid of a non-contact mapping system. Heart 1999;81:570–575.
8. Shah DC, Jais P, Haissaguerre M, et al. Three-dimensional mapping of the common atrial flutter circuit in the right atrium. Circulation 1997;96:3904–3912.
9. Stevenson WG, Delacretaz E, Friedman PL, Ellison KE. Identification and ablation of macroreentrant ventricular tachycardia with the CARTO electroanatomical mapping system. Pacing Clin Electrophysiol 1998;21:1448–1456.
10. Shah D, Sunthorn H, Burri H, et al. Narrow, slow-conducting isthmus dependent left atrial reentry developing after ablation for atrial fibrillation: ECG characterization and elimination by focal RF ablation. J Cardiovasc Electrophysiol 2006;17:508–515.
11. de Groot NM, Schalij MJ, Zeppenfeld K, et al. Voltage and activation mapping: how the recording technique affects the outcome of catheter ablation procedures in patients with congenital heart disease. Circulation 2003;108:2099–2106.
12. Khoury DS, Taccardi B, Lux RL, Ershler PR, Rudy Y. Reconstruction of endocardial potentials and activation sequences from intracavitary probe measurements. Localization of pacing sites and effects of myocardial structure. Circulation 1995;91:845–863.
13. Chinitz LA, Sethi JS. How to perform noncontact mapping. Heart Rhythm 2006;3:120–123.
14. Gregory RL. The Medawar Lecture 2001 knowledge for vision: vision for knowledge. Philos Trans R Soc Lond B Biol Sci 2005;360:1231–1251.
15. Knecht S, Hocini M, Wright M, et al. Left atrial linear lesions are required for successful treatment of persistent atrial fibrillation. Eur Heart J 2008;29:2359–2366.
16. Lellouche N, Jais P, Nault I, et al. Early recurrences after atrial fibrillation ablation: prognostic value and effect of early reablation. J Cardiovasc Electrophysiol 2008;19:599–605.
17. Weerasooriya R, Jais P, Wright M, et al. Catheter ablation of atrial tachycardia following atrial fibrillation ablation. J Cardiovasc Electrophysiol 2009;20:833–838.
18. Harada T, Stevenson WG, Kocovic DZ, Friedman PL. Catheter ablation of ventricular tachycardia after myocardial infarction: relation of endocardial sinus rhythm late potentials to the reentry circuit. J Am Coll Cardiol 1997;30:1015–1023.

References are included in this chapter as well as the References section.[93, 163, 179-194]

4 Ripple Mapping for Atrial Tachycardia

4.1 Aims for this chapter (in combination with Chapter 3)

A1 Design a new method for activation mapping that does not require a user-chosen window of interest.

A2 Avoid the need for local activation time assignment.

A3 Enable the display of electrogram characteristics, such as fractionation or double potentials

A4 Create a prototype for analysis of clinical cases.

4.2 Introduction

The initial study of Ripple Mapping was a proof-of-concept study. Following this, substantial changes were made to the software. The anatomical shell created with the commercial software is used instead of a surface generated from the collected points (see Section 2.3.2 on p51). Also, the interpolated values of the bipolar voltage amplitude are used to shade the atrial shell, giving additional information about underlying substrate. Further software changes to the user interface also allowed for much faster running of the displayed data. This was important so that novice users could assess the raw data without having to rely upon pre-prepared videos. This meant that they could assess a case without any influence from the researcher.

In this chapter, the next rendition of the software is tested more systematically. Specifically, the activation maps of patients with atrial tachycardia are assessed with Ripple Mapping by 4 electrophysiologists of varying experience.

4.3 Design modifications to Ripple Mapping

4.3.1 Surface rendering and voltage information

The Ripple Mapping was changed so that it can run from an exported Carto3 case, as described in Section 2.3.2. The electrograms, triangulated atrial surface, and valve orifices are imported. The Carto3 data also includes voltage amplitude data – the peak-to-peak amplitude of the electrograms is interpolated across the atrial surface. In the initial Ripple Mapping study, the atrial surface was shaded in grey, but this has been modified to include shading according to this voltage data. This allows the user to interpret activation within the context of information about the underlying tissue – low voltage areas being likely related to scar or previous ablation.

4.3.2 Playback speed

The speed at which the Ripple Mapping can run was increased by reducing the total number of graphics objects that are held in memory (it is more efficient to have one graphics object holding information for multiple bars rather than having multiple graphics objects relating to a single bar each). If the user selects particularly fast playback speeds, then the quality of graphics rendering is reduced in order to facilitate the required frame-rate increase. This method allows for a frame rate of playback so that up to 150ms of data can be displayed per second.

4.3.3 Automatic 'window'

In the initial use of Ripple Mapping, the user selected the time-period that was included. However, for this study a fixed time-frame was used (to emphasise that a user-defined window of interest does not need to be used). The time-frame was chosen in relation to the mid-CS electrogram for all LA maps, and in relation to the most proximal CS electrogram for RA maps. For each map, the time-frame was taken from one TCL before the respective electrogram to one TCL afterwards. When the Ripple Map reaches the end of the time-frame the display of all points is briefly suspended, in order to indicate to the user that the Ripple Map is restarting. Using this method, the user sees two complete cycle lengths of the tachycardia being displayed. This guarantees that, for a macroreentrant tachycardia, if any arbitrary 'start point' is chosen then an entire cycle is displayed without interruption. The Ripple GUI is shown in Figure 4-1.

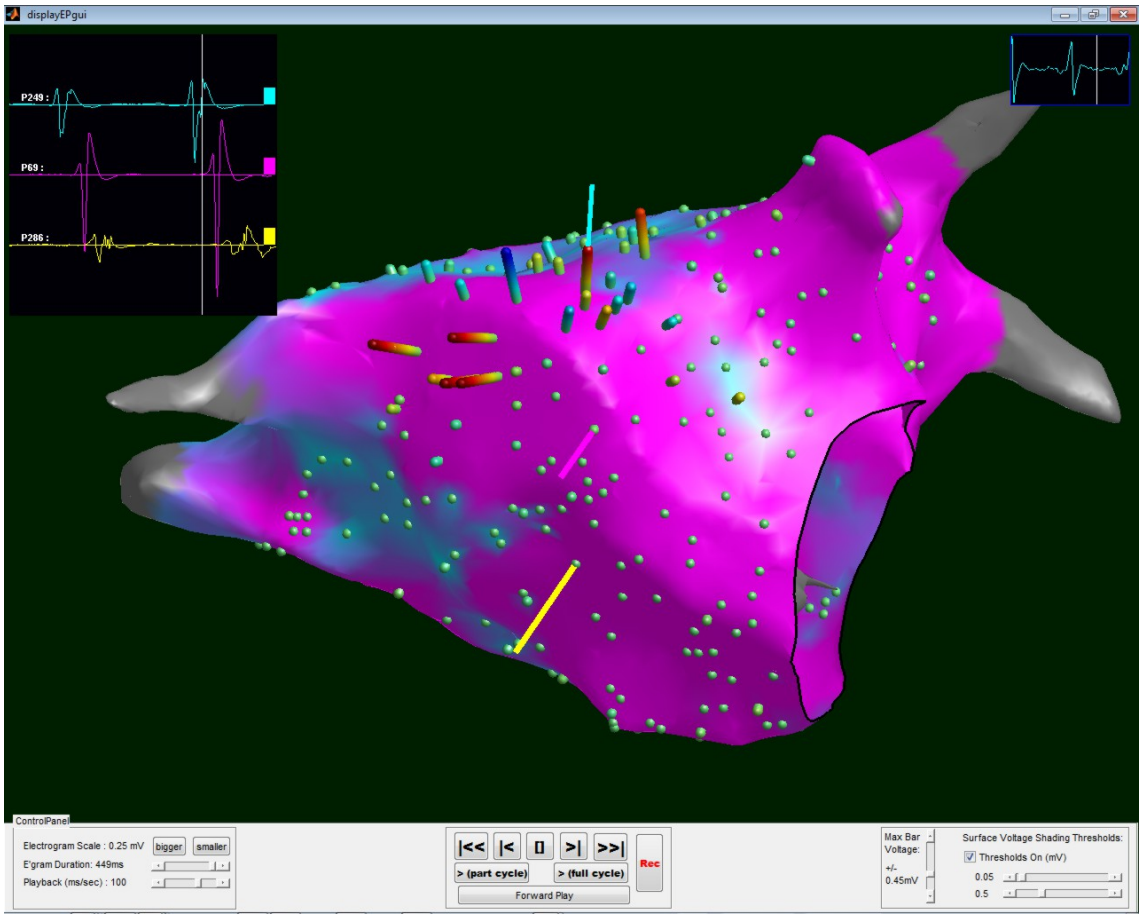

Figure 4-1. The user-interface for Ripple Mapping. The atrial surface is downloaded from Carto3 and coloured according to the interpolated bipolar electrogram voltages. Cyan represents areas with low voltage and magenta high voltage (the sliders in the bottom right corner are used to adjust the scale). The bars extend outward from the cardiac surface according to the electrogram voltage (red for positive and blue for negative voltages). The bars reach their maximum length at a user controlled value (similar to clipping). Additional controls adjust the speed of play. The user can select electrograms and see them displayed at the top left.

4.4 Experimental methods

Carto3 maps for patients with atrial tachycardia were assessed, for the period 01/01/2010 – 01/04/12. All procedures were performed by the same operator and the same mapping strategy. Carto maps were only included where the mechanism of tachycardia was confirmed by successful ablation. Maps for typical right atrial flutter in structurally normal hearts were excluded. In total, 16 cases were identified with a total of 18 mapped atrial tachycardias. Further information about the clinical methods for

creating the Carto3 maps are given in Section 2.2.2, p49. For each tachycardia, the activation of each atrial wall was determined by the researcher using all of the information available (known arrhythmia mechanism, isochronal map, Ripple Map, interpretation of electrograms). The surface voltage scale was chosen to shade all areas >0.5mv as magenta and <0.05 as cyan, as per other studies.

Four electrophysiologists were then asked to interpret the Ripple Maps from each patient. They were given written instructions describing how to interpret Ripple Maps. For each case, they were then asked to fill out a *pro forma* requiring them to identify: the direction of activation of the anterior, posterior, septal, lateral and inferior walls; the difficulty in establishing a diagnosis; the most likely diagnosis; and an ablation target. No information about entrainment manoeuvres was provided. If activation was consistent with a reentrant tachycardia all electrophysiologists confirmed that it was their usual practice to perform entrainment in order to rule out a localised tachycardia adjacent to a line of conduction block.

Isochronal maps were also assessed by the electrophysiologists, after a period of more than 1 month from the initial analysis. The same *pro forma* was used. The proportion of correct responses could then be compared between Ripple Maps and isochronal maps.

The activation maps were also assessed qualitatively in order to assess the utility of the method.

4.5 Results

Table 4-1 gives details about the cases which were included in the study.

Case	CL (ms)	Previous ablation / surgery	Diagnosis
Left atrial cases			
1	410	CTI ablation for typical flutter	Focal from ridge between LUPV and LAA
2	250	Previous PVI for PAF	Exit from posterior aspect of LUPV
3	280	PVI, CTI line, roof line	Localised reentry from a circuit on the septum between the RIPV and CS
4	360	PVI, roof line, mitral line	Localised reentry on anterior wall
5	260	Mitral valve repair, tricuspid annuloplasty, and surgical PVI	Reentry around atriotomy scar and perimitral reentry (2 mechanisms)
6	250	Previous PVI, roof line, mitral line	Activation consistent with roof dependent reentry. Entrainment indicated localised reentry anterior to blocked roof line
7a	260	PVI, roof line.	Roof dependent reentry around L veins. Also perimitral circuit (double loop)
7b	315	Following on from Case 7	Perimitral reentry
8	240	PVI, roof line, mitral line, CTI line	Perimitral reentry
9	345	PVI, roof line, attempted mitral line	Perimitral reentry
10	225	PVI, roof line, mitral line, anterior mitral line	Roof dependent around R veins
11	320	PVI, roof line	Roof dependent flutter (or possible focal next to blocked line)
12	250	PVI, roof line, mitral line, 'maze'	Perimitral flutter
Right atrial cases			
13	240	Previous cardiac surgery with R + L atriotomies	Dual-loop around tricuspid annulus and R atriotomy scar
14a	285	Surgical repair for Tetralogy of Fallot	Dual-loop around tricuspid annulus and R atriotomy scar
14b	305	Following on from case 14, new tachycardia CL 305ms.	Reentry around R atriotomy
15	420	Mitral valve repair (R atriotomy) and surgical PVI	Reentry around R atriotomy scar
16	220	Tetralogy of Fallot repair	Single loop reentry around tricuspid annulus

Table 4-1. Details of the cases for which activation maps were analysed. On average there were 110 (range 34-322) points in each map.

4.5.1 Questionnaire study

Figure 4-2 shows the proportion of correct responses by the electrophysiologists analysing each case using Ripple Mapping, and a similar graph for the isochronal maps. The results have been grouped according to the tachycardia mechanisms. Overall diagnostic accuracy was high for all types of macroreentrant tachycardia, and lower for localised reentry tachycardias.

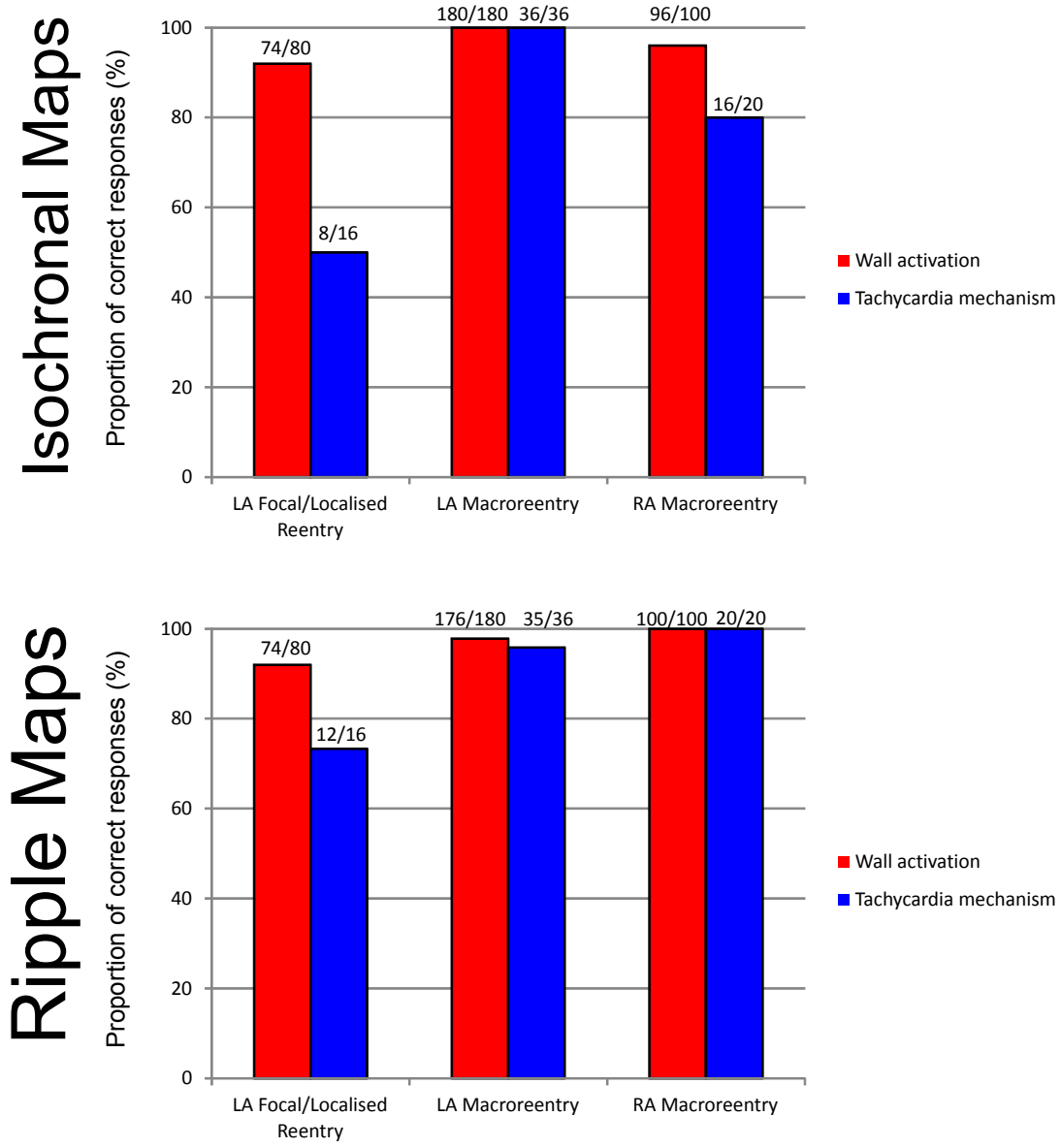

Figure 4-2. Proportion of correct responses for analysis of isochronal maps (above) and Ripple Maps (below). For each type of tachycardia, the proportion of correct responses for wall activation (left bar) and tachycardia mechanism (right bar) is shown. For each chamber, the activation of 5 walls was assessed by 4 observers, giving a total of 5*4=20 responses for each tachycardia. The tachycardia mechanism was assessed 4 times for each tachycardia. Correct responses were less frequent for focal / localised reentry tachycardias (see Text and Discussion on Qualitative analysis, starting on p74).

When comparing the accuracy for determining the direction of activation on each atrial wall, there was no significant difference between isochronal maps and Ripple Mapping for LA macroreentry ($p = 1$), RA macroreentry ($p = 0.17$), or localised

reentry (p = 0.32). Similarly there was no significant difference in the accuracy of diagnosis for LA macroreentry (p = 0.37), RA macroreentry (p = 0.35). There was a trend to increased diagnostic accuracy for the Ripple Maps of localised reentry, but this did not achieve statistical significance (p = 0.18).

Users' ratings of 'case difficulty' and 'diagnostic accuracy' were not significantly different between any of the groups and were not predictive of successful identification of the tachycardia mechanism. Similarly, the number of points used to create the maps was not predictive, although users subjectively reported that a higher number of points was more helpful for the Ripple Maps.

4.5.2 Qualitative analysis

The pre-chosen time interval for Ripple Maps allowed interpretation of the data in all cases. In the LA macroreentry cases, most areas of atrium had voltages >0.5mV. An example of peri-mitral reentry is shown in Movie 4-1. Note that the Ripple Map successfully displays double potentials at the atrial roof, where a linear ablation lesion had been performed at a previous procedure.

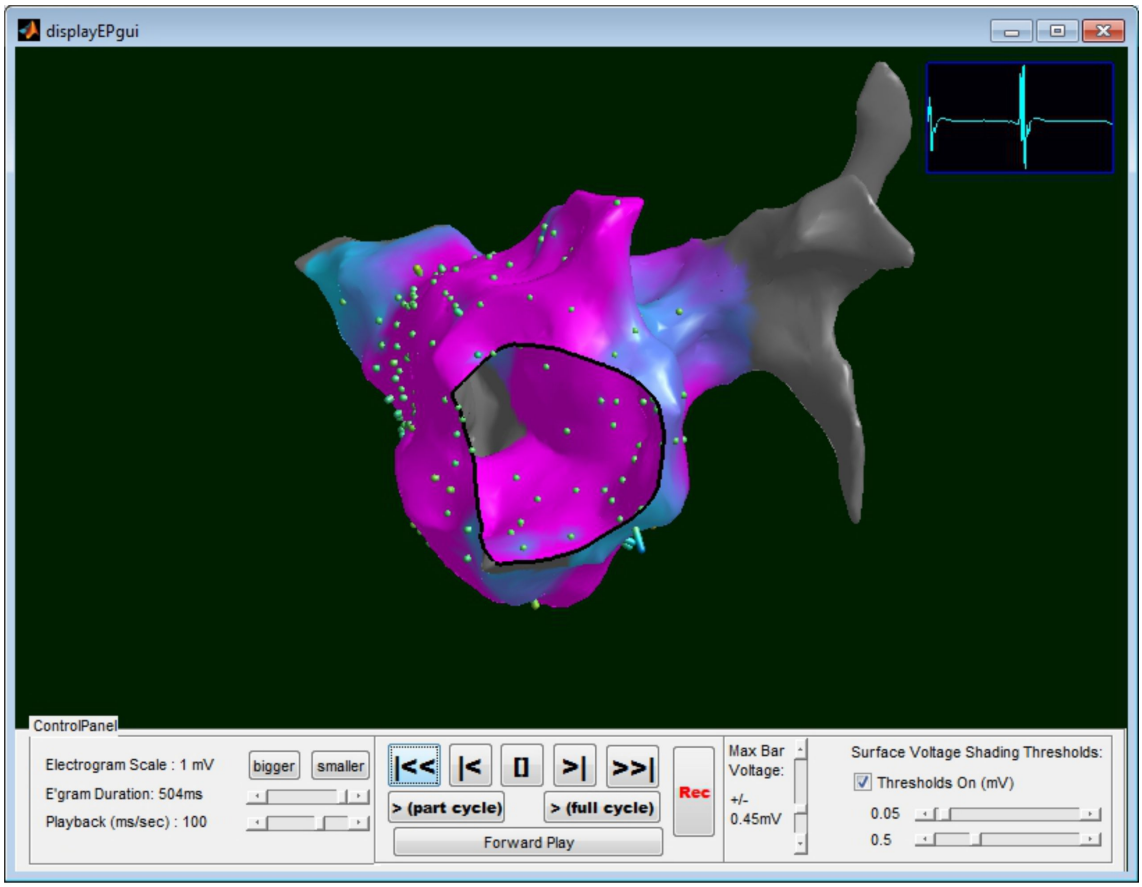

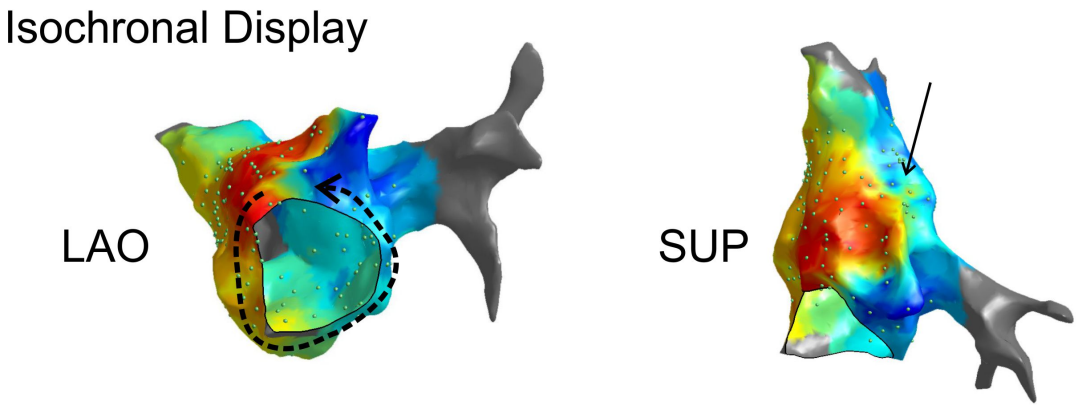

Movie 4-1. [The Movie is included in supplemental data.] Ripple Map from Case 12. The Ripple Map shows activation consistent with anti-clockwise perimitral flutter. There are double potentials at the roof, which successfully convey the impression of activation reaching a previous ablation line from the anterior wall, and then from the posterior wall. Most areas of atrium have a voltage >0.5mV, facilitating interpretation.

In the lower panel, two views of the isochronal map. In the LAO view, the tachycardia mechanism is demonstrated clearly (dotted arrow). In the superior (sup) view, there is ambiguity of LAT assignment at the roof (thin arrow) and the presence of double potentials is not conveyed.

The success rate for focal / localised tachycardias was lower than for macroreentry. In Case 1, there was a focal tachycardia originating from the left superior pulmonary vein, and the LA had normal voltages throughout. In this case, all observers made the correct diagnosis using both the Ripple Map and also the isochronal map. Similarly, in Case 2, there was a focal breakout from the left superior vein in a patient in whom PVI had previously been performed. Reentry could not be ruled out as a mechanism but the activation pattern of the LA was from a 'source' in the pulmonary vein.

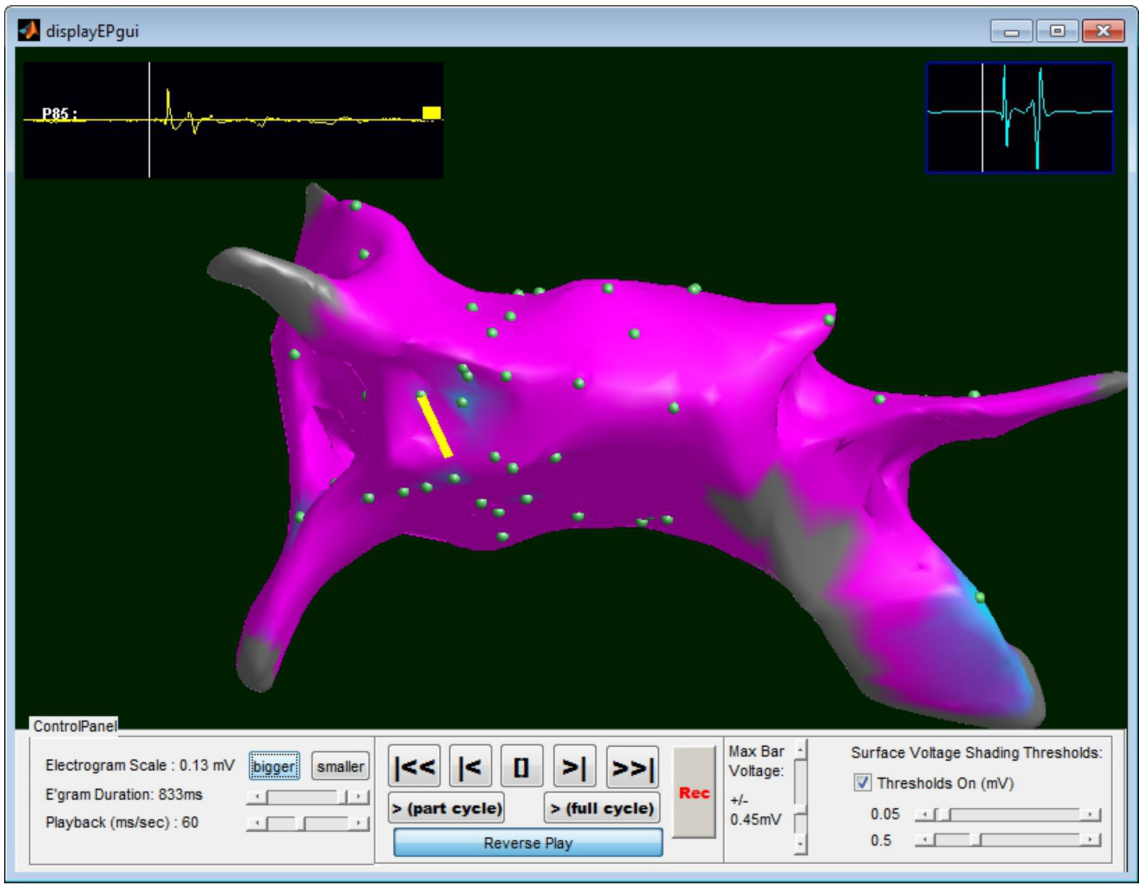

Isochronal Display

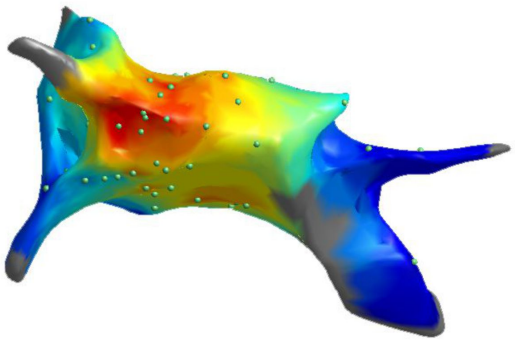

Movie 4-2. [The Movie is included in supplemental data.] Ripple Map from Case 2, viewed from superior/posterior. The Ripple Map shows activation earliest at P85 (electrogram shown). Activation is centrifugal away from this location.
The isochronal display is shown in the lower panel. For this tachycardia all observers correctly interpreted both types of map.

The other cases involving a focal / localised reentry mechanism were Cases 3 and 4. In both of these, a substantial portion of the LA surface had bipolar electrogram voltages <0.5mV and the localised reentry circuit had portions with voltages similar to

the intrinsic noise of the measuring system (<0.05mV). It is notable that during the ablation procedure for Case 3, the correct location of the circuit was not correctly identified and tachycardia terminated when ablation was re-directed to an area of fractionated activity approximately 1cm away from the initial site. In Case 4, interpretation of activation was also difficult. In the clinical case, temporary cessation of tachycardia was noted with catheter pressure during mapping. Ablation at this site resulted in termination and non-inducibility of tachycardia. Figure 4-3 illustrates the localised reentry circuits for these cases.

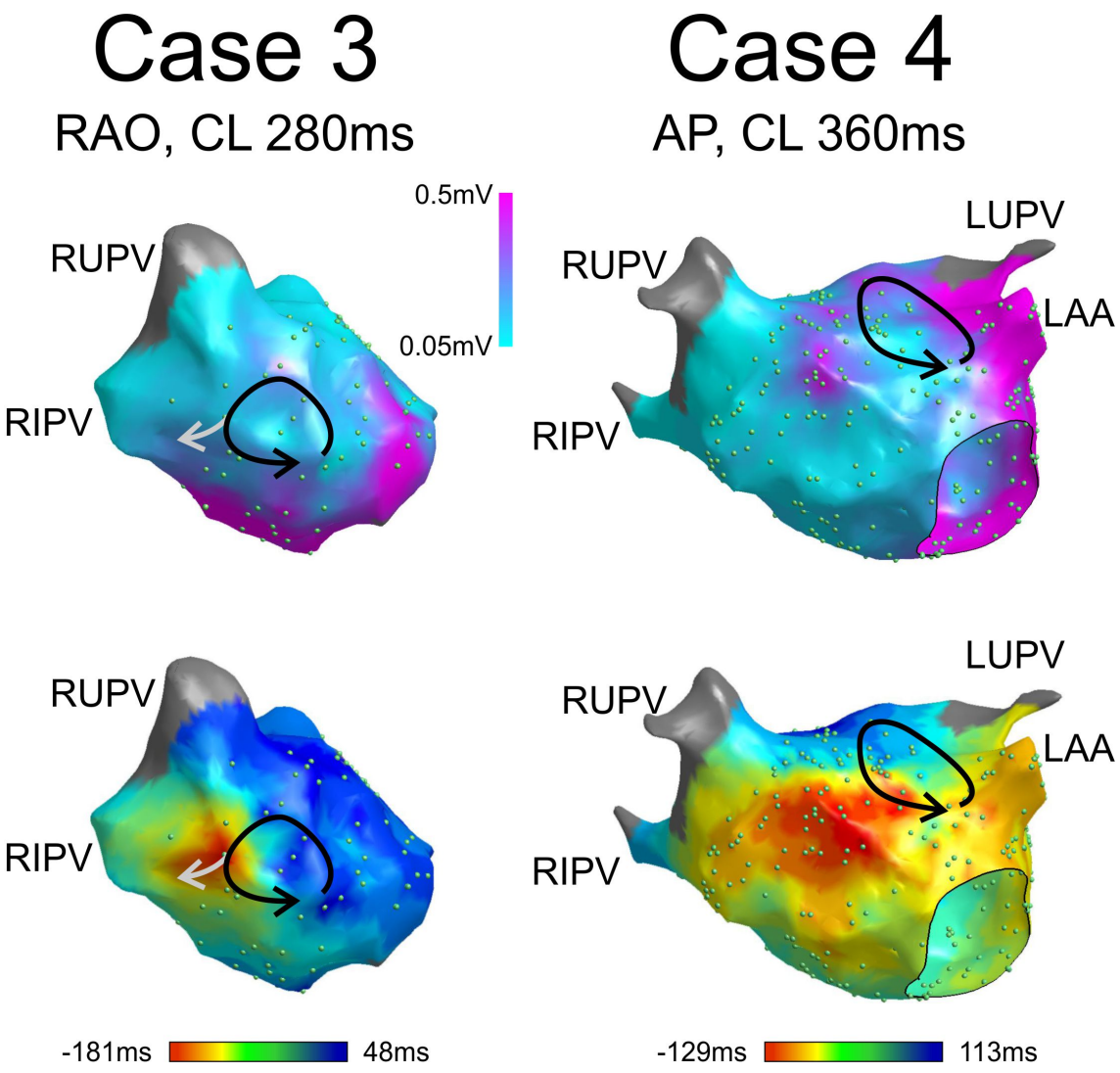

Figure 4-3. Upper Row: Voltage maps for Cases 3 and 4. **Lower Row:** The corresponding isochronal maps. The black arrows represent the localised reentry circuit, which has been inferred by examination of the maps and also *post hoc* knowledge of the location where a single lesion caused tachycardia termination. In each case, large areas of the atrium have electrograms with voltage amplitudes of less than 0.05mV. This limited the number of electrogram points that were recorded, particularly in Case 3, because of the difficulty in assigning activation time when using Carto 3. On each map, the ablation lesion resulting in termination of tachycardia is located at the black arrowhead. In Case 3, ablation was initially attempted at the grey arrowhead because this was where activation appeared to 'break out'. The cases can also be viewed as **Movie 4-3** and **Movie 4-4**.

Cases 3 & 4, illustrated in Figure 4-4, were the tachycardias with the lowest rate of successful interpretation. However, Case 3 had a higher rate of success when the Ripple Mapping was used, in comparison to the isochronal map. The isochronal map

drew users to the 'earliest' electrogram, as it had done in the clinical case, to the site were ablation was directed first without success. However, with the Ripple Map observers did not state a single point for an ablation target but instead correctly identified a larger region of interest. One of the limitations of this study, is that the benefits of mapping systems are best assessed using tachycardias where the activation pattern is difficult to ascertain. Unfortunately, this is a small proportion of the clinical tachycardias that are encountered.

Although it did not reach statistical significance, there was a trend towards higher success rates with interpretation of RA Ripple Maps than with the isochronal maps. All of these patients had previous atriotomy scars. Incorporation of the voltage data onto the Ripple Map was useful for interpreting activation within the context of underlying substrate. See Figure 4-4.

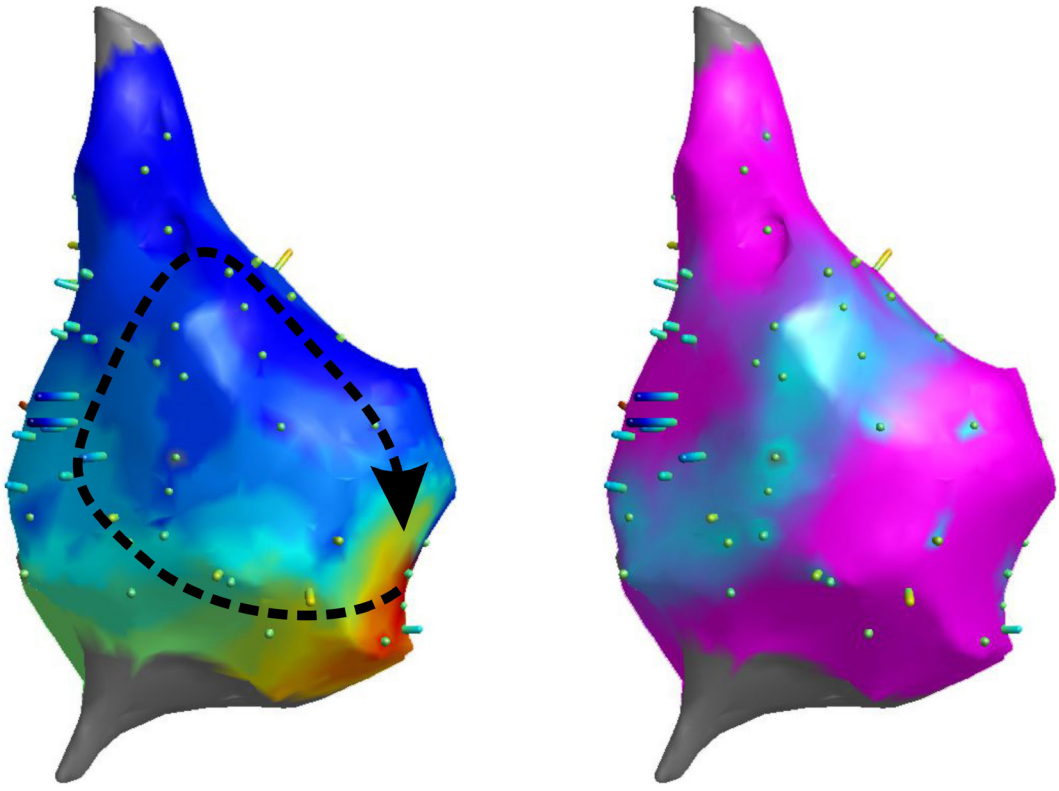

Figure 4-4. Case 13, dual-loop reentry around a right lateral atriotomy and around the tricuspid annulus. There was difficulty in obtaining points with clear activation times, so the density of points is low where 'early meets late' on the isochronal map. The Ripple Map shows the location of the atriotomy scar from the Carto3 data. It can be viewed as **Movie 4-5**.

4.6 Discussion

This study has shown that Ripple Mapping is capable of conveying the correct activation pattern to electrophysiologists who are not practised in its use. The success rates for identifying correct activation were similar to those for identifying activation on isochronal maps. However, Ripple Mapping has the advantage that no user-defined window of interest is required and the user does not need to annotate the local activation time for each individual electrogram. The use of atrial shells produced with Fast Anatomical Maps (FAM) from the Carto3 system allowed interpretation of activation despite being concave in some areas (see Chapter 3).

In cases with macroreentry, the success rate for identifying tachycardia mechanisms was high and the efficacy of Ripple Mapping was, again, similar to isochronal mapping. The success rate for correctly identifying activation patterns was lower in the group of cases that exhibited localised reentry, using any form of activation map. There are several explanations for this finding. First, these tachycardias usually arise from areas of tissue that have been altered by previous ablation. Therefore the electrograms in the area of interest often have low voltages which are similar in amplitude to the noise in the recordings. This makes identification of activation timing difficult, whatever method is used. Second, there is a more varied substrate for localised reentry tachycardias, in contrast to the stereotypical macroreentry circuits with their relatively clear targets for ablation (e.g. see Figure 1-3, p20).

One of the limitations of this study is that electrogram points were collected for the purpose of LAT assignment and incorporation into an isochronal map. In areas with low voltage or ambiguous activation times then some points may not have been collected because of the risk of creating an incorrect isochronal map (see Chapter 3, Figure 3). However, these are the areas where a high density of points might be more useful for the Ripple Mapping because this makes activation easier to identify. For example, in Case 3, Ripple Mapping did suggest a low voltage localised reentry circuit to some users, whereas the isochronal map seemed suggestive of a more focal tachycardia.

In the future, if Ripple Mapping is incorporated into an electroanatomic mapping system then the collection of data will be directed towards interpretation of the Ripple Map rather than an isochronal map. Locations with low voltage and indeterminate activation times could still be collected, without fear that they will adversely affect the map. This may be particularly useful if multi-electrode mapping is employed because this utilises catheters with up to 20 electrodes, which collect 10 bipolar electrograms simultaneously. Although this has the potential to allow much faster and more densely spaced electrogram acquisition, it does require that every electrogram is correctly annotated with the LAT for an isochronal map. This is likely to be the critical factor in enabling an accurate diagnosis to be achieved. In contrast, with Ripple Mapping it is likely that electrograms could be collected much more quickly because they are interpreted 'as is' on the Ripple Map rather than requiring any form of user pre-processing.

Even with a very high density of points, it is likely that interpretation of Ripple Maps will be difficult in areas of low voltage. If there is no recordable signal then no technique will be able to assess direction of activation. In the presence of very small signals, then avoidance of electrical noise in the catheter laboratory is even more important. It is also possible that some signal processing techniques could improve the clarity of the recorded electrograms. In the current study, all electrograms were collected from a 4mm-tip ablation catheter with a 2mm gap to the proximal 2mm ring electrode. If multi-electrode mapping is used, then these catheters usually have smaller electrodes with a wider spacing. The effects of these different electrode dimensions have not been studied.

At present, mapping systems are tools to assist the electrophysiologist. In difficult cases, their skill at incorporating information about the patient, the activation pattern, cycle length variability, and entrainment information is critical to achieving the right ablation strategy. In this study, a questionnaire survey was used to quantify successful interpretation. However, 'offline' analysis does not provide the same time for the electrophysiologists to consider the nuances of the case. Most activation maps were interpreted within approximately 5 minutes – considerably shorter than it would take to create a map in the clinical situation. It is possible that when activation maps

are collected in the context of a mapping strategy that diagnostic accuracy might be higher.

4.7 Conclusion

Ripple Mapping enables assessment of atrial tachycardia activation without requiring assignment of local activation times or a pre-defined window of interest. The prototype software was used successfully by observers to analyse cases and was non-inferior to analysis of isochronal maps. Ripple Mapping was able to indicate activation at points with double potentials. However, where the electrogram voltage was small in comparison to underlying noise, discerning activation was difficult.

5 A New Criterion for Detecting Reentry

5.1 Aims for this chapter

E1 Re-assess the criteria for entrainment to see if the principles can be reformulated into a method that is practical for use during AT procedures.

E2 Re-assess the criteria for entrainment, with a view to detecting double-loop reentry.

5.2 Introduction

The following work has recently been accepted for publication[195], with an accompanying editorial.[196] This has been reorganised to include the appendices within the text, additional discussion, and data from a recently published case report.

Atrial tachycardia occurs commonly in the context of ablation for persistent AF or prior surgery for congenital or acquired heart disease.[31, 95, 197] Successful catheter ablation therapy requires the mechanism to be elucidated, typically using a combination of activation mapping and also overdrive pacing manoeuvres.[3, 86, 198, 199] Overdrive pacing to entrain macroreentry circuits was first described by Waldo and colleagues, and they developed four criteria whose presence indicates reentry (although absence of the criteria does not exclude reentry).[156, 200, 201] These were pivotal in establishing the mechanism of reentry but their applicability can be limited - particularly for atrial tachycardia. This is discussed in Section 1.4.3 on p38.

During atrial ablation procedures, overdrive pacing (entrainment) manoeuvres carry the risk of changing or terminating the tachycardia.[3, 93] Typically, overdrive pacing is performed from a limited number of different positions, seeking a short post-pacing interval, while keeping 'reference' electrodes at the same locations (e.g. coronary sinus and right atrium).[3] Algorithms have been developed to assist with localizing the tachycardia circuit on the basis of post-pacing intervals.[170] However, in order to maximise the diagnostic gain, it would be advantageous to use information from all these available electrode recordings.

This study was conducted in two phases: 1) *Development of the entrainment criterion* using a detailed mathematical description and also illustrated with a mathematical model of uniform conduction; and 2) *Testing of the entrainment criterion* using clinical data.

5.3 Proposed criterion

The proposed criterion relies upon adherence to the definitions of overdrive pacing, FBT, Activation Difference, and centrifugal tachycardia that are listed below, in Table 5-1.

Overdrive pacing	During tachycardia, pacing and capturing the relevant cardiac chamber(s) at a constant rate that is faster than the rate of the spontaneous tachycardia and that fails to interrupt it.
First beat of tachycardia (FBT)	After the termination of overdrive pacing, the first beat of tachycardia (at any particular site) is the first activation where the preceding cycle length is longer than the overdrive pacing cycle length.
Activation Difference	The time difference between the first beat of tachycardia at two sites.
Centrifugal tachycardia	A tachycardia with activation that spreads centrifugally from a small area. The mechanism could be focal automaticity, micro-reentry, or localised reentry.

Table 5-1. Definitions.

The proposed criterion follows in Table 5-2.

After overdrive pacing at two different locations and assessing the first ensuing beats of tachycardia, the difference in activation time recorded between any two stationary positions changes by one or two tachycardia cycle lengths.

$$\left|[T_A - T_B]_{overdrive\ 1} - [T_A - T_B]_{overdrive\ 2}\right| \approx TCL$$

$$\left|[T_A - T_B]_{overdrive\ 1} - [T_A - T_B]_{overdrive\ 2}\right| \approx 2 \times TCL$$

A change of two tachycardia cycle lengths is usually due to double-loop reentry.

Table 5-2. Proposed criterion for reentry. If the criterion is not observed, then this does not exclude the presence of reentry. In the mathematical expressions: *A* and *B* refer to two different locations. T_A is the time of FBT at A following cessation of overdrive pacing, and TCL is the tachycardia cycle length. $[T_A - T_B]_{overdrive\ 1}$ is the Activation Difference between A and B (as defined in Table **5-1**) corresponding to the first overdrive pacing manoeuvre

5.4 Development of the new criterion

5.4.1 An intuitive example – single loop reentry

Consider a 'clockwise' reentrant circuit with catheters positioned at 12 o'clock and 3 o'clock. After overdrive pacing from the first, the difference in timing of the first beat of tachycardia (FBT) is 3 'hours', i.e. activation proceeds from 12 o'clock to 3 o'clock. After overdrive pacing from the second, activation proceeds from 3 o'clock to 12 o'clock: the difference in timing is 9 'hours' and the order of activation is reversed (as long as antidromic penetration of the circuit did not reach the first catheter during entrainment). The change in Activation Difference is 3-(-9) = 12 'hours', which is equal to the tachycardia cycle length (TCL). It will be shown that this proves that reentry is present. The criterion developed in this study can also be applied to situations where pacing and sensing are performed from different catheters that are not close to the tachycardia circuit.

5.4.2 Mathematical development

This section describes the background to the criterion using a mathematical basis. I am grateful to Dr Steven Niederer (Division of Imaging Sciences, KCL) for verifying the

equations that are presented. The concepts are also illustrated in Section 5.4.3 (p96) using a model with uniform conduction across a sheet of tissue.

In the following discussion, geodesic paths between points are represented with "→" and we use the term 'geodesic' to describe a path where the conduction time between any two local points on the path is minimised. The shortest time for activation to travel from x to y is indicated by $T(x \rightarrow y)$. By describing activation in this way, spatially non-uniform and anisotropic conduction can be accounted for. After cessation of overdrive pacing, it is assumed that the relative timing of the first beat of tachycardia between any two points is not significantly perturbed, in comparison to the timing for the following beats. For reentry circuits, it is assumed that the conduction time of any path that circumnavigates the circuit is at least as long as the TCL.

Centrifugal tachycardia

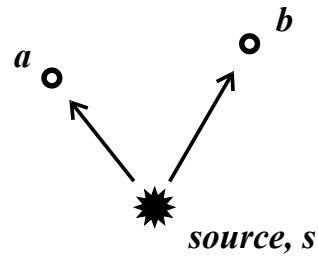

Figure 5-1. Scheme for centrifugal tachycardia.

After entrainment of a centrifugal tachycardia, the first beat of tachycardia emanates from the tachycardia source, s. Therefore, if there are two catheters at a and at b, then the activation difference is:

$$AD_{a,b} = FBT_b - FBT_a = T(s \rightarrow b) - T(s \rightarrow a) \quad [5\text{-}1]$$

The activation pattern of the first beat of tachycardia is independent of the position from which entrainment was performed. If two entrainment manoeuvres are compared, then there will be no significant change in activation difference.

Single loop reentry

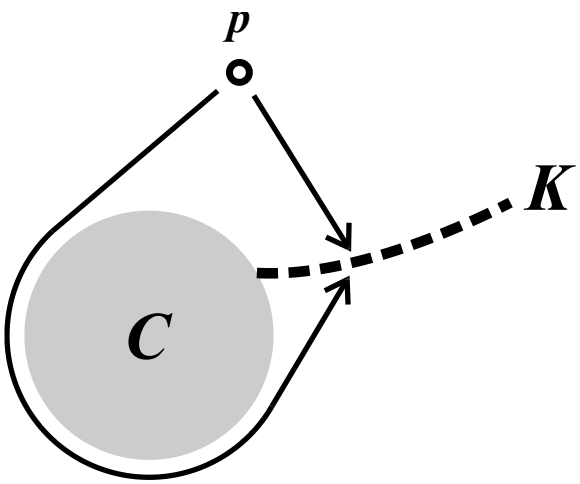

Figure 5-2. Scheme for single loop reentry.

For a single loop reentry circuit, during overdrive pacing from point, p, there is a line of wave collision where the antidromic wavefront collides with the orthodromic wavefront from the previously paced beat. This occurs at a line, K, such that at any location on the line:

$$T(p \to K) = T\left(p \overset{C}{\to} K\right) - PCL \qquad [5\text{-}2]$$

where, PCL is the pacing cycle length, $T(p \to K)$ is the time taken to traverse the shortest geodesic from p to K, and $T\left(p \overset{C}{\to} K\right)$ is the time taken to traverse the shortest geodesic from p to K that also joins the tachycardia circuit, orthodromically, for part of its course.

After the last pacing stimulus, the last paced wavefront continues to activate the surface because there are no further collisions at the line K: activation can continue $p \overset{C}{\to} K \to onwards$. Therefore, the wavefront causing the first beat of tachycardia has originated from the pacing site, then travelled around part of the tachycardia circuit, C, and then passed exactly once through line K.

Let c be a point on $p \overset{C}{\to} K$ that is on the circuit, C. Considering the first beat of tachycardia, the path from p to any recording site, r, must cross the location of the

collision line K exactly once. The alternatives are illustrated in Figure 5-3 and given in [5-3].

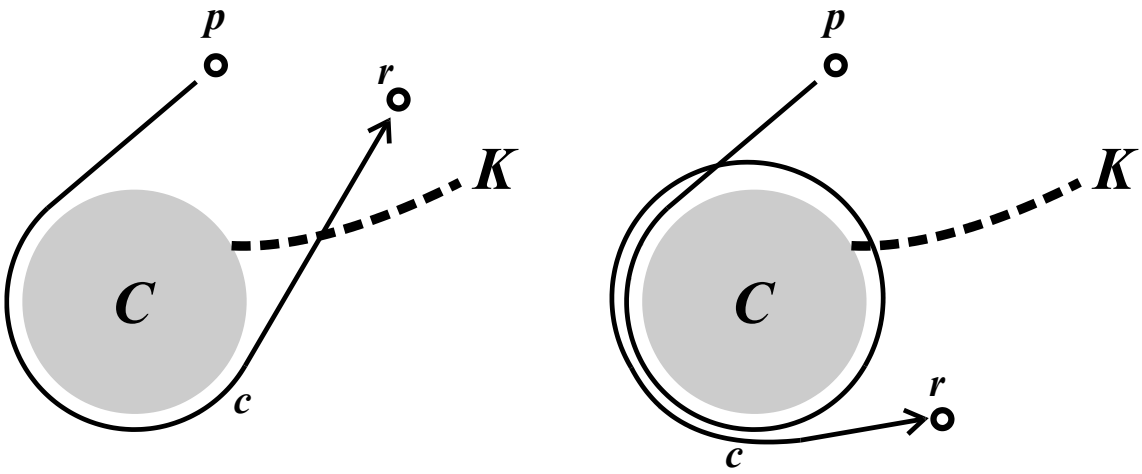

Figure 5-3. Illustration for Equation [5-3].

$$FBT_r = \begin{cases} LPB_p + T(p \to c \to r) \ , & if\ c \overset{K}{\to} r \\ LPB_p + T(p \to c \to K \to c \to r) \ , & otherwise \end{cases} \quad [5\text{-}3]$$

$c \overset{K}{\to} r$ indicates that the path $c \to r$ crosses line K. LPB_p is the time of the last paced beat at the pacing location, p.

In general,

$$T(x \to y \to z) = T(x \to y) + T(y \to z) \quad [5\text{-}4]$$

Also, $T(c \to K \to c)$ is equal to one tachycardia cycle length and so [5-3] can be rearranged:

$$FBT_r = \begin{cases} T(p \to c) + T(c \to r) \ , & if\ c \overset{K}{\to} r \\ T(p \to c) + TCL + T(c \to r) \ , & otherwise \end{cases} \quad [5\text{-}5]$$

Now consider the activation difference, $AD_{a,b}$, at two recording sites a and b, which we define as:

$$AD_{a,b} = FBT_b - FBT_a \quad [5\text{-}6]$$

Then, combining [5-5] and [5-6]:

$$AD_{a,b} = \begin{cases} T(c \to b) - T(c \to a) \ , & if \ c \xrightarrow{K} b \ , \quad c \xrightarrow{K} a \\ T(c \to b) - T(c \to a) - TCL \ , & if \ c \xrightarrow{K} b \ , \quad c \xrightarrow{not\ K} a \\ T(c \to b) + TCL - T(c \to a) \ , & if \ c \xrightarrow{not\ K} b \ , \quad c \xrightarrow{K} a \\ T(c \to b) - T(c \to a) \ , & if \ c \xrightarrow{not\ K} b \ , \quad c \xrightarrow{not\ K} a \end{cases} \quad [5\text{-}7]$$

where c is a constant position on the circuit, C, such that $T(c \to a)$ and $T(c \to b)$ are geodesic paths starting in the orthodromic direction, and c is chosen to minimise these distances, i.e. c is at the 'exit' from the circuit (see Figure 5-3). [5-7] can be restated:

$$AD_{a,b}(K) = \begin{cases} \Delta - TCL, & if \ c \xrightarrow{K} b \ , \quad c \xrightarrow{not\ K} a \\ \Delta + TCL, & if \ c \xrightarrow{not\ K} b \ , \quad c \xrightarrow{K} a \\ \Delta, & otherwise \end{cases} \quad [5\text{-}8]$$

$$\Delta = T(c \to b) - T(c \to a) \quad [5\text{-}9]$$

Equation [5-8] indicates that the relative timing of FBT at two sites depends upon their location and also the position of the collision line, K, that was created during entrainment. Note that, with respect to the activation of the first beat of tachycardia, it is the position of the collision line, K, that is important rather than the position of the pacing location (although the two are related). Consider the change in activation difference with two different manoeuvres, represented by two different collision lines, K_1 and K_2. Using Equation [5-8]:

$$AD_{a,b}(K_2) - AD_{a,b}(K_1)$$

$$= \begin{cases} \pm 2 \times TCL \ , & c \xrightarrow{K_1} b, c \xrightarrow{not\ K_1} a, c \xrightarrow{not\ K_2} b, c \xrightarrow{K_2} a \ \ OR \ \ c \xrightarrow{K_1} a, c \xrightarrow{not\ K_1} b, c \xrightarrow{not\ K_2} a, c \xrightarrow{K_2} b \\ \pm TCL \ , & existence\ of\ intersection\ between\ c \to b\ OR\ c \to a\ with\ K\ change \\ 0 \ , & otherwise \end{cases} \quad [5\text{-}10]$$

This is represented in diagrammatic form below in Figure 5-4.

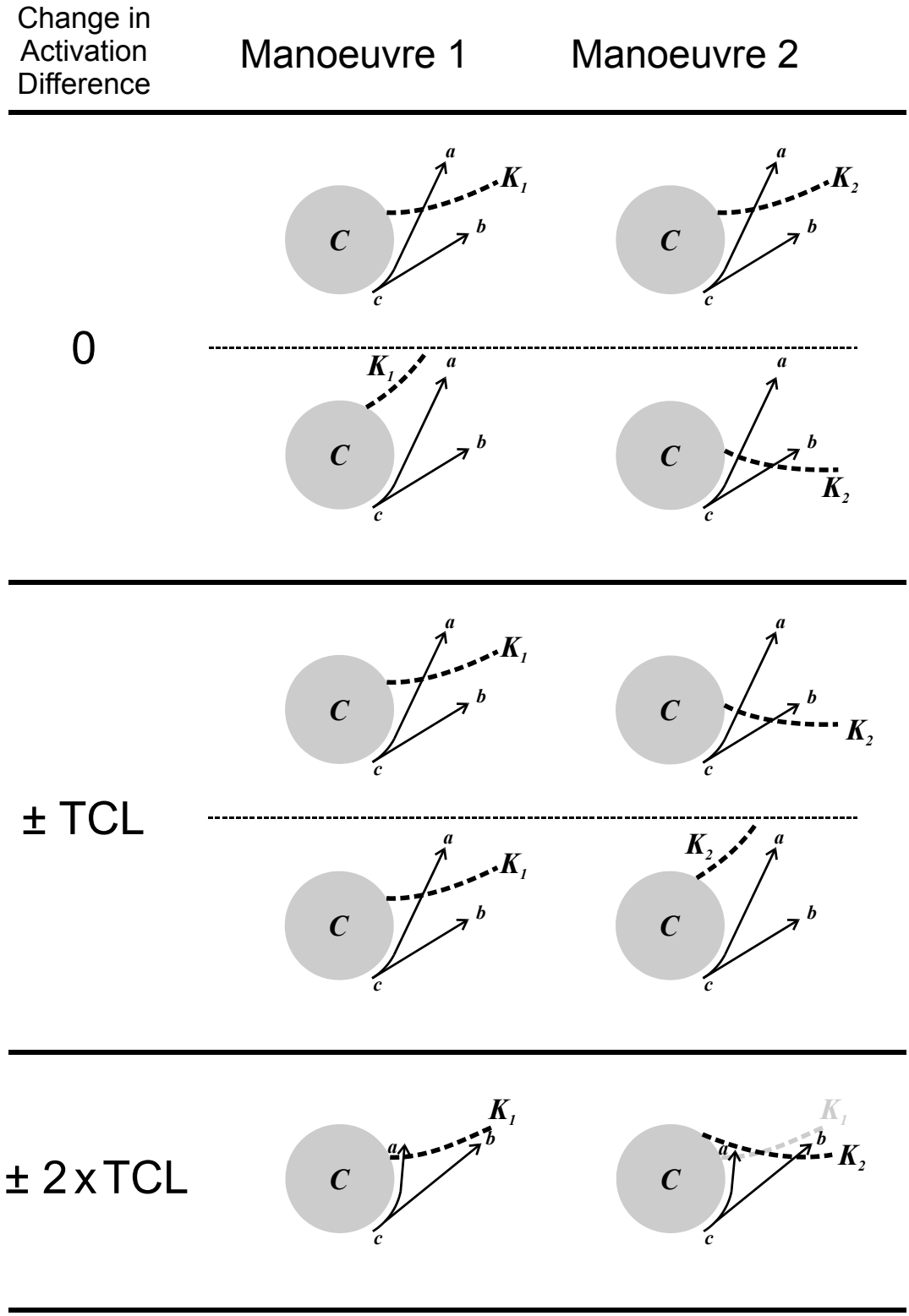

Figure 5-4. Schematic representation of [5-10]. To obtain all mathematical possibilities, the order of the manoeuvres can be reversed and the positions a and b can be interchanged. Further explanation is given in the text. The point c is a position on the circuit, C, such that $T(c \to a)$ and $T(c \to b)$ are geodesic paths starting in the orthodromic direction, and c is chosen to minimise these distances.

In the first row of Figure 5-4, the collision line in Manoeuvre 1 and in Manoeuvre 2 does not change with respect to its intersection with $c \rightarrow a$ or $c \rightarrow b$. Therefore, the Activation Difference in both manoeuvres will be the same and so the change will be 0. This situation is also illustrated in Figure 5-10. In the second row, the collision line intersects neither $c \rightarrow a$ nor $c \rightarrow b$ in Manoeuvre 1, but in Manoeuvre 2 it intersects both $c \rightarrow a$ and $c \rightarrow b$. Thus, in both manoeuvres the wavefront passes through the collision line and then through a and b with the same Activation Difference, so again there is a change of 0.

In the next two rows of Figure 5-4 ("±TCL"), the collision line changes its intersection with only one of $c \rightarrow a$ or $c \rightarrow b$. This results in the Activation Difference changing by ±TCL.

In the final row of Figure 5-4, it is demonstrated that the Activation Difference can change by 2 TCL. This can only occur under conditions where the collision lines of the two manoeuvres intersect each other, as shown. This would require pacing manoeuvres to be performed at different distances from the tachycardia circuit and recordings to be made within both small areas of intersection.

Double loop reentry

Consider a dual loop tachycardia circuit, C and C' - as illustrated in Figure 5-5. It is assumed that there is a common isthmus that has a finite width, and that one of the circuits,C, has a transit time that is less than or equal to the transit time of the other, C'. The TCL is the transit time around the shorter circuit. The situation where the common isthmus is very narrow is discussed later.

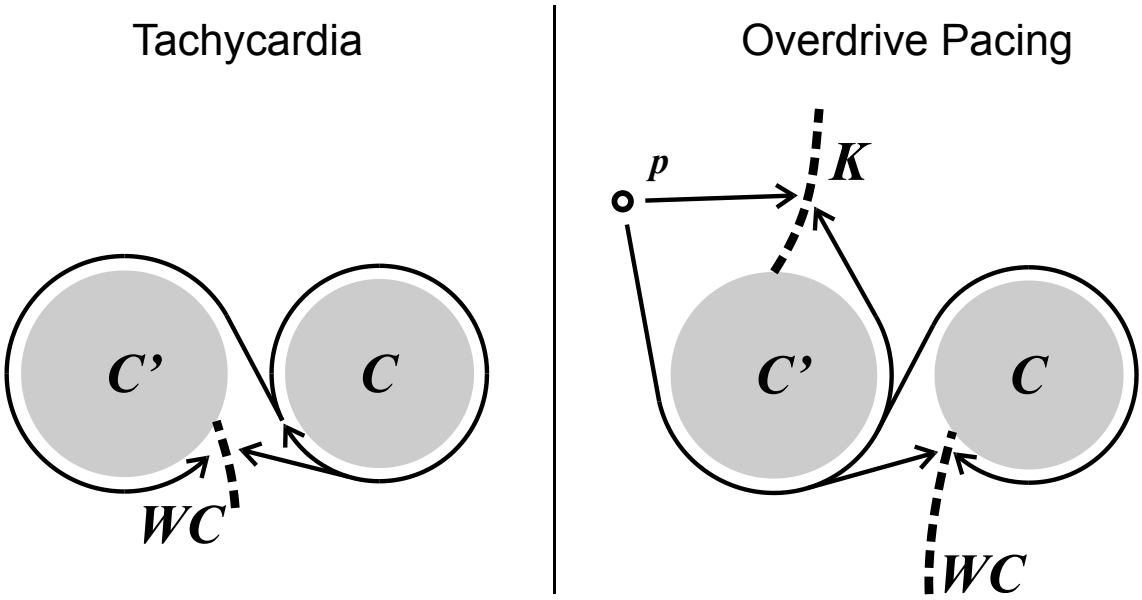

Figure 5-5. Schematic for activation during double loop reentry and also for overdrive pacing of double loop reentry See text for further explanation.

When performing overdrive pacing of a double loop tachycardia, with a cycle length shorter than tachycardia cycle length, there is a line of collision, K, similar to the collision that occurs when overdrive pacing a single-loop reentry tachycardia (refer to Figure 5-2). Additionally, there is a line of wave collision (WC) where wavefronts from each circuit collide with each other. After cessation of overdrive pacing, activation passes through the lines K and WC and tachycardia continues. The line of wave collision, WC, returns to its original location.

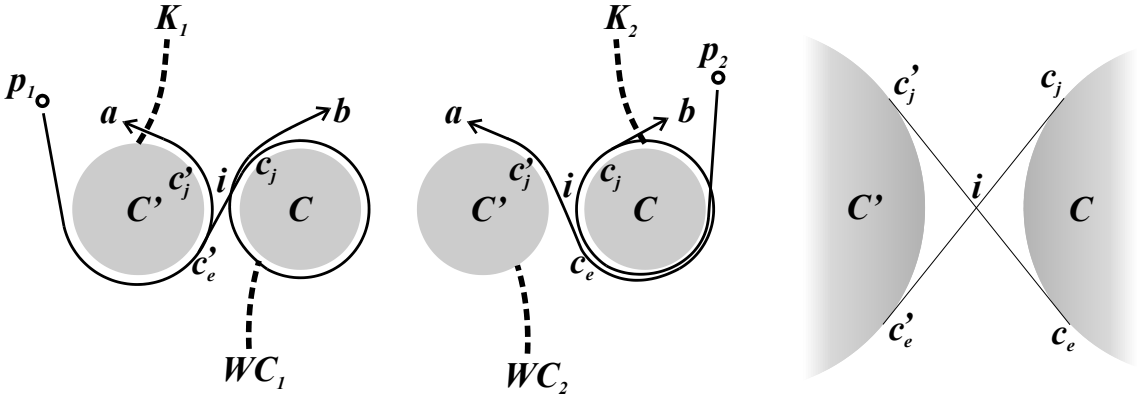

Figure 5-6. Two Overdrive Pacing manoeuvres are illustrated, in a similar way to Figure 5-3. c_e is the location on circuit C where the activation exits the circuit in order to follow a geodesic path to the contralateral circuit C' where it joins at c'_j. c'_e and c_j are corresponding positions on C and on C'. i is the intersection between $c'_e \rightarrow c_j$ and $c_e \rightarrow c_j$.

Figure 5-6 shows a schematic for two different overdrive pacing manoeuvres with a double loop reentry circuit. In the following analysis, we do not consider all possible locations of pacing and recording electrodes. It is assumed that the recording sites, a and b, are on opposite circuits, C and C'. It is also assumed that the paths shown in the figure cross (or do not cross) the lines of collision as illustrated.

The first beat of tachycardia is caused by a wavefront that has travelled through one of the collision lines K or WC exactly one time. Using Figure 5-6, combined with the definition of activation difference in [5-6]:

$$AD_{a,b}(K_1) = T\left(p_1 \rightarrow c'_e \rightarrow i \rightarrow c_j \xrightarrow{C} c_j \rightarrow b\right) - T\left(p_1 \rightarrow c'_e \rightarrow c'_j \rightarrow a\right) \quad [5\text{-}11]$$

$$AD_{a,b}(K_2) = T\left(p_2 \rightarrow c_e \rightarrow c_j \rightarrow b\right) - T\left(p_2 \rightarrow c_e \xrightarrow{C} c_e \rightarrow i \rightarrow c'_j \rightarrow a\right) \quad [5\text{-}12]$$

In equations [5-11] and [5-12], $c_j \xrightarrow{C} c_j$ and $c_e \xrightarrow{C} c_e$ represent entire loops of the tachycardia circuit, C, associated with a transit time of one TCL. Therefore, using [5-4], these equations can be re-written:

$$AD_{a,b}(K_1) = T\left(c'_e \rightarrow i \rightarrow c_j\right) + TCL + T\left(c_j \rightarrow b\right) - T\left(c'_e \rightarrow c'_j\right) - T\left(c'_j \rightarrow a\right) \quad [5\text{-}13]$$

$$AD_{a,b}(K_2) = T\left(c_e \rightarrow c_j\right) + T\left(c_j \rightarrow b\right) - T\left(c_e \rightarrow i \rightarrow c'_j\right) - TCL - T\left(c'_j \rightarrow a\right) \quad [5\text{-}14]$$

Now considering the change in activation difference:

$$AD_{a,b}(K_2) - AD_{a,b}(K_1) = -2 \times TCL + T(c_e \to c_j) - T(c_e \to i \to c_j') - T(c_e' \to i \to c_j) + T(c_e' \to c_j') \quad [5\text{-}15]$$

From Figure 5-6, and the definitions that have been given, we know that:

$$T(c_e \to c_j) < T(c_e \to i) + T(i \to c_j) \quad [5\text{-}16]$$

Therefore, using ε as an error term where $\varepsilon > 0$:

$$T(c_e \to c_j) = T(c_e \to i) + T(i \to c_j) - \varepsilon \quad [5\text{-}17]$$

Similarly, using $\varepsilon' > 0$,

$$T(c_e' \to c_j') = T(c_e' \to i) + T(i \to c_j') - \varepsilon' \quad [5\text{-}18]$$

Now rearranging [5-15] and using [5-17] and [5-18]:

$$AD_{a,b}(K_2) - AD_{a,b}(K_1) = -2 \times TCL + T(c_e \to i) + T(i \to c_j) - \varepsilon - T(c_e \to i) - T(i \to c_j') - T(c_e' \to i) - T(i \to c_j) + T(c_e' \to i) + T(i \to c_j') - \varepsilon' \quad [5\text{-}19]$$

$$AD_{a,b}(K_2) - AD_{a,b}(K_1) = -(2 \times TCL + \varepsilon + \varepsilon') \quad [5\text{-}20]$$

If the manoeuvres were performed in the reverse order, or if the naming of a and b is reversed, then the change in Activation Difference would be positive. Generally:

$$AD_{a,b}(K_2) - AD_{a,b}(K_1) = \pm(2 \times TCL + \varepsilon + \varepsilon') \quad [5\text{-}21]$$

The error terms result from time taken to traverse the isthmus. If there is no width to the isthmus between the circuits, then c_j, c_e, c_j', c_e', and i will all have the same position and so, from [5-17] and [5-18], $\varepsilon = \varepsilon' = 0$.

5.4.3 Illustration of the new criterion

To illustrate the criterion, reentry is modelled around circular obstructions on uniformly conducting sheets: mathematical formulae for all isochrones and lines on the figures were derived using basic geometry, and implemented using Matlab (Mathworks, MA). However, the key results of these models hold with any topological transformation. That is, the sheets and isochrones can be stretched and distorted in order to account for zones of slow conduction, non-uniform conduction velocities and the irregular shape of reentrant circuits in real hearts. It is assumed that conduction properties after the cessation of pacing are stable and similar to those during sustained tachycardia, and that the conduction time of any path that circumnavigates the circuit is at least as long as the TCL.

Single loop reentry

Figure 5-7 illustrates entrainment and the mechanism by which reentry leads to the criterion for single-loop reentry proposed in Table 5-2. During sustained reentry, the tachycardia circuit does not have any 'start' or 'end'. However, during entrainment there is a line of collision where the antidromic wavefront from the pacing electrode meets the orthodromic wavefront from the previously paced beat (or functional block can occur in an area of slow conduction). After cessation of pacing, the paced orthodromic wavefront can pass through the line where the collision occurred and becomes the FBT as it does this.

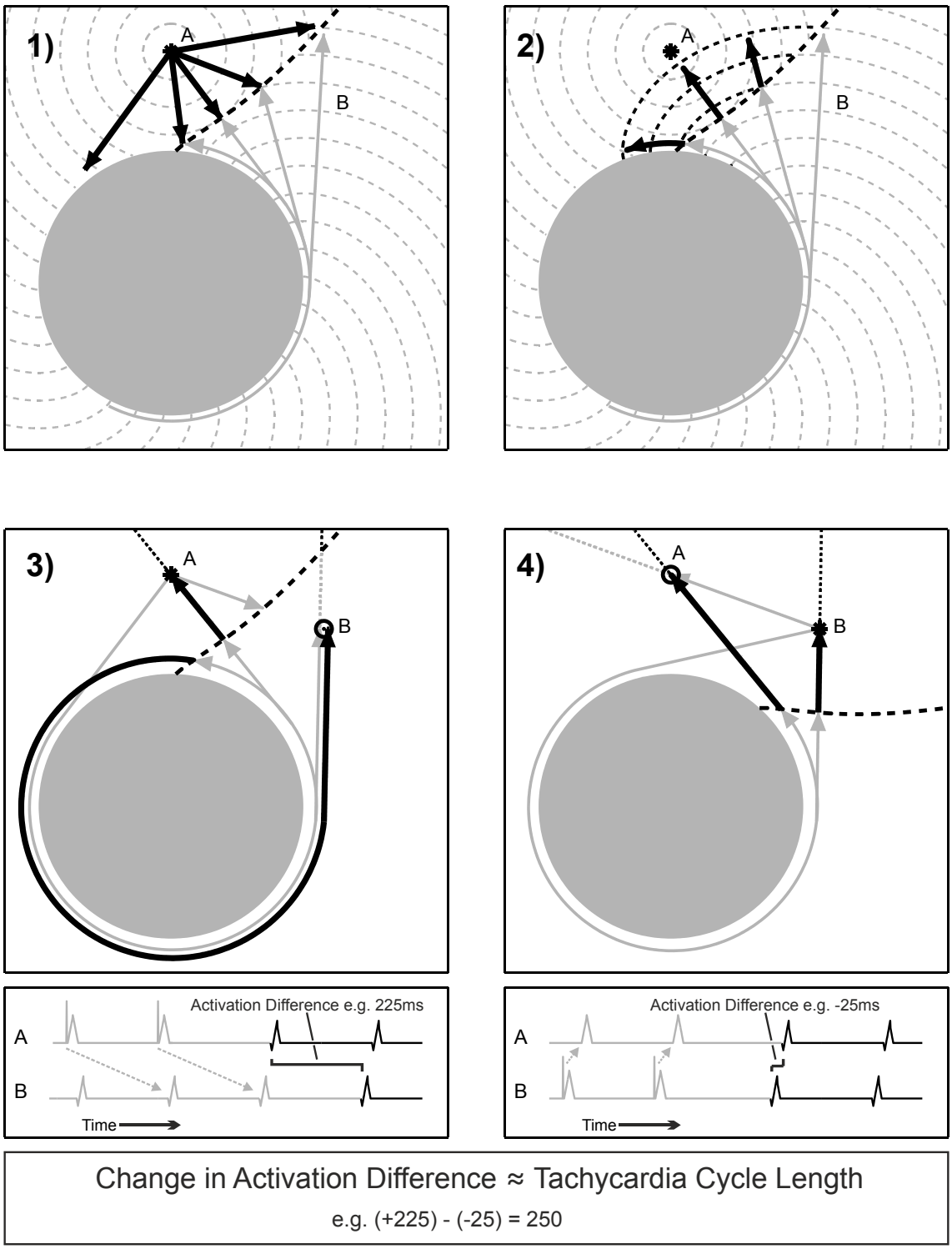

Figure 5-7. Reentry around an obstruction (solid grey circle). Legend follows on next page.

Panel 1 illustrates entrainment with isochrones shown as grey-dashed lines and the pacing site as an asterisk. The orthodromic wavefront from a paced beat has travelled around the circuit (grey) and collided with the antidromic wavefront from the next paced beat (black). In **Panel 2** there is no further paced beat. Transition from last paced beat (grey) to FBT (black) occurs where the activation wavefront passes through the former collision line (thick black dash). This is consistent with the definition of FBT in Table 5-1. Note that close to the circuit, FBT may *precede* the last paced beat at some other locations. **Panel 3** is similar to Panel 2 but without isochrones and includes the complete geodesic paths from the pacing location (A) up to FBT at A and at B. During pacing, antidromic conduction to B is blocked at the collision line, and so activation occurs orthodromically via the circuit with a long transit time (grey arrows). After the last paced beat, the activation wavefront passes through the former collision line to become responsible for FBT (black arrows). Note that the wavefront causing FBT at B has completed almost one revolution of the circuit more than the wavefront causing FBT at A. The corresponding electrograms are illustrated below, with activation at the pacing CL shown in grey: at each site, the FBT is the first complex drawn in black. Difference in the timing of FBT (i.e. Activation Difference) is marked. In **Panel 4**, entrainment has been performed from B and the line of collision (thick-black-dash) has moved so that it no longer intersects the shortest path between the catheters. In contrast to Panel 3, FBT occurs at B and then A in rapid succession. Consequently, as shown on the electrograms below, the relative timing of FBT at these sites has changed by one TCL, fulfilling the criterion for reentry (see Table 5-2).

When transient entrainment is performed from different locations then the sequence of FBT will change because the circuit resumes activation at different phases of tachycardia. It was hypothesised that this change can be detected when the relative timing of FBT, recorded at different sites, changes by one TCL. In contrast, for a centrifugal tachycardia, the activation wavefront causing FBT will always arise from a similar location and so different recording sites will have a comparatively fixed timing relationship. This is illustrated in Figure 5-8. In Figure 5-9, Figure 5-10, and Figure 5-11 illustrations of other catheter positions are shown, with single loop reentry, and different theoretical values of the change in Activation Difference are demonstrated.

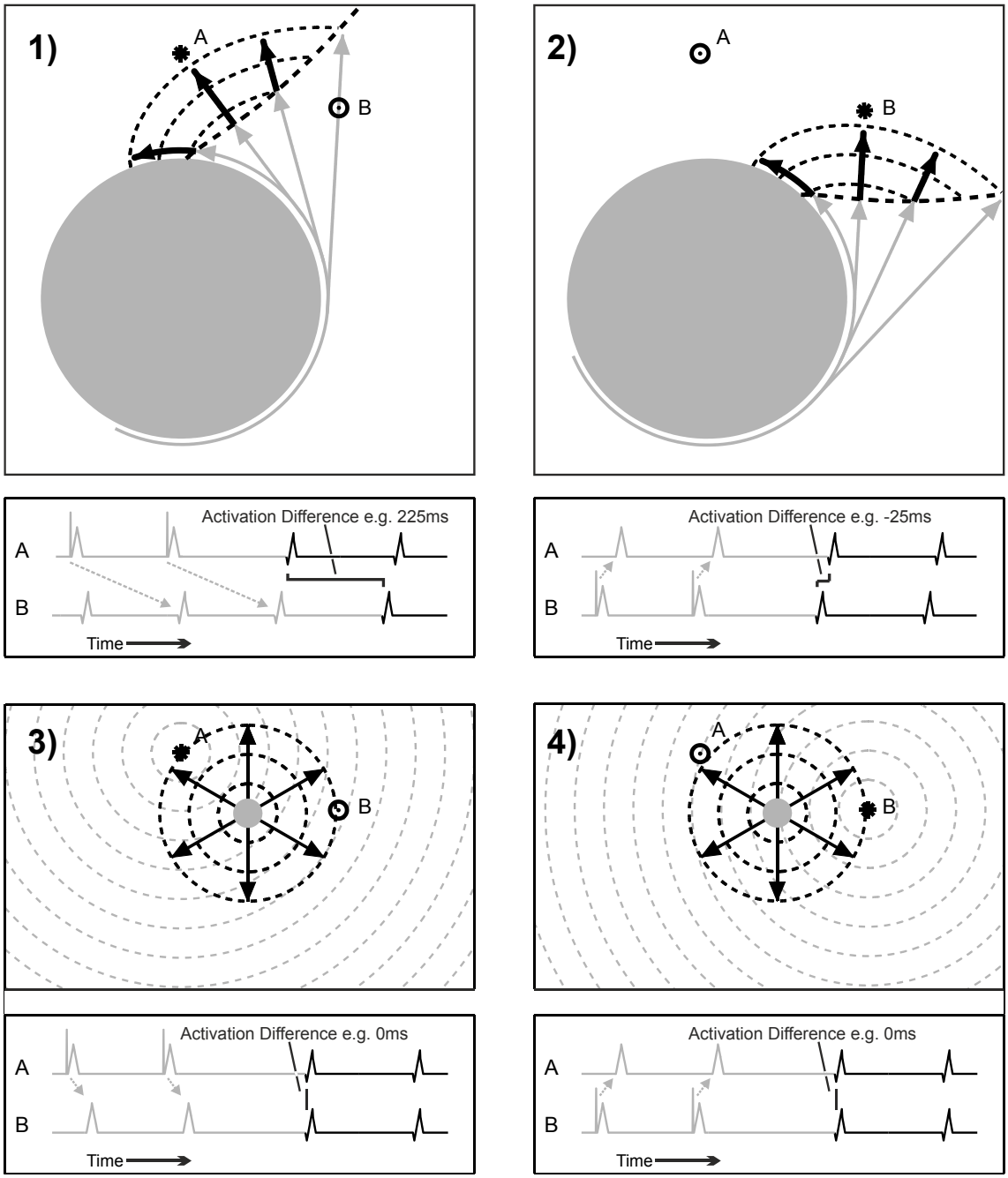

Figure 5-8. Comparison of macroreentry with centrifugal tachycardia. **Panels 1) and 2)** illustrate entrainment of a macroreentrant tachycardia from 2 locations with similar post-pacing intervals. The activation sequence at A and B changes, as described in Figure 5-7. In **Panels 3) and 4)** entrainment of a centrifugal tachycardia is illustrated. The activation sequence remains similar, despite overdrive pacing from different locations. Additionally, the Activation Difference would be similar if the post-pacing interval altered due to transient slowing of the tachycardia.

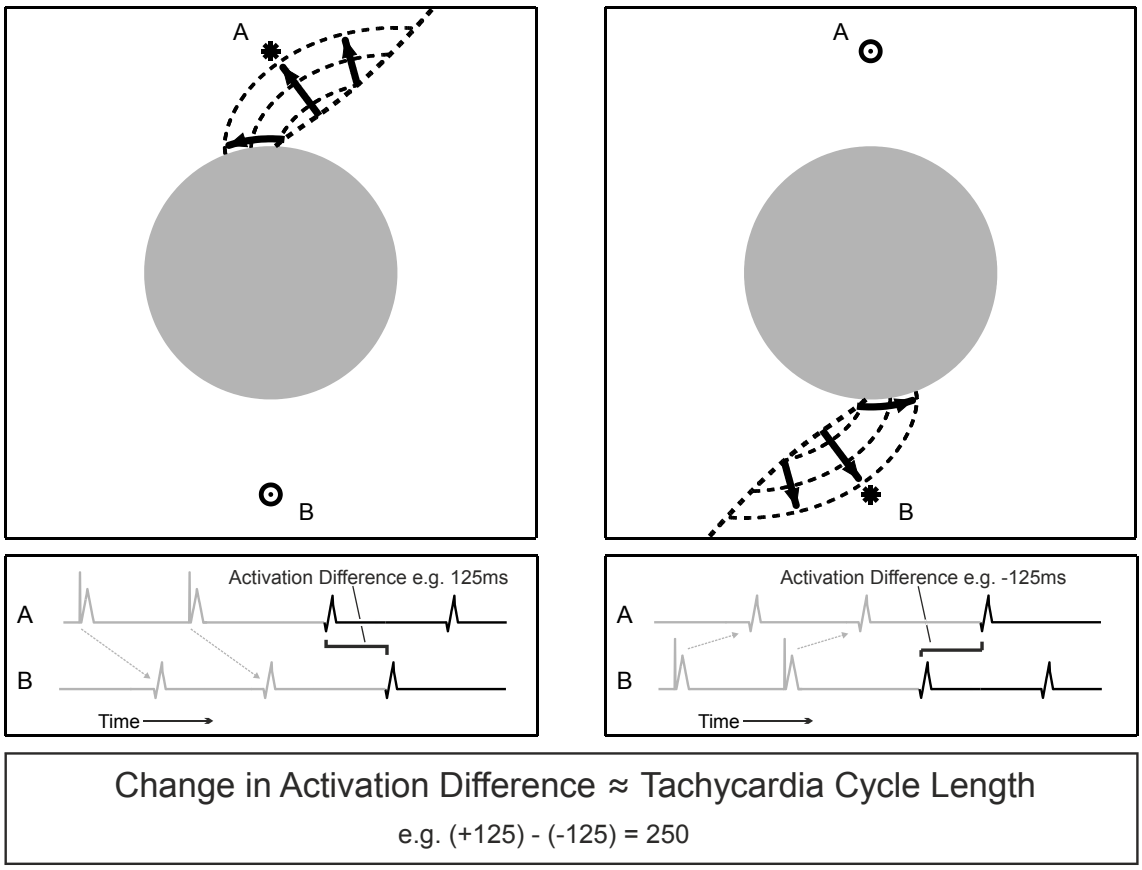

Figure 5-9. Single loop reentry with catheters positioned at opposite sides of the circuit. Activation has been illustrated only after it has passed through the line of collision that was created by pacing. The pacing site is represented by an asterisk. The FBT on the electrogram traces corresponds to the first complex drawn in black (rather than grey). The activation difference changes by one tachycardia cycle length between the manoeuvres.

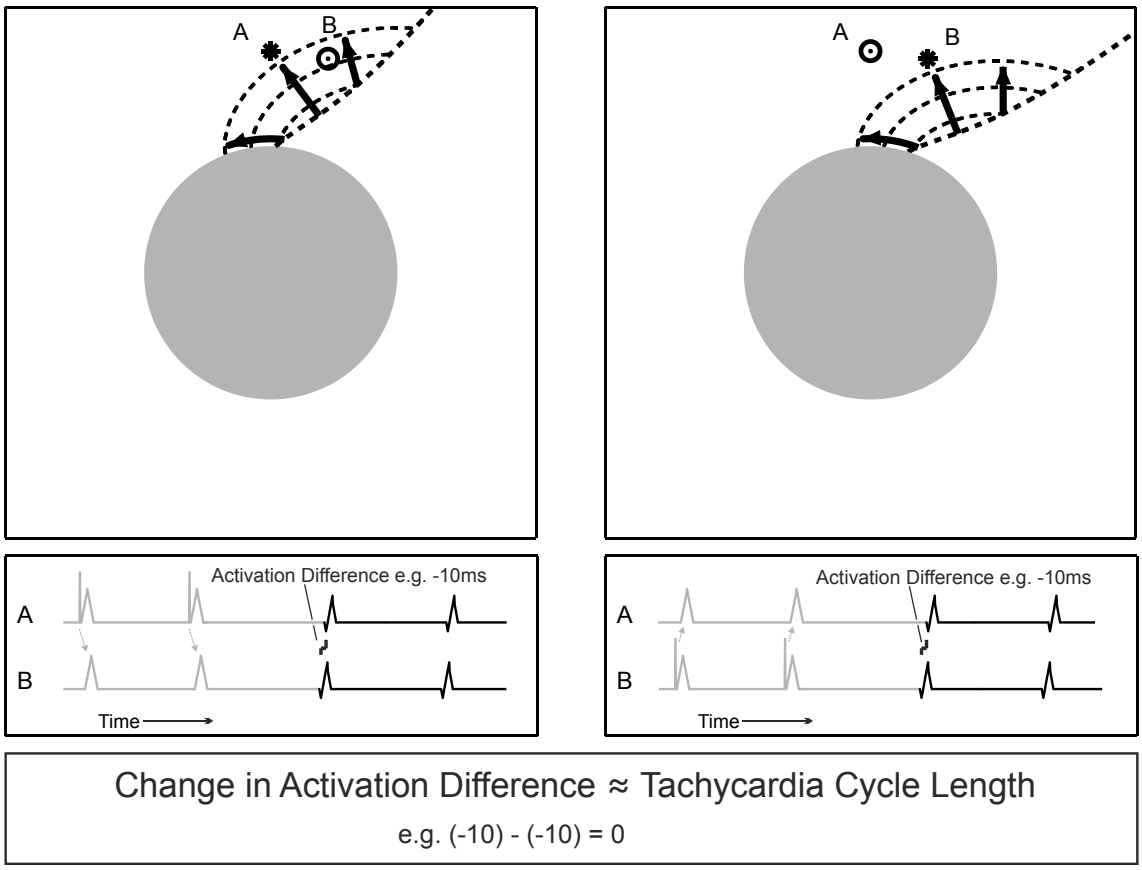

Figure 5-10. The criterion for reentry is not met because A and B are too close together: B has been captured antidromically when pacing from A. Therefore, the relative timing of A and B for the first beat of tachycardia has not changed.

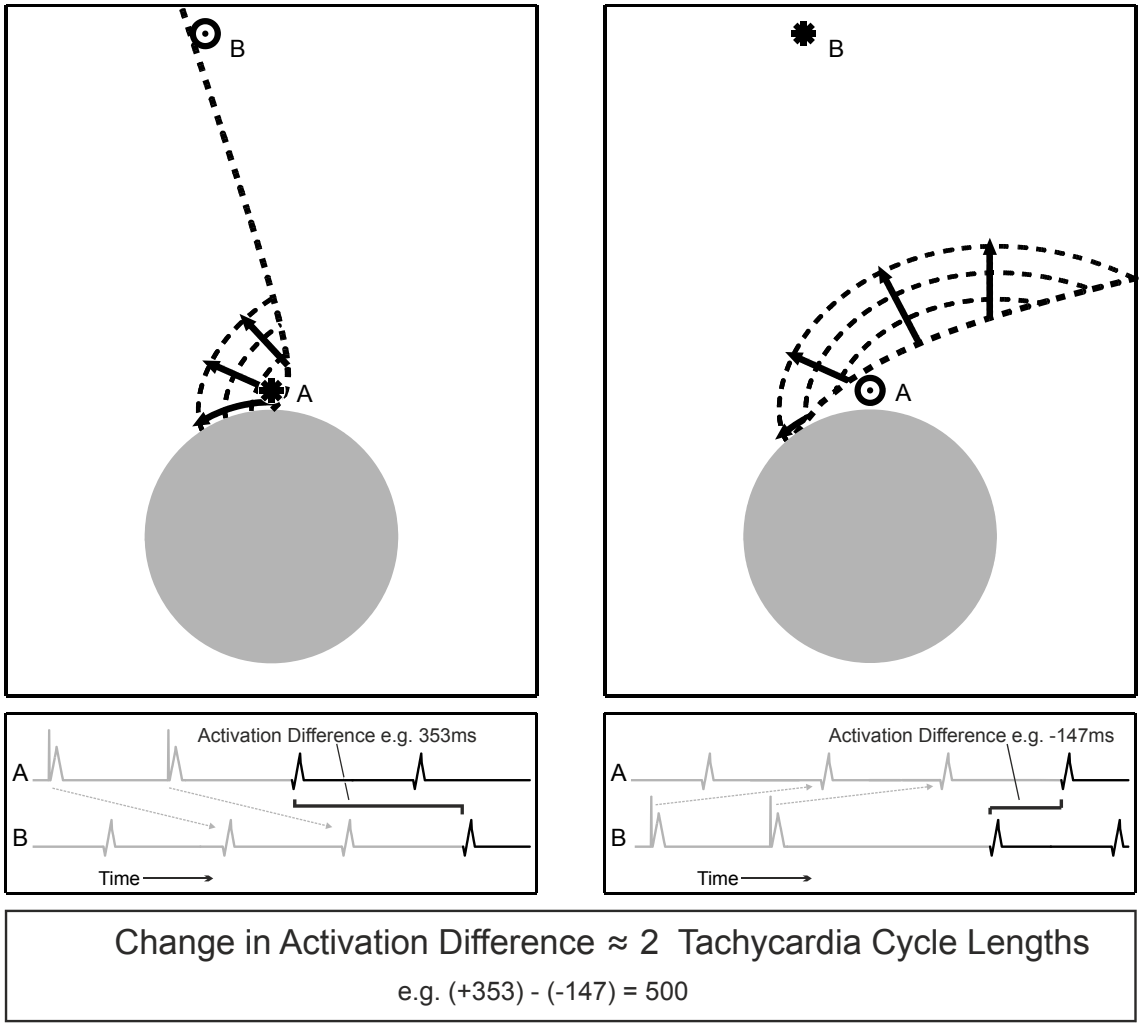

Figure 5-11. A change in Activation Difference of 2 TCL, with single loop reentry. When pacing from A, the shortest path to B is blocked by the collision line (the dashed line between A and B). Additionally, when pacing from B, the shortest path to A is also blocked by the respective collision line. There is a long post-pacing interval at B because it is a long way from the circuit. This can only occur when A and B are positioned in specific locations and one of them must be further from the tachycardia circuit than the other. The result of the positioning shown is that the Activation Difference changes by 2 TCL, despite only a single loop reentry circuit: thus this is an exception to the statement that a change of two tachycardia cycle lengths is usually due to double-loop reentry (see proposed criterion in Table 5-2). In practice, the specific conditions for this situation are unlikely to occur frequently.
This figure is also an example showing that the first beat of tachycardia can precede the last paced beat at other locations (e.g. the first manoeuvre).

Double loop reentry

Figure 5-12 illustrates the description for double-loop reentry proposed in Table 5-2. It is shown on the next page.

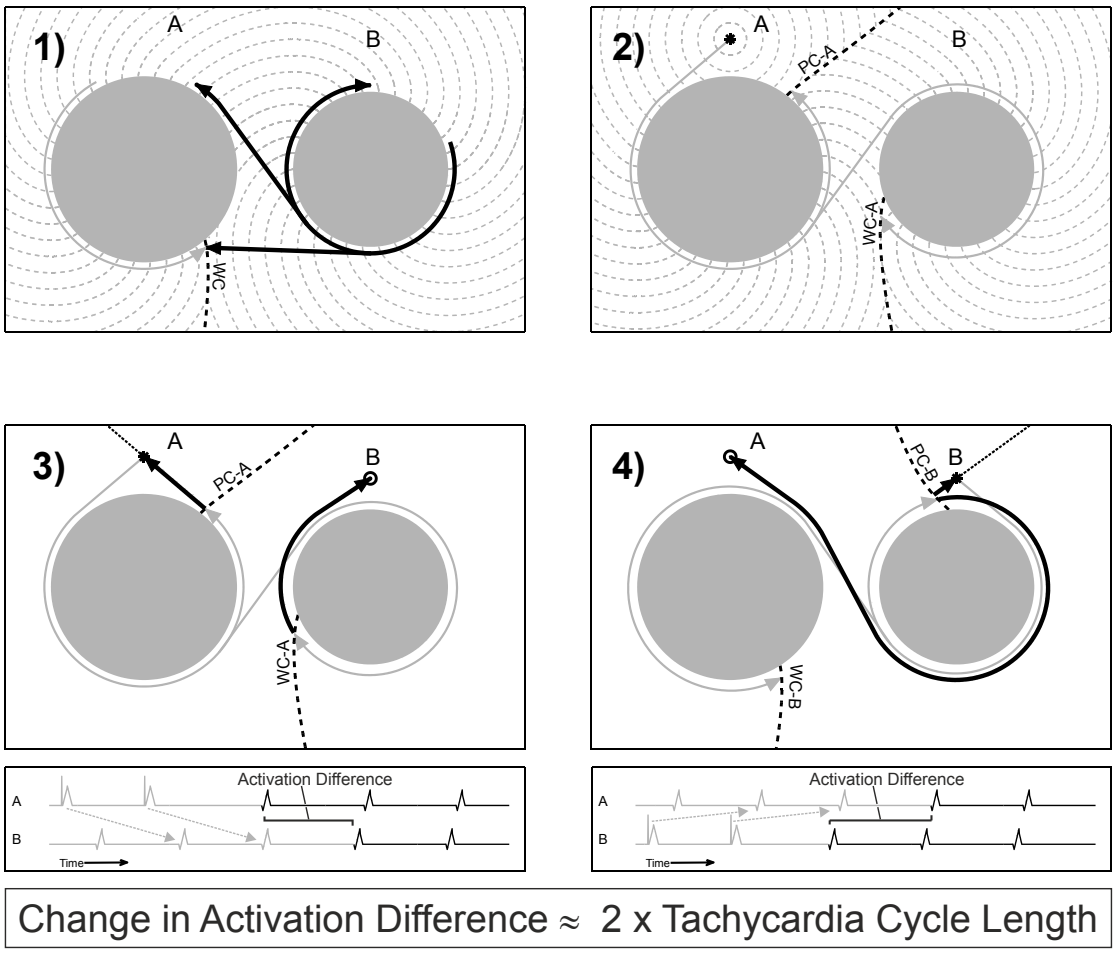

Figure 5-12. Double-loop reentry around slightly unequal obstructions. **Panel 1** - during tachycardia, a wavefront from the shorter circuit (black) drives the longer circuit, where there is a line of collision (WC, black-dash) with the previous activation wavefront (grey). If the cycle lengths around each separate circuit were the same, then this line of wave collision would reach to the isthmus where the wavefronts would fuse. **Panel 2** illustrates activation during overdrive pacing at A, near to the longer circuit. Overdrive pacing is always performed at a CL shorter than TCL (i.e. shorter than the CL around the shortest circuit). Therefore, the line of collision observed in Panel 1 has been advanced onto the shorter circuit, which is now passive (WC-A). There is also a line of collision where the paced antidromic wavefront collides with the orthodromic wavefront from the previous beat (PC-A, similar to Figure 1, Panel 1). Importantly, this has not reached any part of the contralateral circuit so that each paced wavefront must traverse the isthmus orthodromically before activating it (grey arrows). **Panel 3** is similar to Panel 2 but shows transitions from the last paced beat (grey) to FBT (black) where the wavefronts pass through the lines of former collision. (The line where the wavefronts from each circuit collide will then regress to the position in Panel 1.) The wavefront causing FBT at B must complete an additional rotation of the tachycardia circuit, compared to the wavefront causing FBT at A. Corresponding electrograms are shown below, with activation at the pacing CL shown in grey. The difference in activation time of FBT is marked. In **Panel 4**, overdrive pacing has been performed from site B, near to the shorter circuit, and the positions of the collision lines have moved (WC-B and PC-B). Again, the wavefront responsible for FBT at the non-paced circuit has completed an extra revolution of the tachycardia circuit. Therefore, in comparison to Panel 3, the relative timing of FBT has changed by approximately two TCL,

fulfilling the criterion for reentry (see Table 5-2). (The inequality is due to the small additional time associated with traversing the isthmus when pacing the longer circuit (Panel 3).)

Further theoretical implications

In Figure 5-7 through to Figure 5-12, the pacing sites also act as recording sites. In the development of the theoretical background, the recording sites can be separate from the pacing sites. This is demonstrated further in Figure 5-13, as well as the following corollaries:

- Corollary 1: Observation of the single-loop criterion from recording sites on either side of an appropriate anatomical isthmus confirms that the isthmus is critical to the tachycardia mechanism, as long as single-loop reentry is the only tachycardia mechanism present.
- Corollary 2: Observation of the criterion for double loop reentry indicates that the recording sites are usually on different loops, and that neither is positioned at the common isthmus. If the single loop criterion is observed when comparing a passive electrode at a third site with both the previous sites, then this third site is in continuity with the common isthmus (Zone I, Figure 5-13).

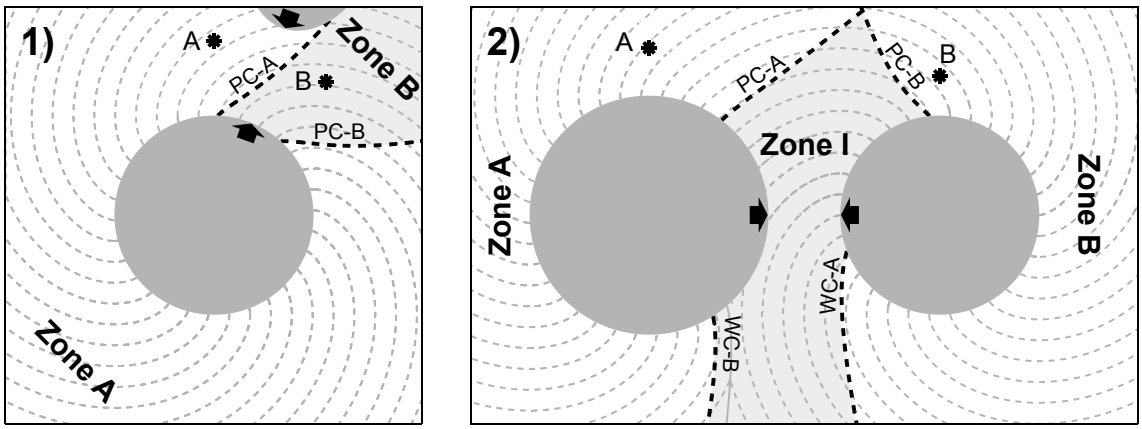

Figure 5-13. Use of passive catheters and isthmus verification. **Panel 1 – single-loop reentry.** Isochrones and lines of functional block are shown, as described in Figure 5-7. After overdrive pacing from A, the last paced wavefront crosses the line where 'paced collision' previously occurred (PC-A) to become the FBT (also see Figure 5-7, Panel 2). It passes through *Zone A then Zone B*. After overdrive pacing from B, the last paced wavefront crosses PC-B, becoming the FBT and passing through *Zone B then Zone A*. Therefore, any pair of passive recording electrodes, where one is positioned in Zone A and the other in Zone B (the zones being caused by pacing at positions A and B), will demonstrate a change in the relative timing of FBT and fulfil the criterion for single-loop entrainment. If B was moved away from A, then Zone B would become larger because PC-B would also move. In the example shown, an isthmus is illustrated (black arrows, with additional grey obstruction). The single-loop criterion confirms that there are two paths between A and B (one passing through an anatomical isthmus and the other around the circuit). The isthmus may be an appropriate ablation target if it is anatomically amenable to ablation and if there are no other coexistent tachycardia mechanisms or double-loops. **Panel 2 – double-loop reentry.** Isochrones and lines of collision are shown, as described in Figure 5-12. Zone I includes the common isthmus.* During overdrive pacing from A, there is 'paced collision' at PC-A, and wave collision between the circuits at WC-A (see Figure 5-12, Panel 3). After pacing, the wavefront crosses PC-A to become the FBT and activate *Zone A, then Zone I*†*, and then Zone B*. After entrainment from B, the last paced wavefront crosses PC-B to become the FBT and activate *Zone B, then Zone I, and then Zone A*. Thus, the criterion for double-loop reentry will be met for any pair of passive electrodes in non-adjacent zones, i.e. one in Zone A and the other in Zone B. Additionally, the criterion for single-loop reentry will be met for any pair in adjacent zones, i.e. one in Zone I, and the other in Zone A or B.

* - Note that Zone I would be larger if electrodes A or B were placed more distally in their respective circuits.

† - Zone I is also activated by a wavefront emanating from WC-B, see Figure 5-12, Panel 3.

5.5 Experimental Methods

5.5.1 Patients with common atrial flutter

Five patients were studied prior to cavotricuspid isthmus ablation. All patients had structurally normal hearts and none had previous cardiac surgery or ablation. After femoral access, a quadripolar catheter was advanced distally into the coronary sinus (CS) and a radiofrequency (RF) ablation catheter was positioned at pre-specified sites distributed around the right atrium (posterior wall, right atrial appendage, lateral, cavotricuspid isthmus, and septal positions). At each position of the RF catheter, overdrive pacing was performed from the CS and then from RF with a cycle length (CL) 20-30ms less than in tachycardia. The electrograms recorded from the CS and RF catheters were analysed and the change in Activation Difference was measured.

5.5.2 Other data

A literature search [Medline Search Terms: Any Field: "entrainment" & "pacing"] identified two publications exhibiting multipolar recordings of transient entrainment from different sites in patients with dual-loop reentry. [172, 202] Two examples are also provided from patients, in routine clinical practice, with double loop reentry in whom the criterion is demonstrated.

5.5.3 Electrogram processing

The criterion requires that the timing of FBT is identified in the relevant electrogram recordings, in order to calculate the change in Activation Difference (see Table 5-1 for definition). Software was written to assist with this process (see Figure 2-1, p50). The user annotates the activation time corresponding to each electrogram complex and the software then plots the calculated CLs. In this way, FBT can be identified as the first activation after the cessation of pacing with a preceding CL greater than the pacing CL.

5.6 Results

5.6.1 Common atrial flutter

Four or 5 pairs of manoeuvres were performed in each of 5 patients (4 male, 1 female, aged 60-80yrs) with common flutter (TCL 220-285ms). In all patients, cavotricuspid isthmus ablation led to arrhythmia termination. After overdrive pacing, FBT could be unambiguously determined in all recordings. The single-loop criterion was observed in

22/23 pairs of recordings, despite a wide range of positions for the RF catheter and placement of the CS electrodes distally in the CS (away from the tachycardia circuit). In 1/23 pair of recordings, the criterion was not observed: the RF catheter was positioned at the low septum and captured the CS antidromically during entrainment. An example of analysis for a recording pair is shown in Figure 5-14 and the data is summarised in Figure 5-15.

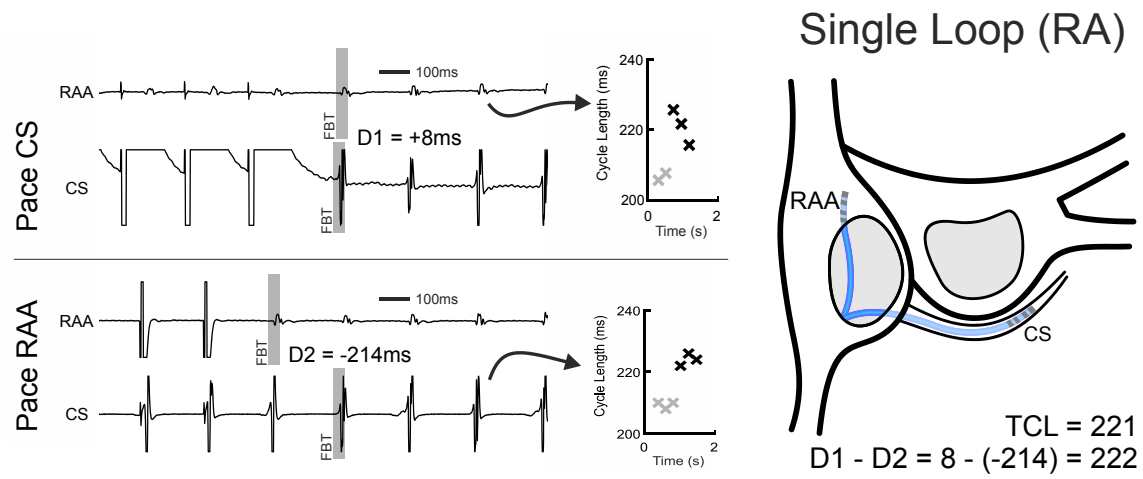

Figure 5-14. Patient with common flutter. In the first manoeuvre, entrainment has been performed from the coronary sinus (CS). In the second, the distal bipole of the other catheter was used for entrainment and this was positioned near the right atrial appendage (RAA). Artefact rendered the recording from distal bipole unusable. Because the entrainment criterion can be applied to any passive catheter, the recording from the proximal bipole can be used legitimately. After pacing, FBT has been identified according to the definition in Table 5-1 (grey highlights). For electrograms displaying concealed entrainment, the CL has been plotted to confirm a change in CL after the cessation of pacing – the black crosses represent intervals after FBT and the grey crosses prior to this. Measurements of activation difference are shown (D1 and D2). The change in Activation Difference (D1-D2) was approximately equal to one TCL, confirming reentry.

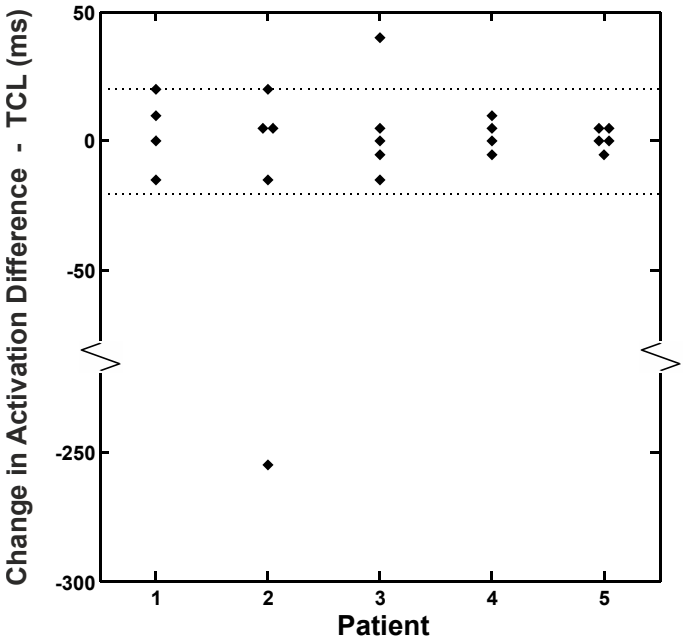

Figure 5-15. Detection of single-loop criterion in 5 patients with common flutter. Pairs of entrainment manoeuvres were performed – with each comprising overdrive pacing from CS1-2 and then overdrive pacing from the RF catheter, which was positioned at 4-5 locations around the tricuspid annulus. For each manoeuvre, the graph shows:

$$Change\ in\ Activation\ Difference - TCL = \left|\left[FBT_{RF} - FBT_{CS1,2}\right]_{overdrive\ RF} - \left[FBT_{RF} - FBT_{CS1,2}\right]_{overdrive\ CS1,2}\right| - TCL$$

For 21/23 manoeuvres, the Change in Activation Difference was within 20ms (dotted lines) of the TCL. There were 2 outliers: in Patient 3, there was a change in CS electrogram morphology and timing suggesting catheter movement; and in Patient 2, when the RF catheter was positioned at the low septum, entrainment from RF captured the CS antidromically and so Activation Difference did not change (see Figure 5-10 for explanation).

5.6.2 Double loop reentry

Three cases were identified from the literature with sufficient data for re-analysis.[172, 202] In each case, there was a dual-loop macroreentrant tachycardia located in the right atrium (RA). Multipolar catheters were positioned in the RA and overdrive pacing was performed from 2 sites that were on separate loops.

Case 1

In Figure 5-16, data are shown from double-loop reentry around a septal surgical scar as well as the tricuspid annulus.[202] The investigators used a multipolar 'basket' catheter to track activation of the last paced beat in order to identify both circuits.

As can be seen in Figure 5-16, each individual spline of the basket catheter has the same activation sequence in each entrainment manoeuvre. Thus, for this particular example, the change in activation difference only depends upon the splines, and not the particular electrodes. Table 5-3 shows the calculated values of change in activation difference, tabulated for each possible pair of splines: for example, the change in activation difference between spline A and spline B was calculated as follows:

$$Activation\ Difference = \left\{\overline{FBT(B)} - \overline{FBT(A)}\right\}_{maneuver\ 2} - \left\{\overline{FBT(B)} - \overline{FBT(A)}\right\}_{maneuver\ 1}$$

where $\overline{FBT(A)}$ is the average activation time of FBT for all electrodes on spline A.

change (ms)	A	B	C	D	E
A	-				
B	289*	-			
C	289*	**578**†	-		
D	286*	**574**†	3	-	
E	288*	**576**†	1	2	-

* - criterion for single-loop reentry met

† - criterion for double-loop reentry met

Table 5-3. Change in the difference of activation time between catheter splines, for the first beats of tachycardia corresponding to Figure 5-16. Tachycardia cycle length 290ms.

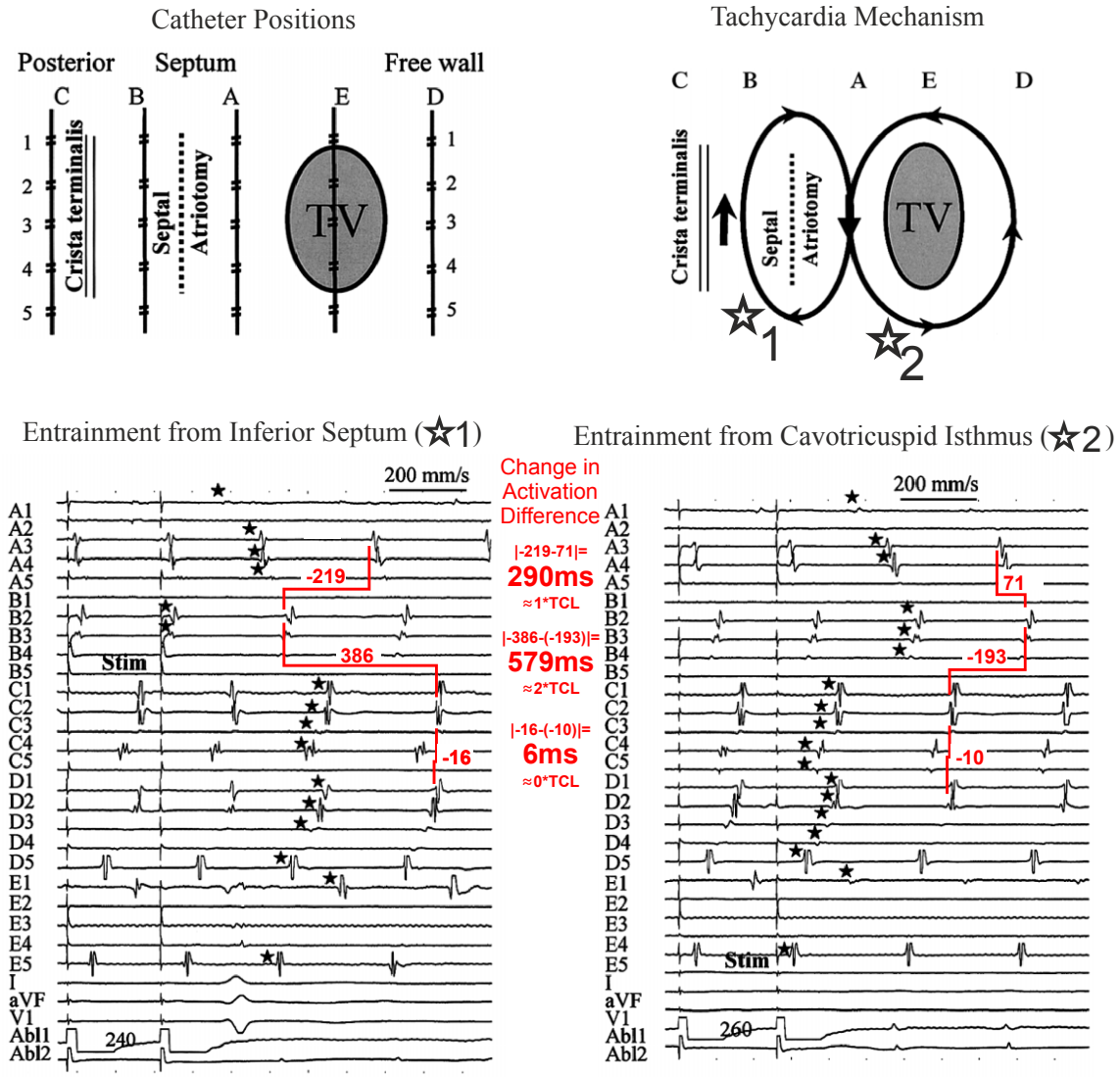

Figure 5-16. Double-loop reentry in a patient with previous mitral valve replacement.[202] Tachycardia cycle length 290ms. Recordings are shown from a basket catheter in the right atrium. A schematic diagram of the catheter spline positions (top left) and the deduced tachycardia mechanism (top right) are shown. Note that splines C and D are adjacent, lying between the tricuspid valve (TV) and the crista terminalis. During entrainment from the inferior septum, the wavefront causing the last paced beat must pass around the septal atriotomy before it can activate the common isthmus and then the circuit around the TV. Electrograms corresponding to the last paced beat are marked (black stars) and FBT is the following complex on each electrogram. The post-pacing interval (at the pacing site) was within 10ms of the TCL. During entrainment from the tricuspid annulus, the wavefront causing the last paced beat must pass around the tricuspid valve before activating the common isthmus and then the circuit around the septal atriotomy. The post-pacing interval (at the pacing site) was the same as the TCL, demonstrating concealed entrainment. Analysis using the criterion for reentry is presented in the Text.

Red parts of the figure illustrate how Change in Activation Difference is calculated (the equation is given in Table 2). The red lines indicate the Activation Difference for A3 vs B2, B2 vs C2, and C2 vs D2, for each manoeuvre. In the central column, the Change in Activation Difference has been calculated and is approximately equal to 1, 2, and 0 TCL respectively.

In Table 5-3, the double-loop criterion is observed when spline B is paired with spline C, D, or E. This confirms double loop reentry, with B on the opposite circuit to C, D, and E. It also excludes the electrodes of B, C, D and E from being positioned at the common isthmus (Corollary 2, Methods). The single-loop criterion is observed between spline A and all other catheters. Thus, spline A is in continuity with the common isthmus (i.e. it is located somewhere in Zone I, Figure 5-13). Note that the common isthmus is not always the best site for ablation (in this case, ablation lines were created from the scar to inferior vena cava and at the cavotricuspid isthmus).

Case 2

In Figure 5-17 data are shown from entrainment manoeuvres in a case of cavotricuspid-isthmus dependent flutter, with one loop around the tricuspid annulus and the other posterior to the superior vena cava.[172] In this particular example, the activation sequence in each entrainment manoeuvre does not change within the following groups of electrodes: CS+TA1-5; PS1-2; TA6-10; and PS3-4. Therefore, these have been pooled in a similar manner as for Case 1.

Table 5-4 shows tabulated values of the change in activation difference, when comparisons are made between these groups. The double-loop criterion is met for TA6-10 and PS3-4, proving that double-loop reentry is present, and that these electrodes are on opposite loops and not at the common isthmus (Corollary 2, Methods). The single-loop criterion is observed between these groups and CS+TA1-5 and PS1-2, demonstrating that CS+TA1-5 and PS1-2 are in continuity with the common isthmus (i.e. Zone I, Figure 5-13). Although anatomically PS1-2 are on the posterior circuit, they were not captured antidromically by pacing from PS3 and so are activated in continuity with the isthmus.

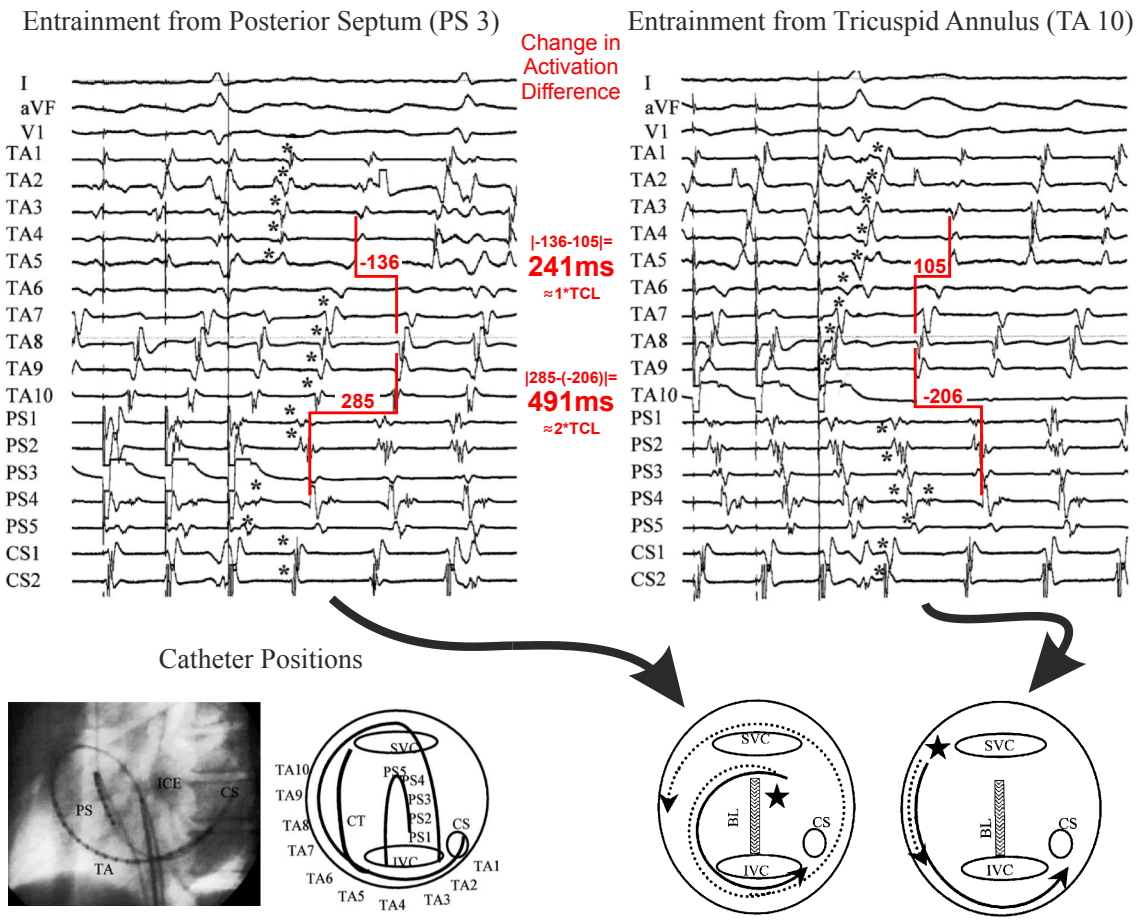

Figure 5-17. Double-loop reentry in a patient with common atrial flutter, consisting of a posterior loop and a loop around the tricuspid annulus. Tachycardia cycle length 245ms. Diagrams and electrograms are reproduced from Fujiki et al,[172] with permission. Recordings are shown from a duodecapolar catheter, a decapolar catheter, and surface ECG leads (I, aVF, and V1). A right anterior oblique x-ray image is shown (bottom left) along with a schematic that indicates the electrode labelling (TA, tricuspid annulus; PS, posterior septum; CS, coronary sinus; SVC, superior vena cava; IVC, inferior vena cava; CT, crista terminalis). During entrainment from PS3, collision with the previous paced beat prevents direct activation of PS2 and PS1. The crista terminalis also prevents direct activation of TA10 – TA6. Thus, the wavefront causing the last paced beat (marked with *) must reach the isthmus (solid arrow on corresponding schematic at bottom right) before activating the circuit around the tricuspid annulus (dotted arrow) to reach TA10-TA6. This was referred to as 'paradoxical delayed capture' by the investigators.[172] When entrainment is performed from TA10, the path to TA6 is shorter than the path to the isthmus.

Red parts of the figure illustrate how Change in Activation Difference is calculated (the equation is given in Table 2 (main manuscript)). The red lines indicate the Activation Difference for TA3 vs TA8, and TA8 vs PS4, for each manoeuvre. In the central column, the Change in Activation Difference has been calculated and is approximately equal to 1 and 2 TCL respectively.

diff (ms)	CS, TA 1-5	PS 1-2	TA 6-10	PS 3-4
CS, TA 1-5	-			
PS 1-2	1	-		
TA 6-10	240*	241*	-	
PS 3-4	250*	249*	**490**†	-

* - criterion for single-loop reentry met

† - criterion for double-loop reentry met

Table 5-4. Change in the difference of activation time between electrode groups, for the first beats of tachycardia corresponding to Figure 5-17. Tachycardia cycle length 245ms.

Another case was presented in the same report as Case 2 with similar results.[172] Of note, the proposed criterion can be applied to any pair of electrodes, even if pacing is performed from other sites. Therefore, for each case, every combination of electrode pairs was analysed by calculating the change in Activation Difference that occurred between the 2 overdrive manoeuvres. The results are presented in Figure 5-18 and show that the change in Activation Difference was approximately equal to 0, 1, or 2 TCL. These changes are related to the position of each electrode as follows (referring to Figure 5-12, Panel 2):

- change ≈ 0 TCL: both electrodes of the pair are positioned in the same Zone
- change ≈ 1 TCL: the electrodes are positioned in adjacent Zones (i.e. Zone A and Zone I, or Zone B and Zone I).
- change ≈ 2 TCL: the electrodes are positioned in non-adjacent Zones (i.e. Zone A and Zone B – opposite 'loops'), *so neither electrode can be at the common isthmus*.

This information allows the location of the zone containing the common isthmus to be identified.

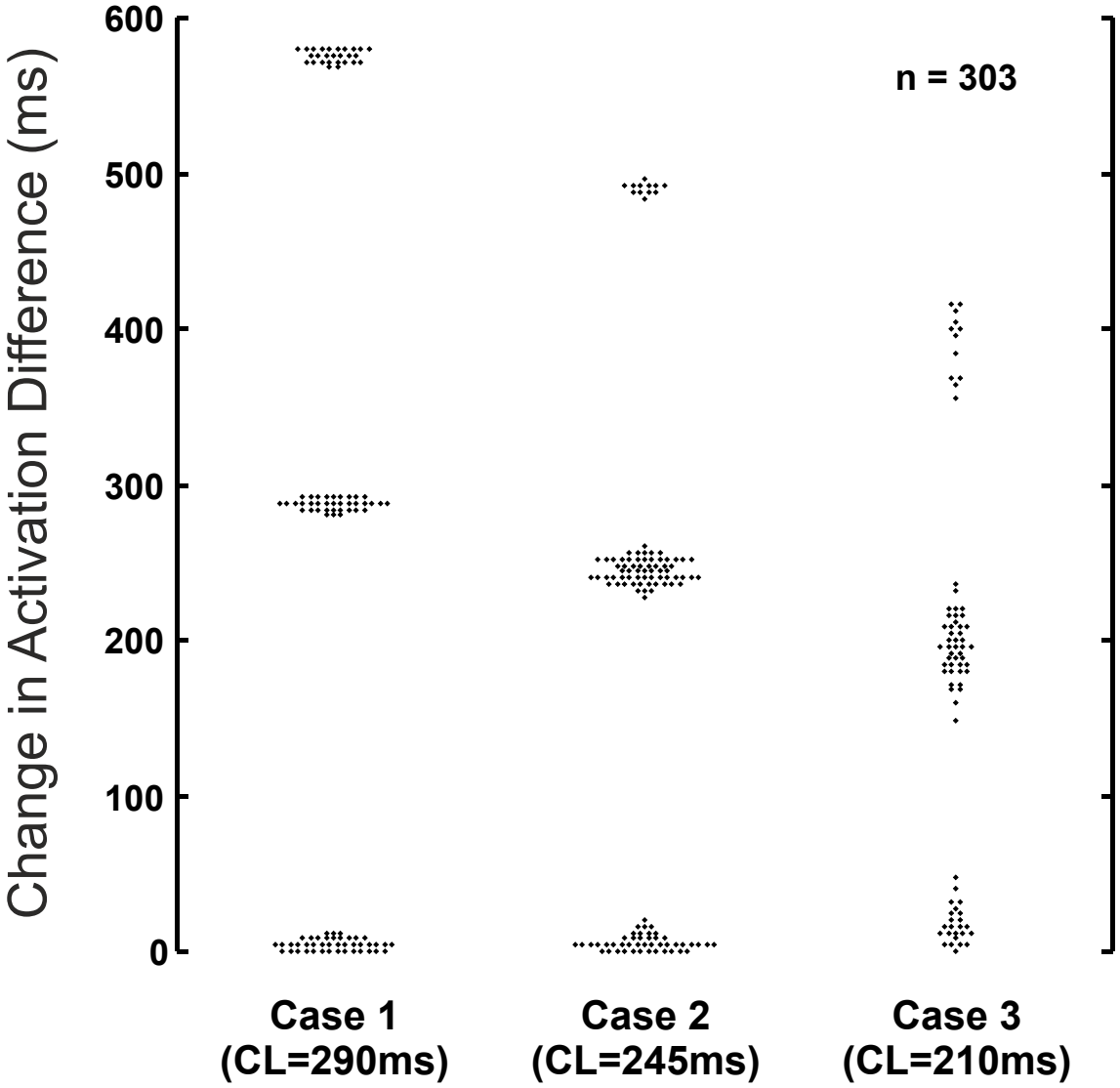

Figure 5-18. Summary of double-loop reentry analysis. Three cases were identified from the literature, in which multipolar catheters were used in the presence of 2 entrainment manoeuvres.[10, 11] For each case, the Activation Difference was calculated for every possible pair of electrodes from the two manoeuvres. The Change in Activation Difference for each pair was approximately equal to 0, 1, or 2 multiples of the TCL (see Text).

5.6.3 Further examples

Figure 5-19 illustrates two cases in which double loop reentry was detected using two catheters.

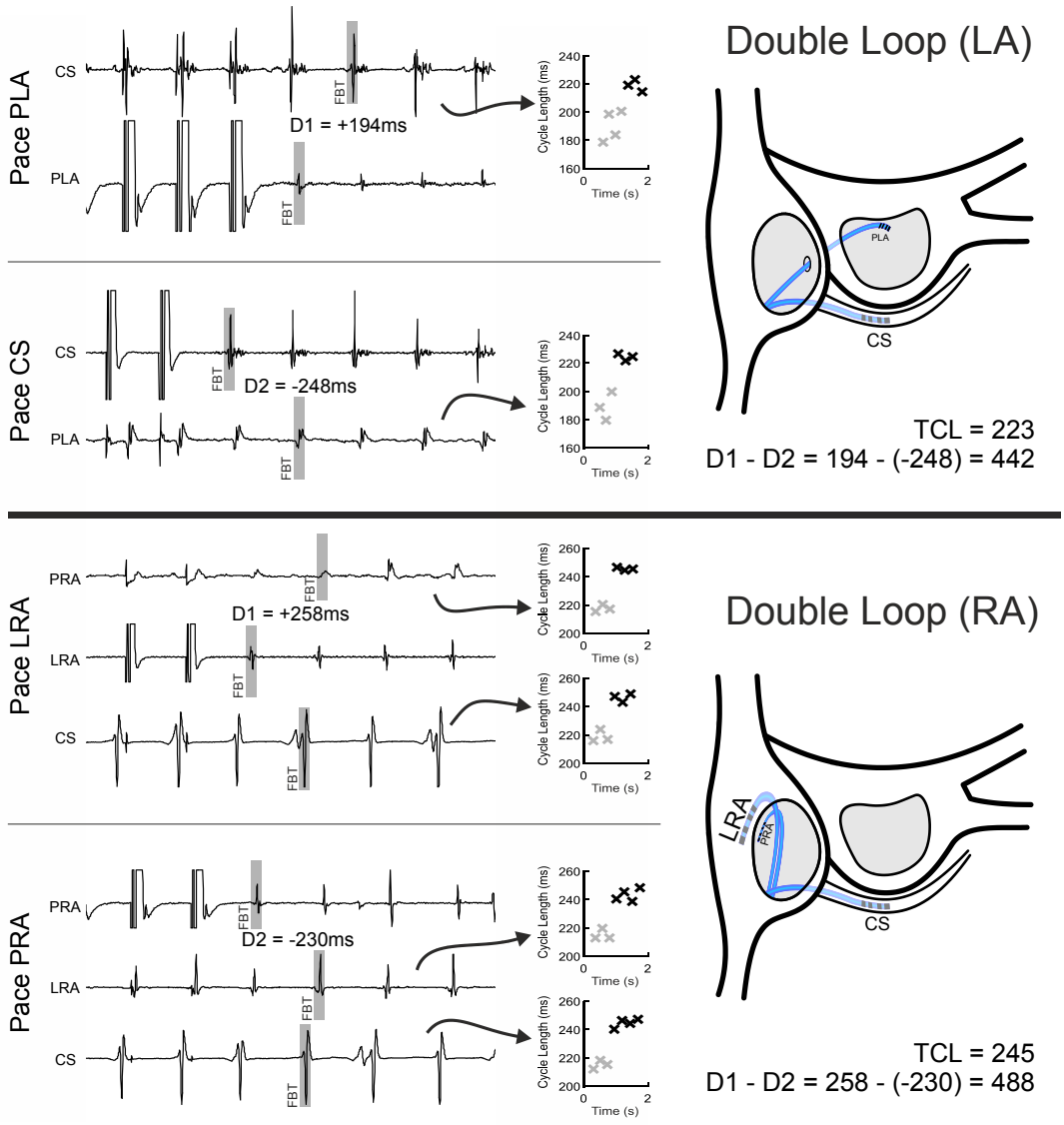

Figure 5-19. Two examples showing the detection of double-loop reentry with two catheters. After pacing, FBT has been identified according to the previous definition (Table 5-1) and it is marked in grey. For electrograms displaying concealed entrainment, the CL has been plotted to confirm a change in CL after the cessation of pacing – the black crosses represent intervals after FBT and the grey crosses prior to this. Measurements of activation difference are shown (D1 and D2). Electrode positions are shown in the schematics to the right.

Upper panel: Double loop reentry – perimitral and roof dependent tachycardia. Electrodes were placed at the high posterior left atrium (PLA) and the mid coronary sinus (CS). The change in Activation Difference (D1-D2) was approximately equal to 2*TCL indicating double-loop reentry. The diagnosis was confirmed by ablation of the LA roof (which caused a change in PPI at the posterior wall) and then termination by ablation at the mitral isthmus.

Lower panel: Common flutter with a double loop. Electrodes were placed at the antero-lateral RA (LRA), the posterior RA (PRA) and the CS. Entrainment was performed from LRA and from PRA. The Activation Difference between LRA and PRA changed by approximately 2*TCL, indicating that these electrodes are positioned on different loops. Comparing the Activation Differences between PRA-to-CS and LRA-to-CS indicated single-loop reentry, confirming that the CS was in continuity with the common isthmus.

There was a recent case report of typical cavotricuspid dependent flutter but with long post-pacing intervals from near to the circuit, in a patient with depressed left ventricular function.[203] The likely explanation for this unusual finding was abnormal, decremental conduction within the tachycardia circuit between the cavotricuspid isthmus and the CS. I am grateful to Kelvin Wong and Tim Betts from the John Radcliffe Hospital, Oxford for sharing the data from this case. All measurements were retaken from the data as presented in Figure 5-20.

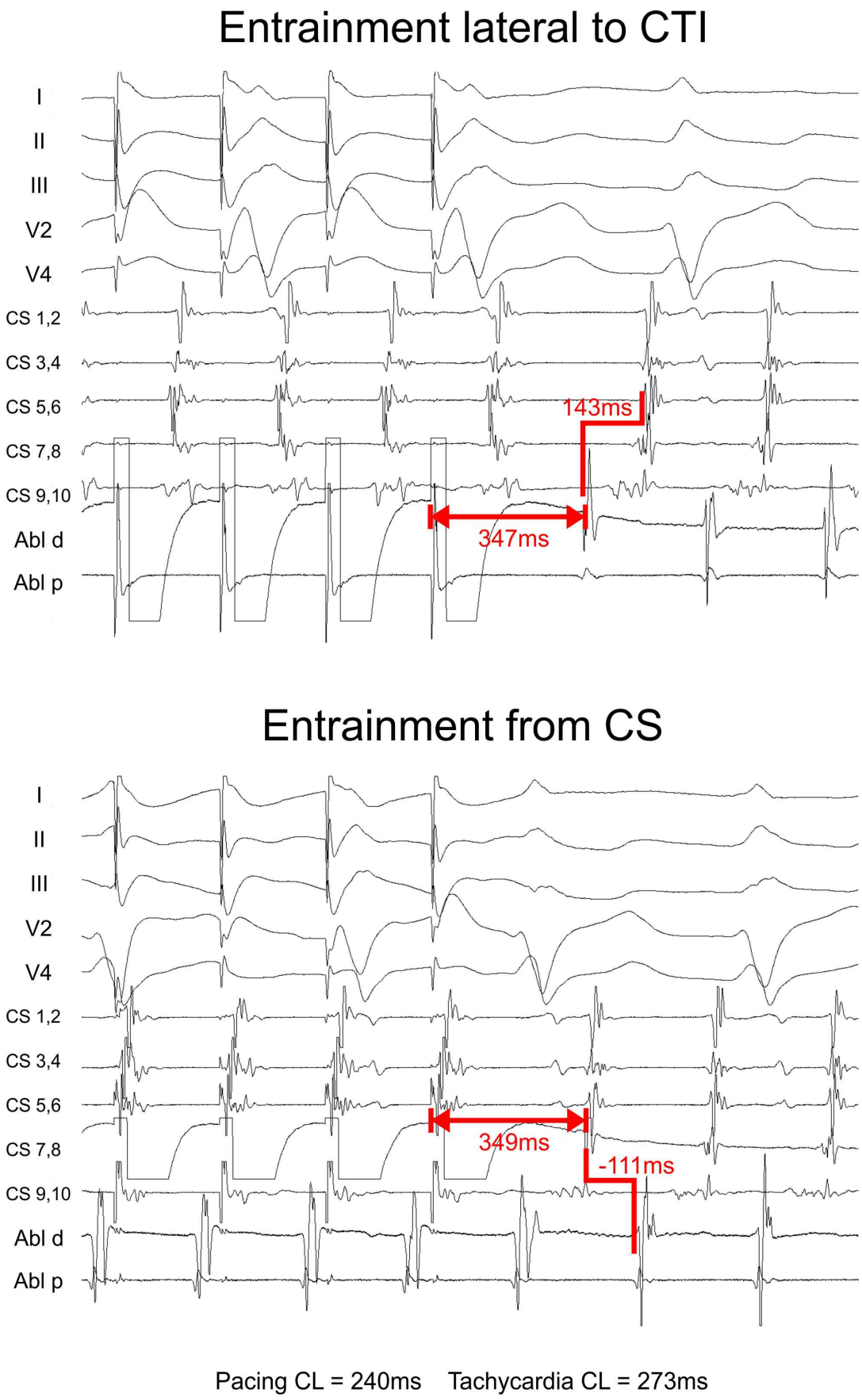

Figure 5-20. An unusual case of typical right atrial flutter. Legend follows on next page.

Data from a previously reported case.[203] The upper panel shows entrainment from the distal pole of the ablation catheter, which is positioned just lateral to the cavotricuspid isthmus. The TCL is 273ms and overdrive pacing was performed with a CL of 240ms. The PPI was 347ms giving a long value for PPI-TCL (74ms). Along with Abl D, CS5,6 was chosen for calculation of the Activation Difference because there is a sharp onset to the electrogram: it was measured at +143ms. In the lower panel, entrainment has been performed from CS7,8 and Abl D was in a similar (but not identical) position. After this entrainment, the Activation Difference was -111ms. Therefore, the change in Activation Difference was 143-(-111)=254ms. This is similar to the TCL (273ms) and therefore consistent with single loop reentry. Additionally, it implies that the cavotricuspid isthmus is an appropriate ablation target (see "Further theoretical implications" on p106) despite the long PPI from near to that location.

5.7 Discussion

An additional criterion for entrainment has been developed. It relies upon the fact that the 'phase' at which a reentrant tachycardia resumes is dependent upon the location from which entrainment was performed. After overdrive pacing, the relative timing of FBT between two locations (the Activation Difference) is dependent upon the location of the collision line(s) present when the last antidromic pacing wavefront collided with the orthodromic wavefront(s) from the previously paced beat. When two entrainment manoeuvres have been performed, the respective collision lines partition the cardiac surface into zones, as shown in Figure 5-13. The Activation Difference between two sites will be: ≈ 0 TCL if both sites are in the same zone; ≈ 1 TCL if the sites are in adjacent zones (demonstrating reentry); and ≈ 2 TCL if the sites are in non-adjacent zones (demonstrating reentry and suggestive of a double loop).

The criterion enables detection of single- and double-loop macroreentry after performing 2 overdrive manoeuvres from 2 different locations. For single-loop reentry, if these locations are reasonably separated with respect to the macroreentry circuit then precise positioning is not required. For double-loop reentry, pacing must be performed from each loop without capturing the other circuit antidromically. The response to overdrive pacing at other (passive) electrodes can also be assessed and may yield further diagnostic information. For example, if activation mapping suggests a double loop reentry circuit then the mechanism can be confirmed and the common isthmus identified using only two overdrive manoeuvres; pacing from electrodes positioned at opposite loops in the presence of a third electrode at the common isthmus.

In developing the entrainment criterion, it has been assumed that conduction times between different parts of the atrium are not affected by pacing. In reality, conduction disturbances are known to be caused by entrainment. In macroreentrant arrhythmias, overdrive pacing can cause a change or termination of tachycardia.[127] However, if this does not occur then changes in conduction times are usually small in comparison to the TCL[164, 204] and so would be unlikely to give a false positive result when the entrainment criterion is applied. Additionally, the conduction affecting the relative timing of FBT has had longer to recover, in comparison to a method relying on the timing of the last paced beat. This hypothesis is supported by reanalysis of a single case report[203] in which overdrive pacing caused significant changes in conduction properties (see Figure 5-20, p119): these cases are unusual[164] and no other cases reported in this thesis had marked decremental conduction associated with entrainment.

For centrifugal arrhythmias, the PPI often varies due to localised conduction disturbances within the tachycardia focus.[169, 204] However, application of the entrainment criterion will not be affected as long as the global atrial activation sequence of the first beat of tachycardia has a similar origin.

The criterion presented here has conceptual similarities with the fourth criterion of transient entrainment, described previously.[156] In the fourth criterion, overdrive pacing is performed from the same site with different pacing rates. The effect of increasing the rate is to advance antidromically the collision line (where the antidromic and orthodromic paced wavefronts meet - refer to Figure 1, Panel 1): this is detected if an electrode is positioned within the small zone where antidromic penetration changes.[156, 205] The criterion presented here is applied to overdrive pacing at different sites, and also relies upon a change in the position of the collision line. A potential disadvantage with the present criterion is that overdrive pacing must be stopped, tachycardia allowed to resume, and then another overdrive pacing manoeuvre performed from a second site. However, in the diagnosis of atrial tachycardia it is common to perform more than one manoeuvre and the present criterion can be observed from a wide range of electrode positions. By contrast, the fourth criterion requires specific positioning of an electrode such that it is sited where antidromic

penetration changes with a change in pacing rate. This may be difficult to achieve without prior knowledge of the tachycardia mechanism.

Previously, double-loop reentry has been identified by extensive entrainment mapping[25], and also by appreciation of subtle changes in cycle length and activation during ablation.[94, 95] Fujiki and colleagues[172, 202] described the careful tracking of activation due to the last paced beat, when entrainment was performed from each loop of double-loop reentry circuits. This allowed both loops to be elucidated, but did require the use of multipolar catheters and pacing close to the tachycardia circuits. The double-loop criterion described in the present study was applied retrospectively to their data, and successfully identified regions that were positioned on opposite circuits as well as regions in continuity with the common isthmus. A potential advantage of the present criterion is that it can be applied to situations with only 2 electrodes, but further information may be gained by application to recordings from any other electrodes within the relevant cardiac chambers. Additionally, the response to overdrive pacing distant from the circuits can be assessed.

5.7.1 Limitations

Demonstration of the criterion proves that reentry is present. If the criterion is not demonstrated then this does not exclude macroreentry. However, pacing from widely separated sites can prevent false negative results that are due to antidromic capture of the recording electrode. Thus, the clinical utility of the criterion will be dependent upon strategic positioning of electrodes in the heart and choice of pacing sites. In turn, this will depend upon the likely tachycardia mechanisms in any particular patient (e.g. as suggested by activation mapping), and a clear understanding of the mechanism by which the criterion can establish reentry.

We have presented a theoretical situation, where the Activation Difference can change by two TCL in the presence of single loop reentry alone. In our small group of patients we did not observe this. However, further study is required to clarify the frequency with which this response can be elicited in clinical practice. A change in Activation Difference of two TCL is more likely to represent double-loop reentry, but this requires the pacing sites to be on different loops.

The present criterion requires correct identification of FBT. It is important to be certain that the last pacing stimulus resulted in successful capture. It is also necessary that overdrive pacing is fast enough to cause a clear change in CL when pacing stops. FBT is often the second complex following the last pacing artefact, but may be one of the subsequent beats if there is a long stimulus-to-electrogram time. In our limited prospective evaluation of the criterion, we used plots of CL to assist this process (Figure 2-1).

After overdrive pacing of a centrifugal tachycardia, the wavefront causing FBT arises from the area where the tachycardia mechanism is located. Thus, the Activation Difference between locations that are distant from this area will be consistent, and so the criterion for reentry will not be met. Conceptually, it is possible that the criterion could be met if sites from within an area of localised reentry or microreentry are recorded. However, these sites are associated with fractionated electrogram recordings. Therefore, if the criterion is used for the identification of macroreentry, we recommend that electrodes with fractionated electrograms are not used. This is subject to further investigation.

6 An Electroanatomic Approach to Entrainment Mapping

6.1 Aims for this chapter

E3 Investigate the theoretical relationship between PPI and the trans-atrial distance from the tachycardia mechanism.

E4 Investigate the theoretical response to overdrive pacing for different tachycardia mechanisms, with respect to the PPI.

E5 Investigate the theoretical response to overdrive pacing for different tachycardia mechanisms, with respect to the response at electrodes distant from the pacing site.

E6 Integrate the theoretical findings from above into a clinical prototype for testing with patients.

6.2 Introduction

As discussed in Chapters 1 and 5, AT is frequent in the context of prior atrial ablation or atrial scars due to previous surgery, and it is often refractory to drug therapy. The first stage of mapping for atrial tachycardia is usually activation mapping.[3, 86] Although not obligatory, electroanatomic mapping systems are commonly used to assist with this process. They may utilise additional anatomic data obtained with MRI, CT, or rotational angiography. After initial activation mapping has been performed, it is usual to perform AOP.

The work described in Chapter 5 focussed upon using AOP effectively to determine the arrhythmia mechanism. This chapter describes the development of an algorithm for providing more detailed information about the arrhythmia location. The aim is to integrate the electroanatomic information obtained from multiple AOP manoeuvres. The steps in this process involve the development of new algorithms for relating the response to AOP to the location of the tachycardia, development of software to display and integrate this information, followed by clinical testing.

6.3 Development of new analysis techniques

6.3.1 Overview

Software was written using Matlab (Mathworks, Natick, MA). An anatomic shell, represented using a triangulation, and electrogram information can be imported. The shell is then color-coded according to the results of entrainment manoeuvres. The user

can decide to perform a 'focal analysis' or a 'macroreentry analysis' of the data, although the software also performs computations to detect the likely mechanism, using the entrainment criterion developed in Chapter 5. All distances between different points on the shell are calculated by finding the shortest geodesic paths (see Section 2.5.3 on p52)

Atrial conduction velocity is anisotropic and heterogeneous. However, a simple model of conduction is used, assuming that the conduction velocity in any direction is less than a user-defined value, v_{max}. This is not a precise model but was chosen for reliability (as long as v_{max} is greater than the true conduction velocity) and simplicity (to facilitate comprehension of the results by the user). We hypothesised that integration of AOP information would be clinically useful, even with a simple underlying model of conduction.

Equations to determine the distance to the tachycardia mechanism, based upon the response to AOP are developed below. Next, Section 6.3.3 describes the way in which AOPs are analysed and information from them is combined visually on the electroanatomic shell.

6.3.2 Modelling post-pacing response to distance from tachycardia

Focal tachycardia - equations for distance to focus

As described in Chapter 1, ‘focal tachycardia’ is used to refer to tachycardias with a localised mechanism and centrifugal activation of the rest of the atrium. The mechanisms include micro-reentry, triggered activity, automatic foci, and localised reentry. After AOP with a focal tachycardia, the PPI is composed of the conduction time from the pacing catheter to the peri-focal junction, the peri-focal conduction time, at least one tachycardia cycle length (TCL), another peri-focal conduction time, and then the conduction time from the peri-focal junction to the pacing catheter. This has been validated by other workers.[169] A schematic is shown below in Figure 6-1.

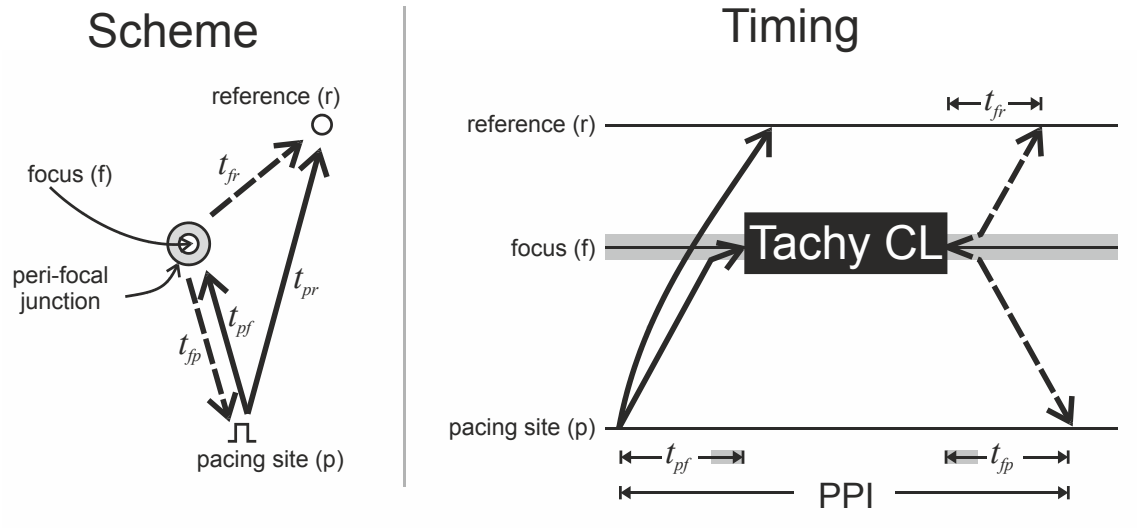

Figure 6-1. Adapted from Mohamed et al.[169] The figure has been extended from Figure 1-8 to include a reference catheter. This schematic is used for the development of equations in the text.

Using the notation in Figure 6-1,

$$t_{pf} + TCL + t_{fp} \leq PPI \quad [6\text{-}1]$$

and so if $t_{pf} \approx t_{fp}$ then

$$t_{fp} \leq \frac{PPI - TCL}{2} \quad [6\text{-}2]$$

If the PPI and the TCL are known, it is possible to estimate the conduction time using [6-2]. Conduction velocity in the atria is anisotropic and heterogeneous. Specifically, areas of low conduction velocity can occur with disease or prior ablation, and an area of slow conduction occurs at the peri-focal zone. However, by combining [6-2] with the use of an upper estimate for the conduction velocity in any direction, v_{max}, then the maximum distance between the focus and the pacing catheter can be estimated. In the following equations, d_{fp} is the distance from the focus to the pacing electrode and $d_{fp,max}$ is the maximum estimate of d_{fp}.

$$d_{fp} \leq v_{max} \times t_{fp} \leq v_{max} \times \frac{PPI - TCL}{2} \quad [6\text{-}3]$$

$$d_{fp} \leq v_{max} \times \frac{PPI - TCL}{2} \quad [6\text{-}4]$$

$$d_{fp,max} = v_{max} \times \frac{PPI - TCL}{2} \quad [6\text{-}5]$$

At the resumption of tachycardia, the relative timing of the reference electrode and the pacing electrode depends upon the relative conduction times from the tachycardia focus. In the following equation, T_r^{T1} and T_p^{T1} represent the timing of the first beat of tachycardia at the reference and pacing electrodes respectively. The conduction time from the focus to the reference electrode is denoted by t_{fr}.

$$T_r^{T1} - T_p^{T1} = t_{fr} - t_{fp} \quad [6\text{-}6]$$

Combining this with [6-1] gives

$$t_{fr} \leq t_{fp} + T_r^{T1} - T_p^{T1} \quad [6\text{-}7]$$

Finally, combining with the maximum conduction velocity and [6-2] yields:

$$d_{fr,max} = v_{max} \times \left(\frac{PPI - TCL}{2} + T_r^{T1} - T_p^{T1}\right) \quad [6\text{-}8]$$

[6-5] and [6-8] provide estimates of the greatest possible distance between an electrode (pacing or reference) and the tachycardia focus, after an AOP. Areas of the atria beyond these boundaries can be excluded from further mapping.

Algorithm for colouring shell

For each electrode response to AOP, Overdrive3D finds all parts of the atrial shell that lie within the maximum possible distance to the tachycardia focus – the focus must lie within this boundary. Areas outside of this boundary can be eliminated and are shaded in grey to denote this. When analysing more than one AOP, including the response at multiple electrodes, the tachycardia focus must lie within the intersection of all boundaries that have been calculated. Areas outside of this intersection are shaded grey, and areas within it are coloured according to the distance from the electrode positions – the recommended site for pacing is located away from the sites that have already been assessed. See Figure 6-2 below.

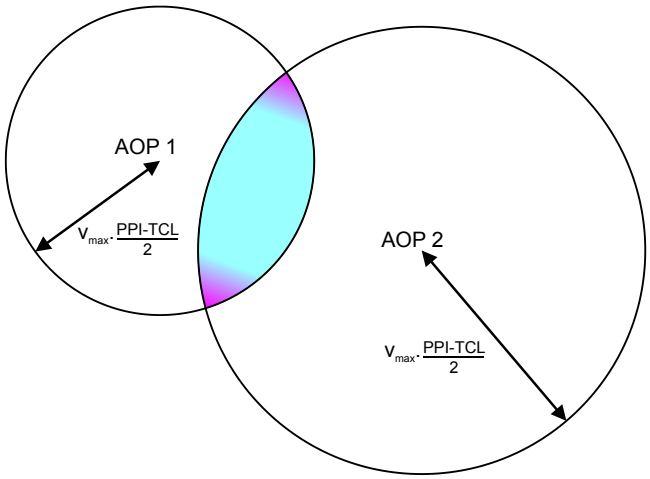

Figure 6-2. 2D schematic to show how the shell is shaded. Let us suppose that there is a focal tachycardia and that 2 AOP manoeuvres have been performed. The maximum distance from AOP 1 to the tachycardia is calculated – the tachycardia focus must lie within a circle of this radius. A similar calculation gives a radius from AOP 2, for the second manoeuvre. When information from these manoeuvres is combined, the focus must lie within the intersection of these circles. This is shaded, with magenta indicating sites furthest from all previous AOP manoeuvres. Thus the recommended next pacing sites are at the apices of this intersection. Note that the information from passive 'reference' catheters could also be included, using [6-8]. As more AOP manoeuvres are performed, the tachycardia is located with increasing accuracy.

Macroreentrant tachycardia – equations for distance to circuit

The relationship between distance to a macroreentrant circuit and the PPI has previously been investigated, for reentry around a circular obstruction on a plane.[174] Here, the analysis is extended to include reentry around a linear scar and also reentry around a truncated cone. Linear scar is a more realistic model for an atriotomy, and a truncated cone is a more realistic representation of reentry around the tricuspid or mitral annulus.

Reentry modelled around a linear scar

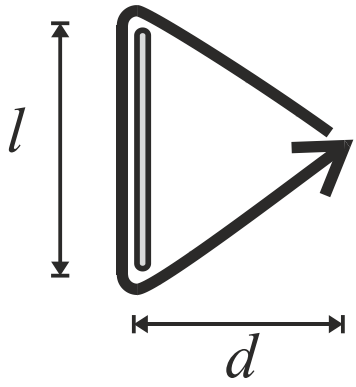

Figure 6-3. Reentry around a linear scar. The scar is modelled as an obstruction with length, l. The pacing site is perpendicular to the middle of the scar (this assumption is discussed in the text) and separated by a distance, d.

Figure 6-3 shows a schematic for reentry around a linear obstruction. The activation wavefront from the last pacing stimulus will travel from the pacing catheter, orthodromically around the reentrant circuit and then return to activate the paced site. For a conduction velocity, v, then using Pythagoras' theorem, the PPI is given by:

$$PPI = \frac{1}{v} \times \left\{ l + 2\sqrt{d^2 + \left({}^{l}/_{2}\right)^2} \right\} \quad [6\text{-}9]$$

The TCL is given by:

$$TCL = {}^{2l}/_{v} \quad \Rightarrow \quad l = TCL.v/2 \quad [6\text{-}10]$$

Now combining [6-9] and [6-10]:

$$d = \frac{v}{2}\sqrt{PPI \times (PPI - TCL)} \quad [6\text{-}11]$$

In the presence of non-uniform conduction velocities, then the distance d must be shorter than the distance calculated by assuming the maximum conduction velocity. Therefore, the maximum distance d_{max} is given by:

$$d_{max} = \frac{v_{max}}{2}\sqrt{PPI \times (PPI - TCL)} \quad [6\text{-}12]$$

It can be shown that this equation also provides a valid over-estimate for pacing positions that are not located perpendicular to the middle of the obstruction.

Reentry modelled around a truncated cone

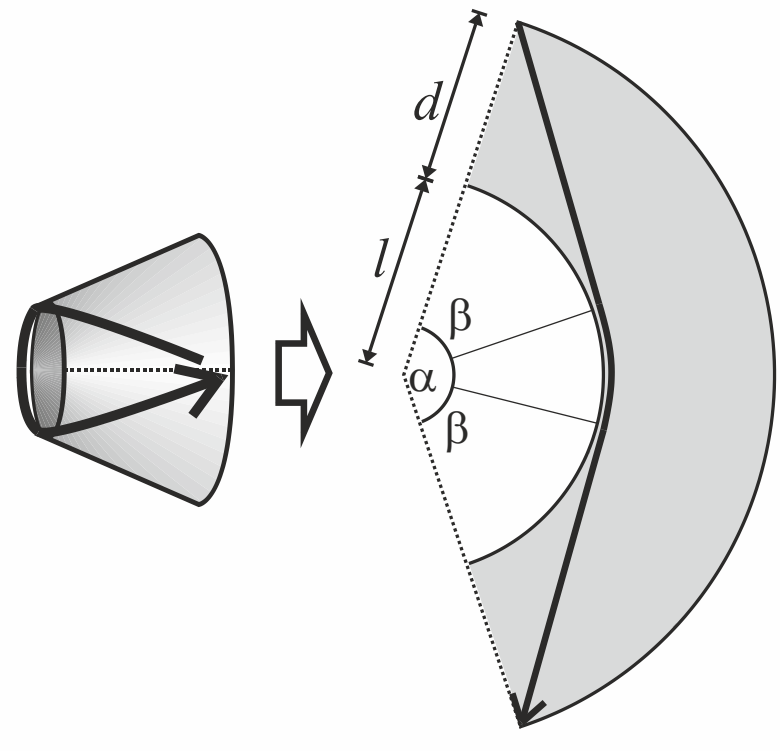

Figure 6-4. Reentry around a truncated cone. The pacing site is a distance, d, from the reentry circuit, which courses around the part of the cone with the smallest radius. The mathematics is simplified by 'cutting' the cone along a meridian (dotted line on left part of figure), and then 'unrolling' it onto a plane.

Using Figure 6-4, let p be the path taken by the last paced wavefront around the cone and then returning to the pacing site.

$$p = 2\sqrt{(l+d)^2 - l^2} + (\alpha - 2\beta).l \quad [6\text{-}13]$$

Let the aperture of the cone be 2θ. The angles, α and β, are in radians and can be related to the cone's dimensions as follows:

$$\alpha = 2\pi \sin(\theta)\ ,\ \beta = \cos^{-1}\left(\frac{l}{l+d}\right) \quad [6\text{-}14]$$

The TCL can be related to l by the distance around the inner circle and the conduction velocity, v:

$$TCL = \frac{\alpha.l}{v} \quad [6\text{-}15]$$

If there is a uniform conduction velocity, v, then $p = PPI \times v$. This can be combined with [6-13], [6-14], and [6-15] to give:

$$d^2 + 2dl + \left(l.\left(2\pi \sin(\theta) - 2\cos^{-1}\left(\frac{l}{l+d}\right)\right) - PPI.v\right)^2 = 0 \qquad [6\text{-}16]$$

Reentry modelled around a circular obstruction

From Figure 6-4, it can be seen that a circular obstruction is a special case of reentry around a truncated cone, where the aperture of the cone is π radians, and so $\theta = \pi/2$ and $\alpha = 2\pi$. Now [6-16] becomes:

$$d^2 + 2dl + \left(l.\left(2\pi - 2\cos^{-1}\left(\frac{l}{l+d}\right)\right) - PPI.v\right)^2 = 0 \qquad [6\text{-}17]$$

This is equivalent to equations derived by previous workers.[174]

Summary – post pacing response and distance to the tachycardia

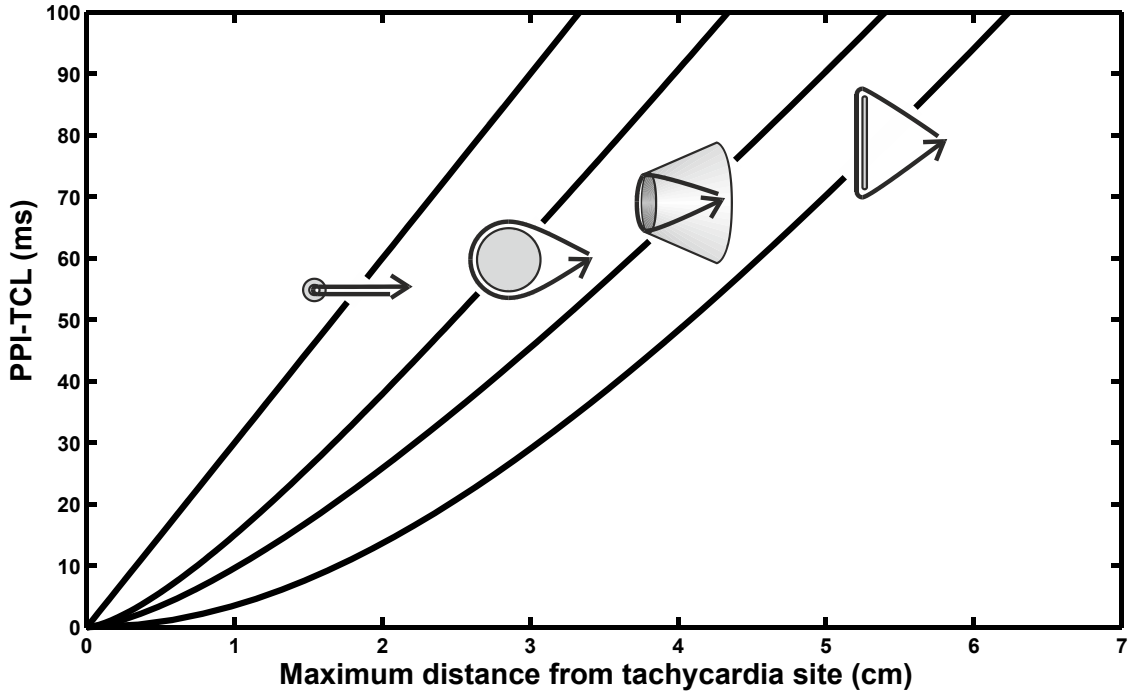

Figure 6-5. A comparison of models for relating PPI to the distance from the tachycardia site. PPI-TCL is related to distance for each of the mathematical models that have been used in the text. From left to right, these are: focal tachycardia, reentry around a circular obstruction, reentry around a truncated cone, and reentry around a linear lesion. Parameters were: TCL 250ms, conduction velocity 0.7m/s, and a conical aperture of 80°. For discussion , see text.

In Figure 6-5, the relationship between PPI and distance to the tachycardia site is summarised. From this graph, it can be seen that for a PPI-TCL=30ms, the maximum possible distance to a scar-related macroreentry circuit is much greater than for a focal tachycardia. In order not to underestimate the distance to a tachycardia site, the equation for a linear obstruction was used for macroreentrant tachycardias ([6-12]).

6.3.3 Development of the Overdrive3D algorithm

Each AOP must be annotated with activation times and assessed for capture of the entire chamber at the pacing CL, and the FBT must be identified for each electrogram. A GUI was written to assist with the interpretation of AOP manoeuvres and this was described in Section 2.2.3 on p49. Following this, the information is incorporated with information from previous AOPs before being displayed on a reconstruction of the electroanatomic shell. Details of this process are given below.

Import and analysis of electrograms

It is usual for reference catheters to remain in the same location between different AOP manoeuvres. The first beat of tachycardia can be compared between every pair of stationary electrodes, for every pair of AOP manoeuvres. This was discussed in detail in Chapter 5. If the difference in timing between a pair of electrodes changes by one TCL, then this is evidence for single loop reentry. If there is a change of two TCL then this suggests double loop reentry. If there are changes that are not a multiple of the TCL, then this suggests that the tachycardia activation pattern is different between the different AOP manoeuvres – i.e. that the tachycardia has changed.

Assimilation of AOP information onto the electroanatomic shell

The assimilation of information onto the electroanatomic shell depends upon the tachycardia mechanism. The user can select ‘focal’ or ‘macro’ analysis. This choice will be informed by previous activation mapping and also by the results of previous AOP analyses: the Overdrive3D program will indicate if the responses are consistent with macroreentry.

For focal analysis, the response at each electrode for each AOP is used to determine the maximum possible distance to the focus, using [6-5] and [6-8]. Areas outside this perimeter are shaded grey. Locations on the shell that are within the

maximum possible distance to each electrode for each AOP are possible locations for the tachycardia. These areas are shaded as previously described in Figure 6-2.

For macroreentry analysis, the maximum distance from the pacing electrode to the tachycardia circuit is estimated using [6-12], for each AOP. The atrial surface within this boundary is then shaded according to the PPI. The tachycardia mechanism must pass through this area. As more AOPs are performed, more information about the location of the circuit is generated. An example is given later, in Section 6.5.3 on p139.

Maximum possible conduction velocity

The software requires an estimate of the maximum possible conduction velocity, v_{max}, in order to relate electrogram timings to distances. This is set by the user and it is important that it is an upper estimate of the actual value: a high value of v_{max}will also compensate for errors in the model, geometrical representation, and electrogram timings. However, the software also provides estimates of conduction velocity from the entrainment manoeuvres, by calculating the shortest geodesic distances between the pacing electrode and reference electrodes during an AOP, and dividing these by the respective conduction times. (Position and timing measurement accuracies are incorporated in order to give appropriate error bars on the graphical display.) Low velocities may be recorded near to zones of slow conduction, or if functional block is created during the entrainment of a macroreentrant tachycardia.

Graphical User-Interface

A GUI for Overdrive3D has been designed. This performs a number of tasks: anatomical geometry can be imported; electrograms can be annotated with assistance for detecting the first beat of tachycardia; basic checks of the data are performed, with alert messages if possible errors are detected; different AOP manoeuvres can be 'hidden' or 'unhidden' from the analysis; and the results are presented. Additionally, the value of v_{max} used for the calculations can be interactively adjusted, and the user can view calculated conduction velocities.

6.4 Methods for clinical testing

Patients undergoing ablation for atrial tachycardia (including atrial flutter) or for pulmonary vein isolation were included in the study. All patients had venous access via

the right femoral vein and transseptal puncture was performed if left atrial access was required for their clinical procedure. As is standard clinical practice, all AOP manoeuvres were performed by pacing with a cycle length 20-30ms shorter than the tachycardia cycle length. For annotation of electrograms at the pacing site, local activation time during pacing was annotated at the onset of the stimulus artefact.

For all patients, a Navistar catheter was used with Carto3 (Biosense Webster, Diamond Bar, CA) to create an anatomical shell. This was then exported to a CD, and imported into the Overdrive3D software on a separate computer. For each AOP site, the x-, y-, z- coordinates were read from Carto3 and imported manually into Overdrive3D. Immediately after each AOP, the electrograms exported from the LabView recording system onto flash memory storage and then imported into Overdrive3D.

Overdrive3D was then used to interpret all AOP manoeuvres that had been performed for the tachycardia being analysed. For focal simulated tachycardias, the 'focal analysis' was used. For other tachycardias, 'focal analysis' was used initially and two manoeuvres were performed from differing locations. Overdrive manoeuvres were assessed using the GUI described in Section 2.2.3. For catheters that remained in the same position between different manoeuvres, the activation pattern of the FBT was assessed. If the relative timing of FBT at two electrodes changed by more than 12.5ms then a warning was activated to indicate that the tachycardia may have changed. If the change was close to a multiple of the TCL, then the warning indicated that this change may be due to underlying macroreentry according to the criterion presented in Chapter 5.

Overdrive3D was evaluated for 6 clinical atrial tachycardias, and 4 simulated tachycardias. For the simulated tachycardias, focal atrial tachycardia was simulated by pacing, with a temporary pacing system in AAI mode, from an additional catheter placed near to the left or right atrial appendage. For all cases, an initial value for v_{max} of 1.25m/s was used and adjusted on the basis of individual conduction velocities measured between the pacing and reference electrodes.

6.5 Results

Table 6-1 includes details of each patient included in the study. The number of AOP required refers to the number of manoeuvres to localise a focal tachycardia (or simulation) within 1cm. For macroreentry circuits, this number refers to identification of macroreentry as the mechanism and also identification of an appropriate ablation strategy (i.e. a critical isthmus).

Patient	Age	Tachycardia	Number of AOP Required
1	63	Focal simulation, LA near LAA	2
2	52	Focal simulation, LA near LAA	3
3	55	Focal simulation, RA near RAA	2
4	58	Focal simulation, RA near RAA	2
		Common flutter	4
5	54	RA macro-reentry, around SVC	4
6	48	Common flutter	3
		Localised-reentry near LSPV	4
7	31	Localised-reentry, inferolateral RA	4
		Localised-reentry, inferoseptal RA	3

Table 6-1. LSPV, left superior pulmonary vein.

Overdrive3D was able to perform all necessary calculations for analysis of an AOP within approximately 20 seconds, after data entry. (This computation time is necessary for the extensive iteration involved in finding shortest geodesic paths around the anatomical shell.) The export of geometry data from Carto3 took approximately 10 minutes, due to the need to write the data to CD. Export of the electrogram data for each entrainment manoeuvre took less than 1 minute. Integration of Overdrive3D into the localisation system would obviate the need for these export times. For most analyses, the pre-set value of v_{max} (1.25m/s) was satisfactory. In some patients, it was increased according to measured values but was always in the range 1.25-1.4m/s.

6.5.1 Simulated Focal Tachycardias

Focal tachycardias were simulated by pacing from a temporary generator in 4 patients (see Table 1). An example is presented in Figure 6-6. For 3 of the patients, the positions (<1cm) of the simulated tachycardia were identified with 2 AOP, and in the other patient 3 AOP were required.

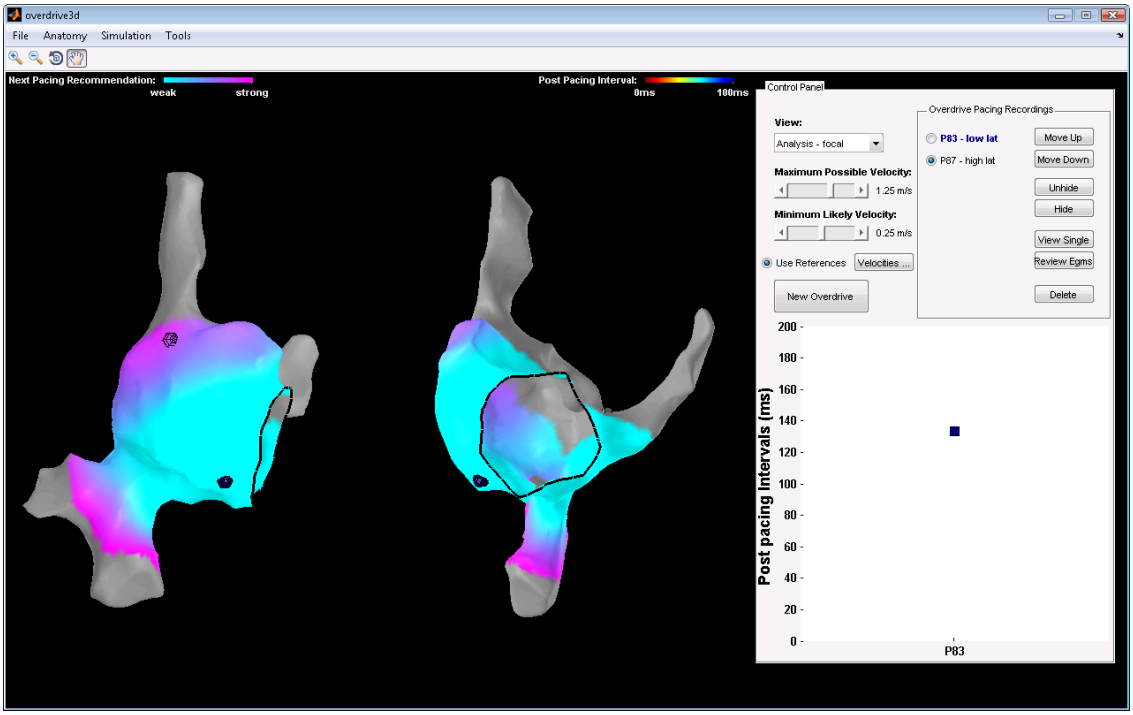

Figure 6-6. Overdrive3D and analysis of a simulated focal tachycardia. To the left, two views of the atrial geometry are displayed (RAO and LAO). The user control panel is to the right. A single Atrial Overdrive Pacing (AOP) manoeuvre has been performed, just lateral to the cavo-tricuspid isthmus. Information from the pacing electrode and from the proximal CS electrode has been used for analysis. The post-pacing interval (at the pacing catheter) was 137ms, and the estimated conduction time from the CS electrode was also long. Therefore, the entire lateral right atrium is within the calculated 'boundaries' (see Text). The software recommends sites to pace – strong recommendations in magenta, weak recommendations in cyan. The recommended sites are within the calculated boundaries but far away from the CS and pacing sites. The algorithm makes these calculations on the basis of the supplied geometry, which extends out of the heart to the IVC in this case. Thus, the recommended site for the next AOP is the high-postero-lateral right atrium and this was close to the site of the simulated tachycardia (open mesh point).

6.5.2 Clinical Localised Reentry Tachycardias

In total, 3 localised reentry tachycardias were mapped in two patients. In Patient 6, there was localised reentry near to the left superior pulmonary vein (the patient had not had any prior ablation or history of AF). AOP was performed at the anterior wall, two locations on the posterior wall and then at the tachycardia site – 4 in total, including the site of tachycardia. Patient 7 had atrial tachycardia in the context of a prior Fontan procedure for congenital heart disease, with a very large right atrium. Analysis of the first tachycardia is illustrated in Figure 6-7, and localisation would have been achieved with 4 AOP: although it was not possible to obtain capture at the 4th site, ablation was performed here and caused a change of cycle length and activation pattern consistent with termination of this tachycardia. Mapping of the next tachycardia localised it to the septal side of the atrium using 3 AOP, where further ablation restored sinus rhythm.

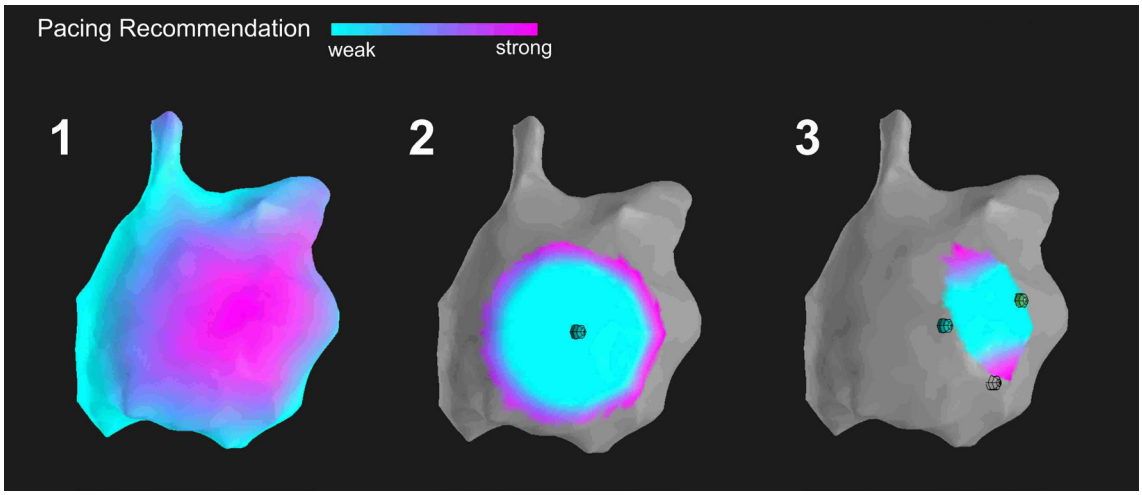

Figure 6-7. Use of Overdrive3D for a patient with a previous Fontan surgery, a huge right atrium, and atrial tachycardia. Analysis provided by the software is shown after 1, 2, and 3 atrial overdrive pacing (AOP) manoeuvres (right lateral view). The atrial surface is shaded according to 'pacing recommendation' (colour bar, top left), and the pacing sites are indicated by a sphere shaded according to the post-pacing interval (PPI, colour bar, top right). A reference catheter was not used for this case (the activation sequence changed, probably due to movement). The first AOP was performed on the septal side of the atrium (site not in view), giving a very long PPI (477ms) and resulting in the recommendation to perform the next AOP at the lateral wall. The second AOP resulted in a much shorter PPI (53ms), and a shorter boundary to define the location of the tachycardia. A third AOP was performed with a similar PPI (63ms), but the combined information gives 'bracketing' of the tachycardia location and two recommended sites for the next AOP. Activation timing at the inferior site was early and therefore this was chosen. However, it was not possible to get capture during pacing (site indicated by open mesh). Due to favourable activation mapping in this region, ablation was performed and resulted in termination of this tachycardia.

6.5.3 Clinical Macroreentrant Tachycardias

Patient 5 had previously undergone CTI ablation. Macroreentry was verified with 2 AOP and 2 further AOP were used to characterise the circuit further, as illustrated in Figure 5. The diagnosis was macroreentry around the SVC, despite a relatively short PPI (19ms) just lateral to the CTI. After termination of tachycardia pre-existing bi-directional CTI block was demonstrated, confirming that the CTI had not participated in the tachycardia. Patient 4 and Patient 6 both had typical CTI dependent flutter. In each case, reentry was identified with 2 AOP and the circuit was further characterised with 2 additional AOP.

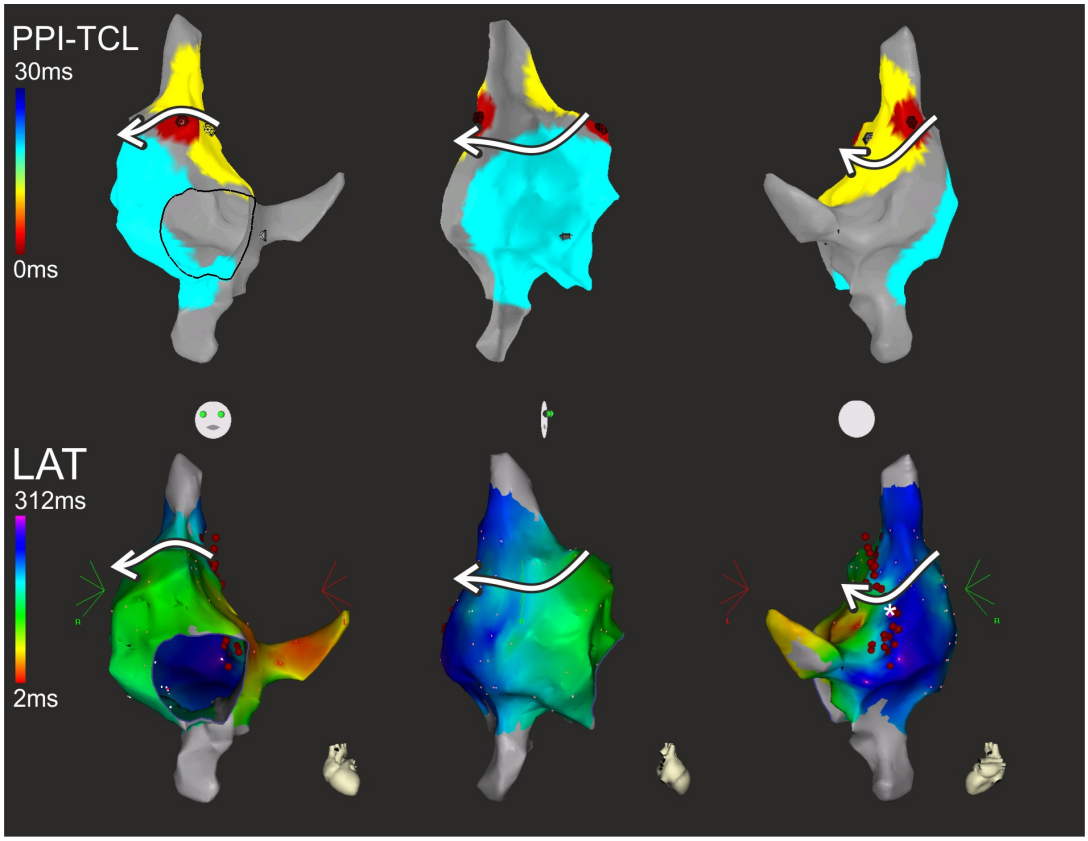

Figure 6-8. Use of Overdrive3D with an unusual case of macroreentry. The patient had previously undergone ablation of the cavotricuspid isthmus, but had not had any other cardiac interventions and had a normal echocardiogram. The right atrium is displayed in 3 views (antero-posterior, right lateral, and postero-anterior). In the top row, the Overdrive3D analysis is shown after 4 atrial overdrive pacing (AOP) manoeuvres. The first AOP was performed at the high septum and gave a short PPI (yellow, PPI-TCL=11ms). Therefore, the mapping catheter was held in the same position and an AOP was performed from a reference catheter at the low lateral wall (pale blue, PPI-TCL=19ms). Combining information from these AOP gave two alert messages: 1) there was no position on the geometry within the boundaries of both AOP, for a focal tachycardia and 2) when comparing the first beat of tachycardia between the AOP manoeuvres, the activation difference between the mapping and reference catheters changed by 402ms (almost equal to the tachycardia cycle length of 399ms) confirming the presence of reentry (see Chapter 5). Therefore, the Overdrive3D analysis was changed to 'Macroreentrant Tachycardia Analysis'. Two further AOP were performed at the right atrial appendage and high posterior wall (both with PPI-TCL=1ms). The shaded areas represent the area that falls within the estimated maximum distance from the pacing site to the tachycardia mechanism, for each AOP, and is shaded according to the PPI. Consequently, the reentry circuit must pass through each shaded zone. Note that the shaded areas are large relative to the short PPIs that were obtained – see Discussion. The activation map is shown in the bottom row. There was a zone of slow conduction at the medial aspect of the posterior wall and so linear ablation was performed here (red points, best seen lower right panel), achieving termination at the site marked with the white asterisk (there was no slowing of tachycardia cycle length with ablation at sites more superior on the line). The tachycardia mechanism is shown with white arrows and is consistent for both Overdrive3D and the activation maps.

6.6 Discussion

The feasibility of a computer assisted approach to the interpretation of AOP manoeuvres has been demonstrated. The software, Overdrive3D, provides a platform for the interpretation of any manoeuvres that have been performed at different stages of the procedure from user-chosen locations, with any number of reference electrodes. This flexibility provides the potential for integration into a combined AOP-mapping and activation-mapping strategy. The expectation is that this will allow maximum diagnostic gain from AOP, minimizing the number of manoeuvres that are required, and therefore contributing to swift and accurate diagnosis.

For the design of Overdrive3D, a simple model of cardiac conduction was used – assuming that velocity in all locations and directions is less than a user-defined value, v_{max}. The value of v_{max} can be adjusted by the user during the procedure, on the basis of measured conduction velocities from the pacing sites to the reference electrodes. However, we recommend a margin for error of at least 30%. We found that values for v_{max} of 1.2-1.4m/s were satisfactory for the patients in this small series. Whilst extremely heterogeneous conduction velocities in a patient might cause some lack of precision, the results should be reliable if v_{max} is set fast enough. Integration of results from multiple AOP then compensates for the simplistic model: Overdrive3D performed adequately, even for a challenging case of atrial tachycardia in a patient with prior Fontan surgery (see Figure 6-7) in which conduction velocities were likely to have been variable across different parts of the atrium.

The analysis of AOP for focal tachycardias builds upon work by other investigators.[169] As noted in an editorial accompanying that study, these may often arise from microreentry or localised reentry rather than from an automatic focus, and the response of automatic foci to overdrive pacing might be more variable.[206] However, provided that AOP causes a return cycle length, at nearby atrial tissue, that is equal to or longer than the TCL, then [6-5] and [6-8] will still give valid (over-) estimates for the distance from the recording electrodes to the tachycardia focus. Overdrive pacing should be performed for long enough to ensure that acceleration of the tachycardia has not occurred.

For macroreentrant tachycardias, the concept of color-coding a geometrical representation of the cardiac anatomy according to results of AOP is not new. Previous investigators used commercially available electroanatomical mapping software to do this, annotating each AOP location according to the PPI and using in-built interpolation of colour between the points.[25, 171] This method has been used for detailed characterisation of flutter circuits using a high number of AOP manoeuvres (range 18-103).[25] In another study, the method was used to assist with diagnosis and ablation strategy for reentrant tachycardias.[171] However, the number of AOP manoeuvres was high (14-77 per patient) and the time taken for PPI mapping was long (12-200 minutes per tachycardia). In contrast to these previous studies, Overdrive3D indicates possible locations of the tachycardia mechanism, calculated from a simple model of conduction and integrating information from a comparatively small number of AOP manoeuvres.

An algorithm for determining macroreentry circuits has previously been described, using up to 3 AOP manoeuvres from predetermined locations in the RA and CS, in patients without complex congenital heart disease.[170] One of 6 possible regions is then identified as being critical to the circuit. This strategy could be used in conjunction with Overdrive3D. Overdrive3D has the added benefit that its design allows flexibility in AOP position, use with macroreentrant as well as focal tachycardias, and also use with patients who have structural cardiac abnormalities including complex congenital heart disease.

There has been little previous investigation of the relationship between PPI and the distance from pacing site to macroreentrant circuit. One study developed theoretical equations for reentry around a circular obstruction on a sheet.[174] Further theoretical work was undertaken for the development of Overdrive3D, investigating simple mathematical models of reentry around a linear obstruction (analogous to an atriotomy scar) and around a truncated cone (analogous to peri-tricuspid or peri-mitral flutter). This analysis suggested that the distance to the tachycardia circuit may be greater than previously appreciated, for a given PPI, and the equation corresponding to a linear lesion was used for Overdrive3D because this represented a 'worst case scenario'. This was vindicated by the analysis of AOP in Patient 5 (see Figure 6-8). The PPI lateral to the CTI was 19ms. However, a relatively large possible distance to the tachycardia circuit was calculated and a large corresponding area was shaded onto the

anatomical representation. Further AOP manoeuvres and activation mapping confirmed that the tachycardia circuit passed near to the limit of this shaded area, i.e. the shaded area was appropriately large.

The equations used for calculating distance to the macroreentry circuit are sensitive to small changes in PPI. Therefore, it is important that the PPIs are accurate and reflect the tachycardia. It has previously been reported that conduction delay at pacing rates faster than TCL can cause transient slowing of the tachycardia circuit,[164] which would give artificially long PPI and artificially long distances to the tachycardia circuit in Overdrive3D. This effect did not noticeably impair the analysis in this feasibility study, but will need further investigation.

Further investigation is also required in order to optimise the way in which Overdrive3D is integrated with results from activation mapping. Currently, the Focal Tachycardia Analysis provides the user with information about the possible location of the tachycardia as well as recommendations for the next AOP location. It is anticipated that selective activation mapping within these areas will help to clarify the best location.

In its current form, Overdrive3D can confirm the presence of reentry using new entrainment criteria (see Chapter 5). There is no similar entrainment criterion for focal tachycardias. However, the presence of focal tachycardias can sometimes be inferred from cycle length variability during tachycardia or in response to AOP.[3, 204] Another limitation of AOP, and its use in Overdrive3D, is that confounding results might be obtained if multiple competing tachycardia mechanisms co-exist. However, if AOP mapping is used close to the dominant mechanism (based on activation mapping) then it should still be reliable: for its most effective use, Overdrive3D must be used in conjunction with the other tools available to the electrophysiologist.

6.7 Conclusion

Using a simple model of conduction, this study has shown the feasibility for integrating electroanatomic information from multiple AOP, in the presence of any chosen recording electrodes. It is hoped that Overdrive3D, integrated into electroanatomic mapping systems, could greatly expedite procedures for atrial tachycardia. Further testing is in progress.

7 Conclusions

7.1 Introduction

Mapping is crucial for the successful ablation treatment of atrial tachycardias, which have formed an increasing clinical burden in the era of AF ablation. Only by determining the mechanism of these tachycardias can lesions be strategically placed at locations which will terminate and prevent recurrence of the arrhythmia. The mechanism must be deduced by mapping and the current gold standard is isochronal mapping followed by attempted entrainment.

It is difficult to quantify the need for better mapping systems precisely because accurate data is not available. However, during 2003-2006 there were at least 4000 patients with persistent AF who received treatment with catheter ablation, worldwide,[1] at a time when the number of ablations was growing at 15% per year in the US.[207] Some of these patients would have required ablation of AT during their index procedure, and approximately 25% would have re-presented with AT afterwards. Therefore, the number of patients requiring treatment of AT, in the context of AF ablation, is substantial and growing. Additionally, AT continues to require treatment in patients with normal hearts and in patients with previous cardiac surgery. Arrhythmia is an important cause of morbidity and mortality in patients with a history of congenital heart disease.

A literature review, in Chapter 1, identified key shortcomings of current approaches (see Sections 1.3.7 and 1.4.7). In brief, activation mapping with isochronal maps requires a user-defined window of interest and also a single LAT to be defined for each electrogram. Existing entrainment criteria are often difficult to apply in the setting of AT and the analysis of electrograms has been limited to interpretation of the PPI at the electrode used for pacing.

The overarching goal of the thesis was to reassess these mapping techniques and to develop new techniques that facilitate and improve the interpretation of information that is collected.

7.2 Original Contributions

This thesis has explored new approaches to the mapping of atrial activation and also interpretation of entrainment manoeuvres.

7.2.1 Activation mapping

In Chapter 3, Ripple Mapping was developed and tested in a variety of different arrhythmias. Computational methods were developed to reconstruct a cardiac surface from the locations of collected electrograms. Software was written to display each electrogram as a bar protruding from the cardiac surface, where the length varies with time according to the electrogram's voltage-time relationship. The method was further developed in Chapter 4, with the cardiac surface being exported from the Carto3 platform and shaded according to the bipolar electrogram voltage. The user-interface was also modified so that cases could be loaded directly and then assessed by other users, with minimal prior instruction (Aim A4).

Interpretation of Ripple Maps was performed without requiring a user-defined window of interest (Aim A1) or LAT assignment (Aim A2). Double potentials were also displayed successfully (Aim A3) although the visualisation of electrogram characteristics was limited if the signal-to-noise ratio was low. This may be one of the reasons why the successful diagnosis of localised reentry tachycardias was lower than for macroreentry.

7.2.2 Entrainment mapping

At an early stage in the research into entrainment, it became clear that the interpretation of the response to overdrive pacing depended critically upon the mechanism of tachycardia: for example, the trans-atrial distance from the tachycardia mechanism could be much longer, for a given PPI, if the mechanism was macroreentry rather than focal. This provided the motivation to search for an improvement in the methods for detecting macroreentry.

Previous criteria for detecting reentry are often difficult to apply to AT, as discussed in Section 1.4.7 on p44. The new entrainment criterion proposed in Chapter 5 is simple to elicit (Aim E1) and can detect reentry from a wide variety of location pairs around the atria. Preliminary testing in clinical cases is presented. It is the first entrainment criterion with the capability to detect double-loop reentry (Aim E2). Integration of the entrainment criterion with anatomical information can also assist with the identification of an appropriate isthmus for ablation (see "Further theoretical

implications" on p106), even if there is decremental conduction that results in a long PPI from this location (see Figure 5-20).

The mathematical development for the entrainment criterion in Chapter 5 sets out the assumptions and conditions for which the criterion will detect single-loop or double-loop reentry. This analysis was useful in providing a framework for understanding limitations of the method: only with the theoretical analysis did it become apparent that the criterion could theoretically suggest the presence of double loop reentry even if only single loop reentry was present. The wording of the entrainment criterion was modified to allow for this.

In Chapter 6, a mathematical approach was continued in order to investigate the relationship between the response to overdrive pacing and the distance from recording electrodes to the tachycardia mechanism. Equations were developed that used conservative assumptions in order to relate the maximum possible trans-atrial distance to the PPI (Aim E3), depending upon the tachycardia mechanism (Aim E4). Additionally, for focal tachycardias the post-pacing response at electrodes that were not used for pacing can be used to give an estimate for this distance (Aim E5).

The rationale behind developing a clinical prototype for electroanatomic integration of overdrive pacing manoeuvres was to assimilate the information using the theoretical analysis that had been developed. Despite the conservative assumptions (and hence possible lack of precision for identifying the tachycardia location from any one piece of information), it was hoped that by using information from all pacing manoeuvres then the utility of the approach would be increased. Feasibility of the method was demonstrated in patients with localised reentry, macroreentry and also with tachycardias simulated by pacing (Aim E6).

7.3 Implications of the research

In recent years, improvements in technology have allowed for more realistic and precise delineation of atrial geometry at the time of ablation procedures. Additionally, mapping can be performed with catheters comprising multiple electrodes. (For the Carto system, this technology has only become available at this institution within the last month.) It is therefore possible to acquire electrogram data much faster than LAT can be properly assessed by the operator or their assistant. Ripple Mapping may be

particularly useful in this context because LAT annotation is not required. The Ripple Map can then be interpreted using a top-down approach that draws upon the knowledge of the electrophysiologist as they interpret cardiac activation.

In this thesis and in much of the literature, activation mapping and entrainment mapping have been considered separately. When they are combined, entrainment information has usually been used to confirm a diagnosis that has been hypothesised from activation mapping. However, there has been no work on closer integration of the two methods.

In the research presented here, a more formal analysis of overdrive pacing in an electro-anatomic context has been undertaken. Methods for analysing overdrive pacing have been developed here that can be used flexibly, or in the future could be integrated into a more prescriptive approach. The prototype Overdrive3d software uses the newly developed entrainment criterion and also mathematical modelling to combine information from multiple electrodes with multiple manoeuvres. For focal tachycardias, the region of atrium containing the tachycardia mechanism is progressively bracketed as this information becomes available. For macroreentry, areas which must contain part of the tachycardia circuit are highlighted.

This raises the possibility of a more iterative approach between the mapping of activation and entrainment. Preliminary overdrive pacing could be performed earlier in the mapping process in order to provide an indication of areas where careful activation mapping should be performed. Further overdrive pacing could then be performed on the basis of all of this information. Even if overdrive pacing is used very sparingly, on occasions where the PPI information is different to the electrophysiologist's expectation then being able to analyse the response at multiple electrodes and integrate this with other manoeuvres is likely to be helpful.

7.4 Future directions

The techniques developed in this thesis involve computational methods for improving the interpretation of signals measured during clinical electrophysiology procedures. The ultimate aim is that the techniques can influence the treatment of patients through their widespread use. This requires their incorporation into the systems that are used around the world in electrophysiology labs.

In this thesis, testing has been performed with off-line analysis because the commercially available systems for electroanatomic mapping do not allow for immediate download of clinical data. This has been a major obstacle to the progress of the research but some progress has been made.

The Ripple Mapping technique has been taken up by Biosense Webster and will be incorporated into the next version of the Carto3 software (personal communication). This will finally allow assessment of the utility of Ripple Mapping in the real clinical setting, used by a broader spectrum of the electrophysiology community. The future improvement of Ripple Mapping should be with two distinct objectives.

The first objective is to improve the usability of the existing method, in order to maximise the diagnostic accuracy of arrhythmias. The user-interface will be modified in the light of user feedback and the strategy for sampling electrical signals around the atria will be refined. The second objective should be to improve the signal processing in order to convey arrhythmia activation better. For example, in atrial tachycardia, algorithms could correct for, or remove, beats with a significant far-field ventricular component. Similarly, for mapping ventricular tachycardia substrate in sinus rhythm, algorithms might also be developed to enhance the components of signals deriving from local late potentials, as opposed to far-field healthy ventricular activation.

For the work on entrainment, there is also some interest from Biosense Webster in assisting us with development. A non-disclosure agreement has been created between King's College London, Bordeaux University, and Biosense Webster. It is hoped that a system will be provided to allow for export of data from Carto3 to a research system during real clinical cases. This will allow for further data gathering for a much larger cohort of patients. Hopefully, this will then support the case for incorporation into commercially available systems.

There has been extensive focus on the theoretical background for the Entrainment Criterion and for the Overdrive 3D software presented in this thesis. One of the substantial advantages of this approach is that the assumptions behind the computer algorithms are explicit. This will allow future developers to refine the software and also to be clearer about its limitations. It is also possible that the

application of the methods might be broadened; this thesis has pursued techniques for the atrium but some of these might also be applied to ventricular arrhythmias.

Although electroanatomic systems have improved the delineation of the atrial shape and the catheter location within it, imaging techniques may have an increasing role in the management of complex arrhythmias in the future. These techniques provide the atrial geometry and this can be aligned to the frame of reference of the electroanatomic system. MRI techniques may also allow delineation of scar and this could be represented on the Ripple Mapping software (in the way that bipolar voltage amplitude is currently used). For the Entrainment Mapping, MRI could be used to inform patient specific models of cardiac activation. These could then be used to improve upon the simplistic modelling that was used for the development of the Overdrive3D software.

7.5 Conclusion

The research presented in this thesis has involved the development of a new method for mapping activation, a new entrainment criterion for detecting macroreentry, and a new framework for integrating information from overdrive pacing manoeuvres. It is hoped that this contribution will help to advance the quality of treatment that patients receive in the future.

8 References

[1] Cappato R, Calkins H, Chen SA, Davies W, Iesaka Y, Kalman J, Kim YH, Klein G, Natale A, Packer D, Skanes A, Ambrogi F, Biganzoli E: Updated worldwide survey on the methods, efficacy, and safety of catheter ablation for human atrial fibrillation. Circ Arrhythm Electrophysiol 2010; 3:32-38.

[2] Saoudi N, Cosio F, Waldo A, Chen SA, Iesaka Y, Lesh M, Saksena S, Salerno J, Schoels W: A classification of atrial flutter and regular atrial tachycardia according to electrophysiological mechanisms and anatomical bases; a Statement from a Joint Expert Group from The Working Group of Arrhythmias of the European Society of Cardiology and the North American Society of Pacing and Electrophysiology. Eur Heart J 2001; 22:1162-1182.

[3] Jais P, Matsuo S, Knecht S, Weerasooriya R, Hocini M, Sacher F, Wright M, Nault I, Lellouche N, Klein G, Clementy J, Haissaguerre M: A deductive mapping strategy for atrial tachycardia following atrial fibrillation ablation: importance of localized reentry. JCE 2009; 20:480-491.

[4] Sanders P, Hocini M, Jais P, Hsu LF, Takahashi Y, Rotter M, Scavee C, Pasquie JL, Sacher F, Rostock T, Nalliah CJ, Clementy J, Haissaguerre M: Characterization of focal atrial tachycardia using high-density mapping. J Am Coll Cardiol 2005; 46:2088-2099.

[5] Man KC, Knight B, Tse HF, Pelosi F, Michaud GF, Flemming M, Strickberger SA, Morady F: Radiofrequency catheter ablation of inappropriate sinus tachycardia guided by activation mapping. J Am Coll Cardiol 2000; 35:451-457.

[6] Man KC, Brinkman K, Bogun F, Knight B, Bahu M, Weiss R, Goyal R, Harvey M, Daoud EG, Strickberger SA, Morady F: 2:1 atrioventricular block during atrioventricular node reentrant tachycardia. J Am Coll Cardiol 1996; 28:1770-1774.

[7] Marrouche NF, Beheiry S, Tomassoni G, Cole C, Bash D, Dresing T, Saliba W, Abdul-Karim A, Tchou P, Schweikert R, Leonelli F, Natale A: Three-dimensional nonfluoroscopic mapping and ablation of inappropriate sinus tachycardia. Procedural strategies and long-term outcome. J Am Coll Cardiol 2002; 39:1046-1054.

[8] Poutiainen AM, Koistinen MJ, Airaksinen KE, Hartikainen EK, Kettunen RV, Karjalainen JE, Huikuri HV: Prevalence and natural course of ectopic atrial tachycardia. Eur Heart J 1999; 20:694-700.

[9] Chen SA, Chiang CE, Yang CJ, Cheng CC, Wu TJ, Wang SP, Chiang BN, Chang MS: Sustained atrial tachycardia in adult patients. Electrophysiological characteristics,

pharmacological response, possible mechanisms, and effects of radiofrequency ablation. Circulation 1994; 90:1262-1278.

[10] Roberts-Thomson KC, Kistler PM, Kalman JM: Focal atrial tachycardia I: clinical features, diagnosis, mechanisms, and anatomic location. Pacing Clin Electrophysiol 2006; 29:643-652.

[11] Higa S, Tai CT, Lin YJ, Liu TY, Lee PC, Huang JL, Hsieh MH, Yuniadi Y, Huang BH, Lee SH, Ueng KC, Ding YA, Chen SA: Focal atrial tachycardia: new insight from noncontact mapping and catheter ablation. Circulation 2004; 109:84-91.

[12] Issa Z, Miller JM, Aipes DP: *Clinical Arrhythmology and Electrophysiology: A Companion to Braunwald's Heart Disease*: Elsevier Saunders, 2012, p. 726.

[13] Seals AA, Lawrie GM, Magro S, Lin HT, Pacifico A, Roberts R, Wyndham CR: Surgical treatment of right atrial focal tachycardia in adults. J Am Coll Cardiol 1988; 11:1111-1117.

[14] McGuire MA, Johnson DC, Nunn GR, Yung T, Uther JB, Ross DL: Surgical therapy for atrial tachycardia in adults. J Am Coll Cardiol 1989; 14:1777-1782.

[15] Kistler PM, Roberts-Thomson KC, Haqqani HM, Fynn SP, Singarayar S, Vohra JK, Morton JB, Sparks PB, Kalman JM: P-wave morphology in focal atrial tachycardia: development of an algorithm to predict the anatomic site of origin. J Am Coll Cardiol 2006; 48:1010-1017.

[16] Dong J, Zrenner B, Schreieck J, Deisenhofer I, Karch M, Schneider M, Von Bary C, Weyerbrock S, Yin Y, Schmitt C: Catheter ablation of left atrial focal tachycardia guided by electroanatomic mapping and new insights into interatrial electrical conduction. Heart Rhythm 2005; 2:578-591.

[17] Baranowski B, Wazni O, Lindsay B, Kanj M, Saliba W, Burkhardt D, Thomas G, Rickard J, Tchou P: Focal ablation versus single vein isolation for atrial tachycardia originating from a pulmonary vein. Pacing Clin Electrophysiol 2010; 33:776-783.

[18] Bazan V, Rodriguez-Font E, Vinolas X, Guerra JM, Bruguera-Cortada J, Marti-Almor J: Atrial tachycardia originating from the pulmonary vein: clinical, electrocardiographic, and differential electrophysiologic characteristics. Revista espanola de cardiologia 2010; 63:149-155.

[19] Teh AW, Kalman JM, Medi C, Rosso R, Balasubramaniam R, Lee G, Halloran K, Sparks PB, Morton JB, Vohra JK, Kistler PM: Long-term outcome following successful catheter ablation of atrial tachycardia originating from the pulmonary veins: absence of late atrial fibrillation. JCE 2010; 21:747-750.

[20] Mayer AG: *Rhythmical pulsation in scyphomedusae*. Washington, DC: Carnegie Institution of Washington, 1906, p. 62.

[21] Mines GR: On dynamic equilibrium in the heart. The Journal of Physiology 1913; 46:349-383.

[22] Kleber AG, Rudy Y: Basic mechanisms of cardiac impulse propagation and associated arrhythmias. Physiol Rev 2004; 84:431-488.

[23] Granada J, Uribe W, Chyou PH, Maassen K, Vierkant R, Smith PN, Hayes J, Eaker E, Vidaillet H: Incidence and predictors of atrial flutter in the general population. J Am Coll Cardiol 2000; 36:2242-2246.

[24] Tai CT, Chen SA: Electrophysiological mechanisms of atrial flutter. Indian Pacing Electrophysiol J 2006; 6:119-132.

[25] Santucci PA, Varma N, Cytron J, Akar JG, Wilber DJ, Al Chekakie MO, Brysiewicz N: Electroanatomic mapping of postpacing intervals clarifies the complete active circuit and variants in atrial flutter. Heart Rhythm 2009; 6:1586-1595.

[26] Cosio FG, Lopez-Gil M, Goicolea A, Arribas F, Barroso JL: Radiofrequency ablation of the inferior vena cava-tricuspid valve isthmus in common atrial flutter. Am J Cardiol 1993; 71:705-709.

[27] Perez FJ, Schubert CM, Parvez B, Pathak V, Ellenbogen KA, Wood MA: Long-term outcomes after catheter ablation of cavo-tricuspid isthmus dependent atrial flutter: a meta-analysis. Circ Arrhythm Electrophysiol 2009; 2:393-401.

[28] Tai CT, Chen SA, Tzeng JW, Kuo BI, Ding YA, Chang MS, Shyu LY: Prolonged fractionation of paced right atrial electrograms in patients with atrial flutter and fibrillation. J Am Coll Cardiol 2001; 37:1651-1657.

[29] Kistler PM, Sanders P, Fynn SP, Stevenson IH, Spence SJ, Vohra JK, Sparks PB, Kalman JM: Electrophysiologic and electroanatomic changes in the human atrium associated with age. J Am Coll Cardiol 2004; 44:109-116.

[30] Medi C, Kalman JM, Ling LH, Teh AW, Lee G, Lee G, Spence SJ, Kaye DM, Kistler PM: Atrial electrical and structural remodeling associated with longstanding pulmonary hypertension and right ventricular hypertrophy in humans. JCE 2012; 23:614-620.

[31] Calkins H, Kuck KH, Cappato R, Brugada J, Camm AJ, Chen SA, Crijns HJ, Damiano RJ, Jr., Davies DW, DiMarco J, Edgerton J, Ellenbogen K, Ezekowitz MD, Haines DE, Haissaguerre M, Hindricks G, Iesaka Y, Jackman W, Jalife J, Jais P, Kalman J, Keane D, Kim YH, Kirchhof P, Klein G, Kottkamp H, Kumagai K, Lindsay BD, Mansour M, Marchlinski FE, McCarthy PM, Mont JL, Morady F, Nademanee K, Nakagawa H, Natale A, Nattel S, Packer DL, Pappone C, Prystowsky E, Raviele A, Reddy V, Ruskin JN, Shemin RJ, Tsao HM, Wilber D, Heart Rhythm Society Task Force on C, Surgical Ablation of Atrial F: 2012 HRS/EHRA/ECAS expert consensus statement on catheter and surgical ablation of atrial fibrillation: recommendations for patient selection, procedural techniques, patient management and follow-up, definitions, endpoints, and research trial design: a report of the Heart Rhythm Society (HRS) Task Force on Catheter and Surgical Ablation of Atrial Fibrillation. Developed in partnership with the European Heart

Rhythm Association (EHRA), a registered branch of the European Society of Cardiology (ESC) and the European Cardiac Arrhythmia Society (ECAS); and in collaboration with the American College of Cardiology (ACC), American Heart Association (AHA), the Asia Pacific Heart Rhythm Society (APHRS), and the Society of Thoracic Surgeons (STS). Endorsed by the governing bodies of the American College of Cardiology Foundation, the American Heart Association, the European Cardiac Arrhythmia Society, the European Heart Rhythm Association, the Society of Thoracic Surgeons, the Asia Pacific Heart Rhythm Society, and the Heart Rhythm Society. Heart Rhythm 2012; 9:632-696 e621.

[32] Miyasaka Y, Barnes ME, Gersh BJ, Cha SS, Bailey KR, Abhayaratna WP, Seward JB, Tsang TSM: Secular Trends in Incidence of Atrial Fibrillation in Olmsted County, Minnesota, 1980 to 2000, and Implications on the Projections for Future Prevalence. Circulation 2006; 114:119-125.

[33] Nathan H, Eliakim M: The junction between the left atrium and the pulmonary veins. An anatomic study of human hearts. Circulation 1966; 34:412-422.

[34] Chen SA, Hsieh MH, Tai CT, Tsai CF, Prakash VS, Yu WC, Hsu TL, Ding YA, Chang MS: Initiation of atrial fibrillation by ectopic beats originating from the pulmonary veins: electrophysiological characteristics, pharmacological responses, and effects of radiofrequency ablation. Circulation 1999; 100:1879-1886.

[35] Haissaguerre M, Jais P, Shah DC, Takahashi A, Hocini M, Quiniou G, Garrigue S, Le Mouroux A, Le Metayer P, Clementy J: Spontaneous initiation of atrial fibrillation by ectopic beats originating in the pulmonary veins. N Engl J Med 1998; 339:659-666.

[36] Tsai CF, Tai CT, Hsieh MH, Lin WS, Yu WC, Ueng KC, Ding YA, Chang MS, Chen SA: Initiation of atrial fibrillation by ectopic beats originating from the superior vena cava: electrophysiological characteristics and results of radiofrequency ablation. Circulation 2000; 102:67-74.

[37] Hsu LF, Jais P, Keane D, Wharton JM, Deisenhofer I, Hocini M, Shah DC, Sanders P, Scavee C, Weerasooriya R, Clementy J, Haissaguerre M: Atrial fibrillation originating from persistent left superior vena cava. Circulation 2004; 109:828-832.

[38] Doshi RN, Wu TJ, Yashima M, Kim YH, Ong JJ, Cao JM, Hwang C, Yashar P, Fishbein MC, Karagueuzian HS, Chen PS: Relation between ligament of Marshall and adrenergic atrial tachyarrhythmia. Circulation 1999; 100:876-883.

[39] Chen PS, Tan AY: Autonomic nerve activity and atrial fibrillation. Heart Rhythm 2007; 4:S61-64.

[40] Gami AS, Somers VK: Implications of obstructive sleep apnea for atrial fibrillation and sudden cardiac death. JCE 2008; 19:997-1003.

[41] Schoonderwoerd BA, Smit MD, Pen L, Van Gelder IC: New risk factors for atrial fibrillation: causes of 'not-so-lone atrial fibrillation'. Europace 2008; 10:668-673.

[42] Anderson RH, Cook AC: The structure and components of the atrial chambers. Europace 2007; 9 Suppl 6:vi3-9.

[43] Allessie M, Ausma J, Schotten U: Electrical, contractile and structural remodeling during atrial fibrillation. Cardiovasc Res 2002; 54:230-246.

[44] Wijffels MC, Kirchhof CJ, Dorland R, Allessie MA: Atrial fibrillation begets atrial fibrillation. A study in awake chronically instrumented goats. Circulation 1995; 92:1954-1968.

[45] Everett THt, Wilson EE, Verheule S, Guerra JM, Foreman S, Olgin JE: Structural atrial remodeling alters the substrate and spatiotemporal organization of atrial fibrillation: a comparison in canine models of structural and electrical atrial remodeling. Am J Physiol Heart Circ Physiol 2006; 291:H2911-2923.

[46] Morillo CA, Klein GJ, Jones DL, Guiraudon CM: Chronic rapid atrial pacing. Structural, functional, and electrophysiological characteristics of a new model of sustained atrial fibrillation. Circulation 1995; 91:1588-1595.

[47] Li D, Fareh S, Leung TK, Nattel S: Promotion of atrial fibrillation by heart failure in dogs: atrial remodeling of a different sort. Circulation 1999; 100:87-95.

[48] Verheule S, Wilson E, Everett Tt, Shanbhag S, Golden C, Olgin J: Alterations in atrial electrophysiology and tissue structure in a canine model of chronic atrial dilatation due to mitral regurgitation. Circulation 2003; 107:2615-2622.

[49] Sinno H, Derakhchan K, Libersan D, Merhi Y, Leung TK, Nattel S: Atrial ischemia promotes atrial fibrillation in dogs. Circulation 2003; 107:1930-1936.

[50] Schuessler RB, Grayson TM, Bromberg BI, Cox JL, Boineau JP: Cholinergically mediated tachyarrhythmias induced by a single extrastimulus in the isolated canine right atrium. Circ Res 1992; 71:1254-1267.

[51] Everett THt, Wilson EE, Hulley GS, Olgin JE: Transmural characteristics of atrial fibrillation in canine models of structural and electrical atrial remodeling assessed by simultaneous epicardial and endocardial mapping. Heart Rhythm 2010; 7:506-517.

[52] Shinagawa K, Shi YF, Tardif JC, Leung TK, Nattel S: Dynamic nature of atrial fibrillation substrate during development and reversal of heart failure in dogs. Circulation 2002; 105:2672-2678.

[53] Yu WC, Lee SH, Tai CT, Tsai CF, Hsieh MH, Chen CC, Ding YA, Chang MS, Chen SA: Reversal of atrial electrical remodeling following cardioversion of long-standing atrial fibrillation in man. Cardiovasc Res 1999; 42:470-476.

[54] Nguyen BL, Fishbein MC, Chen LS, Chen PS, Masroor S: Histopathological substrate for chronic atrial fibrillation in humans. Heart Rhythm 2009; 6:454-460.

[55] Frustaci A, Chimenti C, Bellocci F, Morgante E, Russo MA, Maseri A: Histological substrate of atrial biopsies in patients with lone atrial fibrillation. Circulation 1997; 96:1180-1184.

[56] Burstein B, Nattel S: Atrial fibrosis: mechanisms and clinical relevance in atrial fibrillation. J Am Coll Cardiol 2008; 51:802-809.

[57] Boldt A, Wetzel U, Lauschke J, Weigl J, Gummert J, Hindricks G, Kottkamp H, Dhein S: Fibrosis in left atrial tissue of patients with atrial fibrillation with and without underlying mitral valve disease. Heart 2004; 90:400-405.

[58] Mahnkopf C, Badger TJ, Burgon NS, Daccarett M, Haslam TS, Badger CT, McGann CJ, Akoum N, Kholmovski E, Macleod RS, Marrouche NF: Evaluation of the Left Atrial Substrate in Patients with Lone Atrial Fibrillation Using Delayed-Enhanced MRI: Implications for Disease Progression and Response to Catheter Ablation. Heart Rhythm 2010 (EPub).

[59] Oral H, Knight BP, Tada H, Ozaydin M, Chugh A, Hassan S, Scharf C, Lai SW, Greenstein R, Pelosi F, Jr., Strickberger SA, Morady F: Pulmonary vein isolation for paroxysmal and persistent atrial fibrillation. Circulation 2002; 105:1077-1081.

[60] Tan ES, Mulder BA, Rienstra M, Wiesfeld AC, Ahmed S, Zijlstra F, Van Gelder IC: Pulmonary vein isolation of symptomatic refractory paroxysmal and persistent atrial fibrillation: A single centre and single operator experience in the Netherlands. Netherlands heart journal : monthly journal of the Netherlands Society of Cardiology and the Netherlands Heart Foundation 2009; 17:366-372.

[61] Nademanee K, Lockwood E, Oketani N, Gidney B: Catheter ablation of atrial fibrillation guided by complex fractionated atrial electrogram mapping of atrial fibrillation substrate. J Cardiol 2010; 55:1-12.

[62] Nademanee K, McKenzie J, Kosar E, Schwab M, Sunsaneewitayakul B, Vasavakul T, Khunnawat C, Ngarmukos T: A new approach for catheter ablation of atrial fibrillation: mapping of the electrophysiologic substrate. J Am Coll Cardiol 2004; 43:2044-2053.

[63] Berenfeld O: Quantifying activation frequency in atrial fibrillation to establish underlying mechanisms and ablation guidance. Heart Rhythm 2007; 4:1225-1234.

[64] O'Neill MD, Jais P, Hocini M, Sacher F, Klein GJ, Clementy J, Haissaguerre M: Catheter ablation for atrial fibrillation. Circulation 2007; 116:1515-1523.

[65] Brooks AG, Stiles MK, Laborderie J, Lau DH, Kuklik P, Shipp NJ, Hsu LF, Sanders P: Outcomes of long-standing persistent atrial fibrillation ablation: a systematic review. Heart Rhythm 2010; 7:835-846.

[66] Arantes L, Klein GJ, Jais P, Lim KT, Matsuo S, Knecht S, Hocini M, O'Neill MD, Clementy J, Haissaguerre M: Tachycardia Transition During Ablation of Persistent Atrial Fibrillation. JCE 2010.

[67] Ammar S, Hessling G, Reents T, Paulik M, Fichtner S, Schon P, Dillier R, Kathan S, Jilek C, Kolb C, Haller B, Deisenhofer I: Importance of sinus rhythm as endpoint of persistent atrial fibrillation ablation. JCE 2013; 24:388-395.

[68] Haissaguerre M, Hocini M, Sanders P, Sacher F, Rotter M, Takahashi Y, Rostock T, Hsu LF, Bordachar P, Reuter S, Roudaut R, Clementy J, Jais P: Catheter ablation of long-lasting persistent atrial fibrillation: clinical outcome and mechanisms of subsequent arrhythmias. JCE 2005; 16:1138-1147.

[69] O'Neill MD, Wright M, Knecht S, Jais P, Hocini M, Takahashi Y, Jonsson A, Sacher F, Matsuo S, Lim KT, Arantes L, Derval N, Lellouche N, Nault I, Bordachar P, Clementy J, Haissaguerre M: Long-term follow-up of persistent atrial fibrillation ablation using termination as a procedural endpoint. Eur Heart J 2009; 30:1105-1112.

[70] Ammar S, Hessling G, Reents T, Fichtner S, Wu J, Zhu P, Kathan S, Estner HL, Jilek C, Kolb C, Haller B, Deisenhofer I: Arrhythmia type after persistent atrial fibrillation ablation predicts success of the repeat procedure. Circ Arrhythm Electrophysiol 2011; 4:609-614.

[71] Gerstenfeld EP, Callans DJ, Dixit S, Russo AM, Nayak H, Lin D, Pulliam W, Siddique S, Marchlinski FE: Mechanisms of organized left atrial tachycardias occurring after pulmonary vein isolation. Circulation 2004; 110:1351-1357.

[72] Chugh A, Oral H, Lemola K, Hall B, Cheung P, Good E, Tamirisa K, Han J, Bogun F, Pelosi F, Jr., Morady F: Prevalence, mechanisms, and clinical significance of macroreentrant atrial tachycardia during and following left atrial ablation for atrial fibrillation. Heart Rhythm 2005; 2:464-471.

[73] Deisenhofer I, Estner H, Zrenner B, Schreieck J, Weyerbrock S, Hessling G, Scharf K, Karch MR, Schmitt C: Left atrial tachycardia after circumferential pulmonary vein ablation for atrial fibrillation: incidence, electrophysiological characteristics, and results of radiofrequency ablation. Europace 2006; 8:573-582.

[74] Choi JI, Pak HN, Park JS, Kwak JJ, Nagamoto Y, Lim HE, Park SW, Hwang C, Kim YH: Clinical significance of early recurrences of atrial tachycardia after atrial fibrillation ablation. JCE 2010; 21:1331-1337.

[75] Cappato R, Negroni S, Pecora D, Bentivegna S, Lupo PP, Carolei A, Esposito C, Furlanello F, De Ambroggi L: Prospective assessment of late conduction recurrence across radiofrequency lesions producing electrical disconnection at the pulmonary vein ostium in patients with atrial fibrillation. Circulation 2003; 108:1599-1604.

[76] Takahashi Y, Takahashi A, Miyazaki S, Kuwahara T, Takei A, Fujino T, Fujii A, Kusa S, Yagishita A, Nozato T, Hikita H, Sato A, Hirao K, Isobe M: Electrophysiological characteristics of localized reentrant atrial tachycardia occurring after catheter ablation of long-lasting persistent atrial fibrillation. JCE 2009; 20:623-629.

[77] Cummings JE, Schweikert R, Saliba W, Hao S, Martin DO, Marrouche NF, Burkhardt JD, Kilicaslan F, Verma A, Beheiry S, Belden W, Natale A: Left atrial flutter following pulmonary

vein antrum isolation with radiofrequency energy: linear lesions or repeat isolation. JCE 2005; 16:293-297.

[78] Thomas SP, Wallace EM, Ross DL: The effect of a residual isthmus of surviving tissue on conduction after linear ablation in atrial myocardium. J Interv Card Electrophysiol 2000; 4:273-281.

[79] Pappone C, Manguso F, Vicedomini G, Gugliotta F, Santinelli O, Ferro A, Gulletta S, Sala S, Sora N, Paglino G, Augello G, Agricola E, Zangrillo A, Alfieri O, Santinelli V: Prevention of iatrogenic atrial tachycardia after ablation of atrial fibrillation: a prospective randomized study comparing circumferential pulmonary vein ablation with a modified approach. Circulation 2004; 110:3036-3042.

[80] Anousheh R, Sawhney NS, Panutich M, Tate C, Chen WC, Feld GK: Effect of mitral isthmus block on development of atrial tachycardia following ablation for atrial fibrillation. Pacing Clin Electrophysiol 2010; 33:460-468.

[81] Sawhney N, Anousheh R, Chen W, Feld GK: Circumferential pulmonary vein ablation with additional linear ablation results in an increased incidence of left atrial flutter compared with segmental pulmonary vein isolation as an initial approach to ablation of paroxysmal atrial fibrillation. Circ Arrhythm Electrophysiol 2010; 3:243-248.

[82] Chae S, Oral H, Good E, Dey S, Wimmer A, Crawford T, Wells D, Sarrazin JF, Chalfoun N, Kuhne M, Fortino J, Huether E, Lemerand T, Pelosi F, Bogun F, Morady F, Chugh A: Atrial tachycardia after circumferential pulmonary vein ablation of atrial fibrillation: mechanistic insights, results of catheter ablation, and risk factors for recurrence. J Am Coll Cardiol 2007; 50:1781-1787.

[83] Gerstenfeld EP, Callans DJ, Sauer W, Jacobson J, Marchlinski FE: Reentrant and nonreentrant focal left atrial tachycardias occur after pulmonary vein isolation. Heart Rhythm 2005; 2:1195-1202.

[84] Ouyang F, Antz M, Ernst S, Hachiya H, Mavrakis H, Deger FT, Schaumann A, Chun J, Falk P, Hennig D, Liu X, Bansch D, Kuck KH: Recovered pulmonary vein conduction as a dominant factor for recurrent atrial tachyarrhythmias after complete circular isolation of the pulmonary veins: lessons from double Lasso technique. Circulation 2005; 111:127-135.

[85] Satomi K, Bansch D, Tilz R, Chun J, Ernst S, Antz M, Greten H, Kuck KH, Ouyang F: Left atrial and pulmonary vein macroreentrant tachycardia associated with double conduction gaps: a novel type of man-made tachycardia after circumferential pulmonary vein isolation. Heart Rhythm 2008; 5:43-51.

[86] Patel AM, d'Avila A, Neuzil P, Kim SJ, Mela T, Singh JP, Ruskin JN, Reddy VY: Atrial tachycardia after ablation of persistent atrial fibrillation: identification of the critical isthmus with a combination of multielectrode activation mapping and targeted entrainment mapping. Circ Arrhythm Electrophysiol 2008; 1:14-22.

[87] Jais P, Hocini M, Hsu LF, Sanders P, Scavee C, Weerasooriya R, Macle L, Raybaud F, Garrigue S, Shah DC, Le Metayer P, Clementy J, Haissaguerre M: Technique and results of linear ablation at the mitral isthmus. Circulation 2004; 110:2996-3002.

[88] Matsuo S, Wright M, Knecht S, Nault I, Lellouche N, Lim KT, Arantes L, O'Neill MD, Hocini M, Jais P, Haissaguerre M: Peri-mitral atrial flutter in patients with atrial fibrillation ablation. Heart Rhythm 2010; 7:2-8.

[89] Cosio FG, Pastor A, Nunez A, Montero MA: How to map and ablate atrial scar macroreentrant tachycardia of the right atrium. Europace 2000; 2:193-200.

[90] Feld GK, Fleck RP, Chen PS, Boyce K, Bahnson TD, Stein JB, Calisi CM, Ibarra M: Radiofrequency catheter ablation for the treatment of human type 1 atrial flutter. Identification of a critical zone in the reentrant circuit by endocardial mapping techniques. Circulation 1992; 86:1233-1240.

[91] Hocini M, Jais P, Sanders P, Takahashi Y, Rotter M, Rostock T, Hsu LF, Sacher F, Reuter S, Clementy J, Haissaguerre M: Techniques, evaluation, and consequences of linear block at the left atrial roof in paroxysmal atrial fibrillation: a prospective randomized study. Circulation 2005; 112:3688-3696.

[92] Guiraudon GM, Ofiesh JG, Kaushik R: Extended vertical transatrial septal approach to the mitral valve. The Annals of thoracic surgery 1991; 52:1058-1060; discussion 1060-1052.

[93] Nakagawa H, Shah N, Matsudaira K, Overholt E, Chandrasekaran K, Beckman KJ, Spector P, Calame JD, Rao A, Hasdemir C, Otomo K, Wang Z, Lazzara R, Jackman WM: Characterization of reentrant circuit in macroreentrant right atrial tachycardia after surgical repair of congenital heart disease: isolated channels between scars allow "focal" ablation. Circulation 2001; 103:699-709.

[94] Shah D, Jais P, Takahashi A, Hocini M, Peng JT, Clementy J, Haissaguerre M: Dual-loop intra-atrial reentry in humans. Circulation 2000; 101:631-639.

[95] Seiler J, Schmid DK, Irtel TA, Tanner H, Rotter M, Schwick N, Delacretaz E: Dual-loop circuits in postoperative atrial macro re-entrant tachycardias. Heart 2007; 93:325-330.

[96] Kalman JM, VanHare GF, Olgin JE, Saxon LA, Stark SI, Lesh MD: Ablation of 'incisional' reentrant atrial tachycardia complicating surgery for congenital heart disease. Use of entrainment to define a critical isthmus of conduction. Circulation 1996; 93:502-512.

[97] Cosio FG, Martin-Penato A, Pastor A, Nunez A, Goicolea A: Atypical flutter: a review. Pacing Clin Electrophysiol 2003; 26:2157-2169.

[98] De Ponti R, Marazzi R, Zoli L, Caravati F, Ghiringhelli S, Salerno-Uriarte JA: Electroanatomic mapping and ablation of macroreentrant atrial tachycardia: comparison between successfully and unsuccessfully treated cases. JCE 2010; 21:155-162.

[99] Waldo AL, Atienza F: *Atrial Flutter*. In Zipes DP, Jalife J, eds: Cardiac electrophysiology: from cell to bedside: Suanders, 2009, pp. 567-576.

[100] Ellenbogen KA, Stambler BS, Wood MA: *Atrial Tachycardia*. In Zipes DP, Jalife J, eds: Cardiac electrophysiology: from cell to bedside: Suanders, 2009, pp. 589-603.

[101] Gerstenfeld EP, Dixit S, Bala R, Callans DJ, Lin D, Sauer W, Garcia F, Cooper J, Russo AM, Marchlinski FE: Surface electrocardiogram characteristics of atrial tachycardias occurring after pulmonary vein isolation. Heart Rhythm 2007; 4:1136-1143.

[102] Chugh A, Latchamsetty R, Oral H, Elmouchi D, Tschopp D, Reich S, Igic P, Lemerand T, Good E, Bogun F, Pelosi F, Jr., Morady F: Characteristics of cavotricuspid isthmus-dependent atrial flutter after left atrial ablation of atrial fibrillation. Circulation 2006; 113:609-615.

[103] Ramanathan C, Ghanem RN, Jia P, Ryu K, Rudy Y: Noninvasive electrocardiographic imaging for cardiac electrophysiology and arrhythmia. Nat Med 2004; 10:422-428.

[104] Messinger-Rapport B, Rudy Y: Noninvasive recovery of epicardial potentials in a realistic heart- torso geometry. Normal sinus rhythm. Circ Res 1990; 66:1023-1039.

[105] Nash MP, Pullan AJ: Challenges Facing Validation of Noninvasive Electrical Imaging of the Heart. The Annals of Noninvasive Electrocardiology 2005; 10:73-82.

[106] Anselma I, Robert NG, Ping J, Charulatha R, Kyungmoo R, Bartolomeo G, Robert G, Bruce SS, Pedro B, William GS, Yoram R, Albert LW: Electrocardiographic imaging (ECGI), a novel diagnostic modality used for mapping of focal left ventricular tachycardia in a young athlete. Heart rhythm : the official journal of the Heart Rhythm Society 2005; 2:1250-1252.

[107] Ramanathan C, Jia P, Ghanem R, Ryu K, Rudy Y: Activation and repolarization of the normal human heart under complete physiological conditions. Proc Natl Acad Sci U S A 2006; 103:6309-6314.

[108] Wang Y, Cuculich PS, Woodard PK, Lindsay BD, Rudy Y: Focal atrial tachycardia after pulmonary vein isolation: noninvasive mapping with electrocardiographic imaging (ECGI). Heart Rhythm 2007; 4:1081-1084.

[109] Shah AJ, Hocini M, Xhaet O, Pascale P, Roten L, Wilton SB, Linton N, Scherr D, Miyazaki S, Jadidi AS, Liu X, Forclaz A, Nault I, Rivard L, Pedersen ME, Derval N, Sacher F, Knecht S, Jais P, Dubois R, Eliautou S, Bokan R, Strom M, Ramanathan C, Cakulev I, Sahadevan J, Lindsay B, Waldo AL, Haissaguerre M: Validation of novel 3-dimensional electrocardiographic mapping of atrial tachycardias by invasive mapping and ablation: a multicenter study. J Am Coll Cardiol 2013; 62:889-897.

[110] Scheinman M, Gerstenfeld E: Mapping of Complex Atrial Tachycardia Circuits by 3-Dimensional Body Surface Mapping: The First Step in the Dawn of a New Era. J Am Coll Cardiol 2013; 62:898-899.

[111] Stinnett-Donnelly JM, Thompson N, Habel N, Petrov-Kondratov V, Correa de Sa DD, Bates JH, Spector PS: Effects of electrode size and spacing on the resolution of intracardiac electrograms. Coronary artery disease 2012; 23:126-132.

[112] Stevenson WG, Soejima K: Recording techniques for clinical electrophysiology. JCE 2005; 16:1017-1022.

[113] Okumura Y, Watanabe I, Ashino S, Kofune M, Ohkubo K, Takagi Y, Kawauchi K, Yamada T, Hashimoto K, Shindo A, Sugimura H, Nakai T, Saito S: Electrophysiologic and anatomical characteristics of the right atrial posterior wall in patients with and without atrial flutter: analysis by intracardiac echocardiography. Circ J 2007; 71:636-642.

[114] Olgin JE, Kalman JM, Fitzpatrick AP, Lesh MD: Role of right atrial endocardial structures as barriers to conduction during human type I atrial flutter. Activation and entrainment mapping guided by intracardiac echocardiography. Circulation 1995; 92:1839-1848.

[115] Tada H, Oral H, Sticherling C, Chough SP, Baker RL, Wasmer K, Pelosi F, Jr., Knight BP, Strickberger SA, Morady F: Double potentials along the ablation line as a guide to radiofrequency ablation of typical atrial flutter. J Am Coll Cardiol 2001; 38:750-755.

[116] Spach MS, Barr RC: Effects of cardiac microstructure on propagating electrical waveforms. Circ Res 2000; 86:E23-28.

[117] Spach MS, Heidlage JF, Dolber PC, Barr RC: Mechanism of origin of conduction disturbances in aging human atrial bundles: experimental and model study. Heart Rhythm 2007; 4:175-185.

[118] Jacquemet V, Henriquez C: Genesis of complex fractionated atrial electrograms in zones of slow conduction: A computer model of microfibrosis. Heart Rhythm 2009; 6:803-810.

[119] Pytkowski M, Jankowska A, Maciag A, Kowalik I, Sterlinski M, Szwed H, Saumarez RC: Paroxysmal atrial fibrillation is associated with increased intra-atrial conduction delay. Europace 2008; 10:1415-1420.

[120] Correa de Sa DD, Thompson N, Stinnett-Donnelly J, Znojkiewicz P, Habel N, Muller JG, Bates JH, Buzas JS, Spector PS: Electrogram fractionation: the relationship between spatiotemporal variation of tissue excitation and electrode spatial resolution. Circ Arrhythm Electrophysiol 2011; 4:909-916.

[121] Callans DJ, Ren JF, Michele J, Marchlinski FE, Dillon SM: Electroanatomic left ventricular mapping in the porcine model of healed anterior myocardial infarction. Correlation with intracardiac echocardiography and pathological analysis. Circulation 1999; 100:1744-1750.

[122] Kettering K, Weig HJ, Reimold M, Schwegler AC, Busch M, Laszlo R, Gawaz M, Schreieck J: Catheter ablation of ventricular tachycardias in patients with ischemic cardiomyopathy: validation of voltage mapping criteria for substrate modification by myocardial viability

assessment using FDG PET. Clinical research in cardiology : official journal of the German Cardiac Society 2010; 99:753-760.

[123] Marchlinski FE, Callans DJ, Gottlieb CD, Zado E: Linear ablation lesions for control of unmappable ventricular tachycardia in patients with ischemic and nonischemic cardiomyopathy. Circulation 2000; 101:1288-1296.

[124] Sanders P, Morton JB, Davidson NC, Spence SJ, Vohra JK, Sparks PB, Kalman JM: Electrical remodeling of the atria in congestive heart failure: electrophysiological and electroanatomic mapping in humans. Circulation 2003; 108:1461-1468.

[125] Sanders P, Morton JB, Kistler PM, Spence SJ, Davidson NC, Hussin A, Vohra JK, Sparks PB, Kalman JM: Electrophysiological and electroanatomic characterization of the atria in sinus node disease: evidence of diffuse atrial remodeling. Circulation 2004; 109:1514-1522.

[126] Harrison JL, Jensen HK, Peel SA, Chiribiri A, Grondal AK, Bloch LO, Pedersen SF, Bentzon JF, Kolbitsch C, Karim R, Williams SE, Linton NW, Rhode KS, Gill J, Cooklin M, Rinaldi CA, Wright M, Kim WY, Schaeffter T, Razavi RS, O'Neill MD: Cardiac magnetic resonance and electroanatomical mapping of acute and chronic atrial ablation injury: a histological validation study. Eur Heart J 2014.

[127] Jais P, Shah DC, Haissaguerre M, Hocini M, Peng JT, Takahashi A, Garrigue S, Le Metayer P, Clementy J: Mapping and ablation of left atrial flutters. Circulation 2000; 101:2928-2934.

[128] Huang SK, Wood MA: *Catheter ablation of cardiac arrhythmias*. Philadelphia, PA: Saunders, 2011, p. 650.

[129] Packer DL: Three-dimensional mapping in interventional electrophysiology: techniques and technology. JCE 2005; 16:1110-1116.

[130] Scaglione M, Biasco L, Caponi D, Anselmino M, Negro A, Di Donna P, Corleto A, Montefusco A, Gaita F: Visualization of multiple catheters with electroanatomical mapping reduces X-ray exposure during atrial fibrillation ablation. Europace 2011; 13:955-962.

[131] Sporton SC, Earley MJ, Nathan AW, Schilling RJ: Electroanatomic versus fluoroscopic mapping for catheter ablation procedures: a prospective randomized study. JCE 2004; 15:310-315.

[132] Ben-Haim SA, Osadchy D, Schuster I, Gepstein L, Hayam G, Josephson ME: Nonfluoroscopic, in vivo navigation and mapping technology. Nat Med 1996; 2:1393-1395.

[133] Gepstein L, Hayam G, Ben-Haim SA: A novel method for nonfluoroscopic catheter-based electroanatomical mapping of the heart. In vitro and in vivo accuracy results. Circulation 1997; 95:1611-1622.

[134] Jiang Y, Farina D, Bar-Tal M, Dossel O: An impedance-based catheter positioning system for cardiac mapping and navigation. IEEE Trans Biomed Eng 2009; 56:1963-1970.

[135] Wittkampf FH, Wever EF, Derksen R, Wilde AA, Ramanna H, Hauer RN, Robles de Medina EO: LocaLisa: new technique for real-time 3-dimensional localization of regular intracardiac electrodes. Circulation 1999; 99:1312-1317.

[136] Okumura Y, Watanabe I, Kofune M, Nagashima K, Sonoda K, Mano H, Ohkubo K, Nakai T, Sasaki N, Kogawa R, Maruyama A, Hirayama A: Effect of catheter tip-tissue surface contact on three-dimensional left atrial and pulmonary vein geometries: potential anatomic distortion of 3D ultrasound, fast anatomical mapping, and merged 3D CT-derived images. JCE 2013; 24:259-266.

[137] Muller H, Burri H, Gentil P, Lerch R, Shah D: Measurement of left atrial volume in patients undergoing ablation for atrial fibrillation: comparison of angiography and electro-anatomic (CARTO) mapping with real-time three-dimensional echocardiography. Europace 2010; 12:792-797.

[138] Beinart R, Kabra R, Heist KE, Blendea D, Barrett CD, Danik SB, Collins R, Ruskin JN, Mansour M: Respiratory compensation improves the accuracy of electroanatomic mapping of the left atrium and pulmonary veins during atrial fibrillation ablation. J Interv Card Electrophysiol 2011; 32:105-110.

[139] Dong J, Dickfeld T, Dalal D, Cheema A, Vasamreddy CR, Henrikson CA, Marine JE, Halperin HR, Berger RD, Lima JA, Bluemke DA, Calkins H: Initial experience in the use of integrated electroanatomic mapping with three-dimensional MR/CT images to guide catheter ablation of atrial fibrillation. JCE 2006; 17:459-466.

[140] Kistler PM, Earley MJ, Harris S, Abrams D, Ellis S, Sporton SC, Schilling RJ: Validation of three-dimensional cardiac image integration: use of integrated CT image into electroanatomic mapping system to perform catheter ablation of atrial fibrillation. JCE 2006; 17:341-348.

[141] Okumura Y, Henz BD, Johnson SB, Bunch TJ, O'Brien CJ, Hodge DO, Altman A, Govari A, Packer DL: Three-dimensional ultrasound for image-guided mapping and intervention: methods, quantitative validation, and clinical feasibility of a novel multimodality image mapping system. Circ Arrhythm Electrophysiol 2008; 1:110-119.

[142] Caponi D, Corleto A, Scaglione M, Blandino A, Biasco L, Cristoforetti Y, Cerrato N, Toso E, Morello M, Gaita F: Ablation of atrial fibrillation: does the addition of three-dimensional magnetic resonance imaging of the left atrium to electroanatomic mapping improve the clinical outcome?: a randomized comparison of Carto-Merge vs. Carto-XP three-dimensional mapping ablation in patients with paroxysmal and persistent atrial fibrillation. Europace 2010; 12:1098-1104.

[143] Kistler PM, Rajappan K, Harris S, Earley MJ, Richmond L, Sporton SC, Schilling RJ: The impact of image integration on catheter ablation of atrial fibrillation using electroanatomic mapping: a prospective randomized study. Eur Heart J 2008; 29:3029-3036.

[144] Del Carpio Munoz F, Buescher TL, Asirvatham SJ: Three-dimensional mapping of cardiac arrhythmias: what do the colors really mean? Circ Arrhythm Electrophysiol 2010; 3:e6-11.

[145] Del Carpio Munoz F, Buescher TL, Asirvatham SJ: Teaching points with 3-dimensional mapping of cardiac arrhythmia: how to overcome potential pitfalls during substrate mapping? Circ Arrhythm Electrophysiol 2011; 4:e72-75.

[146] Del Carpio Munoz F, Buescher TL, Asirvatham SJ: Teaching points with 3-dimensional mapping of cardiac arrhythmias: teaching point 3: when early is not early. Circ Arrhythm Electrophysiol 2011; 4:e11-14.

[147] Ikeguchi S, Peters NS: Novel use of postpacing interval mapping to guide radiofrequency ablation of focal atrial tachycardia with long intra-atrial conduction time. Heart Rhythm 2004; 1:88-93.

[148] De Ponti R, Verlato R, Bertaglia E, Del Greco M, Fusco A, Bottoni N, Drago F, Sciarra L, Ometto R, Mantovan R, Salerno-Uriarte JA: Treatment of macro-re-entrant atrial tachycardia based on electroanatomic mapping: identification and ablation of the mid-diastolic isthmus. Europace 2007; 9:449-457.

[149] Drago F, Russo MS, Marazzi R, Salerno-Uriarte JA, Silvetti MS, De Ponti R: Atrial tachycardias in patients with congenital heart disease: a minimally invasive simplified approach in the use of three-dimensional electroanatomic mapping. Europace 2011; 13:689-695.

[150] Veenhuyzen GD, Knecht S, O'Neill MD, Phil D, Wright M, Nault I, Weerasooriya R, Miyazaki S, Sacher F, Hocini M, Jais P, Haissaguerre M: Atrial tachycardias encountered during and after catheter ablation for atrial fibrillation: part I: classification, incidence, management. Pacing Clin Electrophysiol 2009; 32:393-398.

[151] Hayden WG, Hurley EJ, Rytand DA: The mechanism of canine atrial flutter. Circ Res 1967; 20:496-505.

[152] Rytand DA: Atrial flutter and the circus movement hypothesis. Circulation 1966; 34:713-714.

[153] Waldo AL, MacLean WA, Karp RB, Kouchoukos NT, James TN: Entrainment and interruption of atrial flutter with atrial pacing: studies in man following open heart surgery. Circulation 1977; 56:737-745.

[154] Waldo AL: From bedside to bench: entrainment and other stories. Heart Rhythm 2004; 1:94-106.

[155] Cooper MW: Transient entrainment: the evolution of a medical concept from description to prescription. Pacing Clin Electrophysiol 1996; 19:1162-1176.

[156] Henthorn RW, Okumura K, Olshansky B, Plumb VJ, Hess PG, Waldo AL: A fourth criterion for transient entrainment: the electrogram equivalent of progressive fusion. Circulation 1988; 77:1003-1012.

[157] Okumura K, Henthorn RW, Epstein AE, Plumb VJ, Waldo AL: Further observations on transient entrainment: importance of pacing site and properties of the components of the reentry circuit. Circulation 1985; 72:1293-1307.

[158] Stevenson WG, Sager PT, Friedman PL: Entrainment techniques for mapping atrial and ventricular tachycardias. JCE 1995; 6:201-216.

[159] Veenhuyzen GD, Quinn FR: Principles of entrainment: diagnostic utility for supraventricular tachycardia. Indian Pacing Electrophysiol J 2008; 8:51-65.

[160] Deo R, Berger R: The clinical utility of entrainment pacing. JCE 2009; 20:466-470.

[161] Stevenson WG, Khan H, Sager P, Saxon LA, Middlekauff HR, Natterson PD, Wiener I: Identification of reentry circuit sites during catheter mapping and radiofrequency ablation of ventricular tachycardia late after myocardial infarction. Circulation 1993; 88:1647-1670.

[162] Morton JB, Sanders P, Deen V, Vohra JK, Kalman JM: Sensitivity and specificity of concealed entrainment for the identification of a critical isthmus in the atrium: relationship to rate, anatomic location and antidromic penetration. J Am Coll Cardiol 2002; 39:896-906.

[163] Shah D, Sunthorn H, Burri H, Gentil-Baron P, Pruvot E, Schlaepfer J, Fromer M: Narrow, slow-conducting isthmus dependent left atrial reentry developing after ablation for atrial fibrillation: ECG characterization and elimination by focal RF ablation. JCE 2006; 17:508-515.

[164] Cosio F, Lopez Gil M, Arribas F, Palacios J, Goicolea A, Nunez A: Mechanisms of entrainment of human common flutter studied with multiple endocardial recordings. Circulation 1994; 89:2117-2125.

[165] Kalman JM, Olgin JE, Saxon LA, Lee RJ, Scheinman MM, Lesh MD: Electrocardiographic and electrophysiologic characterization of atypical atrial flutter in man: use of activation and entrainment mapping and implications for catheter ablation. JCE 1997; 8:121-144.

[166] Olshansky B, Okumura K, Hess PG, Waldo AL: Demonstration of an area of slow conduction in human atrial flutter. J Am Coll Cardiol 1990; 16:1639-1648.

[167] Tai CT, Chen SA, Chiang CE, Lee SH, Ueng KC, Wen ZC, Huang JL, Chen YJ, Yu WC, Feng AN, Chiou CW, Chang MS: Characterization of low right atrial isthmus as the slow conduction zone and pharmacological target in typical atrial flutter. Circulation 1997; 96:2601-2611.

[168] Feld GK, Mollerus M, Birgersdotter-Green U, Fujimura O, Bahnson TD, Boyce K, Rahme M: Conduction velocity in the tricuspid valve-inferior vena cava isthmus is slower in patients with type I atrial flutter compared to those without a history of atrial flutter. JCE 1997; 8:1338-1348.

[169] Mohamed U, Skanes AC, Gula LJ, Leong-Sit P, Krahn AD, Yee R, Subbiah R, Klein GJ: A novel pacing maneuver to localize focal atrial tachycardia. JCE 2007; 18:1-6.

[170] Miyazaki H, Stevenson WG, Stephenson K, Soejima K, Epstein LM: Entrainment mapping for rapid distinction of left and right atrial tachycardias. Heart Rhythm 2006; 3:516-523.

[171] Esato M, Hindricks G, Sommer P, Arya A, Gaspar T, Bode K, Bollmann A, Wetzel U, Hilbert S, Kircher S, Eitel C, Piorkowski C: Color-coded three-dimensional entrainment mapping for analysis and treatment of atrial macroreentrant tachycardia. Heart Rhythm 2009; 6:349-358.

[172] Fujiki A, Nishida K, Sakabe M, Sugao M, Tsuneda T, Mizumaki K, Inoue H: Entrainment mapping of dual-loop macroreentry in common atrial flutter: new insights into the atrial flutter circuit. JCE 2004; 15:679-685.

[173] Delacretaz E, Ganz LI, Soejima K, Friedman PL, Walsh EP, Triedman JK, Sloss LJ, Landzberg MJ, Stevenson WG: Multi atrial maco-re-entry circuits in adults with repaired congenital heart disease: entrainment mapping combined with three-dimensional electroanatomic mapping. J Am Coll Cardiol 2001; 37:1665-1676.

[174] Hammer PE, Brooks DH, Triedman JK: Estimation of entrainment response using electrograms from remote sites: validation in animal and computer models of reentrant tachycardia. JCE 2003; 14:52-61.

[175] Triedman JK, Alexander ME, Berul CI, Bevilacqua LM, Walsh EP: Estimation of atrial response to entrainment pacing using electrograms recorded from remote sites. JCE 2000; 11:1215-1222.

[176] Van Hare GF: Entrainment in the age of three-dimensional computer mapping. JCE 2003; 14:62-64.

[177] Del Carpio Munoz F, Buescher T, Asirvatham SJ: Teaching points with 3-dimensional mapping of cardiac arrhythmias: taking points: activation mapping. Circ Arrhythm Electrophysiol 2011; 4:e22-25.

[178] Linton NW, Koa-Wing M, Francis DP, Kojodjojo P, Lim PB, Salukhe TV, Whinnett Z, Davies DW, Peters NS, O'Neill MD, Kanagaratnam P: Cardiac ripple mapping: a novel three-dimensional visualization method for use with electroanatomic mapping of cardiac arrhythmias. Heart Rhythm 2009; 6:1754-1762.

[179] Tai CT, Chen SA, Chiang CE, Lee SH, Wen ZC, Huang JL, Chen YJ, Yu WC, Feng AN, Lin YJ, Ding YA, Chang MS: Long-term outcome of radiofrequency catheter ablation for typical atrial flutter: risk prediction of recurrent arrhythmias. JCE 1998; 9:115-121.

[180] Dixit S, Callans DJ: Mapping for ventricular tachycardia. Card Electrophysiol Rev 2002; 6:436-441.

[181] Marchlinski F, Callans D, Gottlieb C, Rodriguez E, Coyne R, Kleinman D: Magnetic electroanatomical mapping for ablation of focal atrial tachycardias. Pacing Clin Electrophysiol 1998; 21:1621-1635.

[182] Earley MJ, Showkathali R, Alzetani M, Kistler PM, Gupta D, Abrams DJ, Horrocks JA, Harris SJ, Sporton SC, Schilling RJ: Radiofrequency ablation of arrhythmias guided by non-fluoroscopic catheter location: a prospective randomized trial. Eur Heart J 2006; 27:1223-1229.

[183] Nakagawa H, Jackman WM: Use of a three-dimensional, nonfluoroscopic mapping system for catheter ablation of typical atrial flutter. Pacing Clin Electrophysiol 1998; 21:1279-1286.

[184] Schilling RJ, Peters NS, Davies DW: Mapping and ablation of ventricular tachycardia with the aid of a non-contact mapping system. Heart 1999; 81:570-575.

[185] Shah DC, Jais P, Haissaguerre M, Chouairi S, Takahashi A, Hocini M, Garrigue S, Clementy J: Three-dimensional mapping of the common atrial flutter circuit in the right atrium. Circulation 1997; 96:3904-3912.

[186] Stevenson WG, Delacretaz E, Friedman PL, Ellison KE: Identification and ablation of macroreentrant ventricular tachycardia with the CARTO electroanatomical mapping system. Pacing Clin Electrophysiol 1998; 21:1448-1456.

[187] de Groot NM, Schalij MJ, Zeppenfeld K, Blom NA, Van der Velde ET, Van der Wall EE: Voltage and activation mapping: how the recording technique affects the outcome of catheter ablation procedures in patients with congenital heart disease. Circulation 2003; 108:2099-2106.

[188] Khoury DS, Taccardi B, Lux RL, Ershler PR, Rudy Y: Reconstruction of endocardial potentials and activation sequences from intracavitary probe measurements. Localization of pacing sites and effects of myocardial structure. Circulation 1995; 91:845-863.

[189] Chinitz LA, Sethi JS: How to perform noncontact mapping. Heart Rhythm 2006; 3:120-123.

[190] Gregory RL: The Medawar Lecture 2001 knowledge for vision: vision for knowledge. Philos Trans R Soc Lond B Biol Sci 2005; 360:1231-1251.

[191] Knecht S, Hocini M, Wright M, Lellouche N, O'Neill MD, Matsuo S, Nault I, Chauhan VS, Makati KJ, Bevilacqua M, Lim KT, Sacher F, Deplagne A, Derval N, Bordachar P, Jais P, Clementy J, Haissaguerre M: Left atrial linear lesions are required for successful treatment of persistent atrial fibrillation. Eur Heart J 2008; 29:2359-2366.

[192] Lellouche N, Jais P, Nault I, Wright M, Bevilacqua M, Knecht S, Matsuo S, Lim KT, Sacher F, Deplagne A, Bordachar P, Hocini M, Haissaguerre M: Early recurrences after atrial fibrillation ablation: prognostic value and effect of early reablation. JCE 2008; 19:599-605.

[193] Weerasooriya R, Jais P, Wright M, Matsuo S, Knecht S, Nault I, Sacher F, Deplagne A, Bordachar P, Hocini M, Haissaguerre M: Catheter ablation of atrial tachycardia following atrial fibrillation ablation. JCE 2009; 20:833-838.

[194] Harada T, Stevenson WG, Kocovic DZ, Friedman PL: Catheter ablation of ventricular tachycardia after myocardial infarction: relation of endocardial sinus rhythm late potentials to the reentry circuit. J Am Coll Cardiol 1997; 30:1015-1023.

[195] Linton NW, Wilton SB, Scherr D, Shah AJ, Derval N, Sacher F, Wright M, Hocini M, O'Neill MD, Haissaguerre M, Jais P: A practical criterion for the rapid detection of single-loop and double-loop reentry tachycardias. JCE 2013; 24:544-552.

[196] Michaud GF, Stevenson WG: Feeling a little loopy? JCE 2013; 24:553-555.

[197] Raviele A, Natale A, Calkins H, Camm JA, Cappato R, Ann Chen S, Connolly SJ, Damiano Jr R, R DEP, Edgerton JR, Haissaguerre M, Hindricks G, Ho SY, Jalife J, Kirchhof P, Kottkamp H, Kuck KH, Marchlinski FE, Packer DL, Pappone C, Prystowsky E, Reddy VK, Themistoclakis S, Verma A, Wilber DJ, Willems S: Venice Chart International Consensus Document on Atrial Fibrillation Ablation: 2011 Update. JCE 2012; 23:890-923.

[198] Gerstenfeld EP, Marchlinski FE: Mapping and ablation of left atrial tachycardias occurring after atrial fibrillation ablation. Heart Rhythm 2007; 4:S65-72.

[199] Wilber DJ: Catheter ablation of ventricular tachycardia: two decades of progress. Heart Rhythm 2008; 5:S59-63.

[200] Waldo AL: Atrial flutter: entrainment characteristics. JCE 1997; 8:337-352.

[201] Waldo AL, Plumb VJ, Arciniegas JG, MacLean WA, Cooper TB, Priest MF, James TN: Transient entrainment and interruption of the atrioventricular bypass pathway type of paroxysmal atrial tachycardia. A model for understanding and identifying reentrant arrhythmias. Circulation 1983; 67:73-83.

[202] Nishida K, Fujiki A, Nagasawa H, Sakabe M, Mizumaki K, Inoue H, Misaki T: Complex atrial reentrant circuits evaluated by entrainment mapping using a multielectrode basket catheter. Circ J 2004; 68:168-171.

[203] Wong KC, Rajappan K, Bashir Y, Betts TR: Entrainment with long postpacing intervals from within the flutter circuit: what is the mechanism? Circ Arrhythm Electrophysiol 2012; 5:e90-91; discussion e92.

[204] Colombowala IK, Massumi A, Rasekh A, Saeed M, Cheng J, Fakhri B, Shuraih M, Razavi M: Variability in post-pacing intervals predicts global atrial activation pattern during tachycardia. JCE 2008; 19:142-147.

[205] Asami K, Ashikawa H, Terai T, Ishihara N, Nawata H, Hirao K, Miyasaka N, Kawara T, Hiejima K, Harada T, Suzuki F: Atypical form of the fourth criterion for transient entrainment. Pacing Clin Electrophysiol 1998; 21:352-366.

[206] Kalman JM, Kistler PM, Waldo AL: Localization of focal atrial tachycardias--back to the future...when (old) electrophysiologic first principles complement sophisticated technology. JCE 2007; 18:7-8.

[207] Kneeland PP, Fang MC: Trends in catheter ablation for atrial fibrillation in the United States. Journal of hospital medicine : an official publication of the Society of Hospital Medicine 2009; 4:E1-5.

9 Publications arising from this work

Linton NW, Wilton SB, Scherr D, Shah AJ, Derval N, Sacher F, Wright M, Hocini M, O'Neill MD, Haissaguerre M, Jais P. A practical criterion for the rapid detection of single-loop and double-loop reentry tachycardias. JCE. 2013;24:544-552

Linton NW, Koa-Wing M, Francis DP, Kojodjojo P, Lim PB, Salukhe TV, Whinnett Z, Davies DW, Peters NS, O'Neill MD, Kanagaratnam P. Cardiac ripple mapping: A novel three-dimensional visualization method for use with electroanatomic mapping of cardiac arrhythmias. Heart Rhythm. 2009;6:1754-1762

Linton N, Wilton S, Scherr D, Knecht S, Jadidi A, Pederson M, Miyazaki S, Shah A, Derval N, Sacher F, Wright M, Hocini M, O'Neill M, Haïssaguerre M, Jaïs P. A Criterion for Transient Entrainment of Double-Loop Reentry Tachycardias. Heart Rhythm 2011

Linton N, Wilton S, Scherr D, Knecht S, Jadidi A, Pederson M, Miyazaki S, Shah A, Derval N, Sacher F, Wright M, Hocini M, O'Neill M, Haïssaguerre M, Jaïs P. Computer assisted electroanatomic interpretation of overdrive pacing maneuvers. Heart Rhythm 2011

Linton N, Wilton S, Scherr D, Knecht S, Jadidi A, Pederson M, Miyazaki S, Shah A, Derval N, Sacher F, Wright M, Hocini M, O'Neill M, Haïssaguerre M, Jaïs P. A Criterion for Transient Entrainment of Single-Loop Reentry Tachycardias. Heart Rhythm 2011

Linton N, Wright M, Harrison J, O'Neill M. Ripple mapping in combination with Carto3 fast anatomical mapping. Heart Rhythm 2011